Biochemical characterization of Fucoxanthin Chlorophyll *a/c* binding proteins in the diatom *Phaeodactylum tricornutum*

Dissertation

for attaining the PhD degree

of Natural Sciences

submitted to the Faculty of Biological Sciences

of the Johann Wolfgang Goethe University

in Frankfurt am Main

by

Jidnyasa Joshi

from

Goregaon, India

Frankfurt (2011)

(D 30)

accepted by the Faculty…………………………………………………………………………

of the Johann Wolfgang Goethe University as a dissertation.

Dean:..……………………………………………………………………………………..

Expert assessor: …………………………………………………………………………...

Date of the disputation:……………………………………………………………………

All that is gold does not glitter,
Not all those who wander are lost;
The old that is strong does not wither,
Deep roots are not reached by the frost

-chapter ten 'Strider'

J.R.R.Tolkien, The Lord of the Rings

Table of Contents

List of figures

List of tables

Abbreviations and Symbols

2D	2 dimensional
3D	3 dimensional
° C	degrees celcius
%	percentage
x: y	ratio of x to y
::	corresponding to
λ	wavelength in nanometer
A°	angstrom units
APS	ammonium persulfate
ATP	adenosine triphosphate
Chl	chlorophyll
C.V.	column volume
ca	circa
DDE	diadinoxanthin deepoxidase
DDM	dodecyl maltoside
ddH_2O	double distilled water
Ddx	diadinoxanthin
DEAE	diethylaminoethyl
Det	detergent
Dtx	diatoxanthin
ECL	enhanced chemiluminescence
ESI	electrospray ionization
Fx	fucoxanthin
$FcpA_{His}$	his-tagged FcpA purified via IMAC
g	gram(s)
*g	times gravity
hr	hour(s)
H^+	proton
HPLC	high performance liquid chromatography
kDa	kilodalton
LC	liquid chromatography
LHCI	light harvesting complex of photosystem I
LHCII	light harvesting complex of photosystem II
ml	milli-liter
mM	milli molar
min	minute(s)
mg	milligram(s)
mm	millimeter(s)
mA	milliampere
mbar	millibar
μ	micrometer
MGDG	monogalactosyl diacylglycerol
MS	mass spectrometry
NADP	nicotinamide adenine dinucleotide phosphate
NG	nonylglucoside
Ni-NTA	nickel nitrilotriacetate
nm	nanometer

NPQ	nonphotochemical quenching
OEC	oxygen evolving center
PAGE	polyacrylamide gel electrophoresis
PBS	phosphate buffered saline
PC	phosphatidylcholine
PCR	polymerase chain reaction
PDA	piperazine diacrylamide
PS	photosytem
Psi	pounds per square inch
PQ	plastoquinone
PVDF	polyvinyldifluoridine
PBS	phosphate buffered saline
qE	energy dependant component of NPQ
RC	reaction center
rpm	rotations per minute
s	second(s)
SDS	sodium dodecyl sulfate
SQDG	sulfoquinovosyl diacylglycerol
TEM	transmission electron microscope
TEMED	tetramethylethylenediamine
V	volt(s)
Vx	violaxanthin
WT	wildtype
w/w	weight by weight
w/v	weight by volume
XC	xanthophyll cycle

1 Introduction

----

1   Introduction

Phaeodactylum tricornutum, an established model organism in photosynthesis research, was used in this thesis to investigate in detail the biochemical aspects of the light harvesting complexes: the Fucoxanthin Chlorophyll *a/c* binding proteins (FCPs) and their interactions with photosystems.

1.1   Diatoms

Diatoms (Phylum: Heterokontophyta, Classes: Bacillariophyceae, Fragilariophyceae and Mediophyceae) are unicellular photosynthetic organisms believed to be derived from a secondary endosymbiosis process between a red alga and a heterotrophic eukaryote around 1 billion years ago (Bhattacharya and Medlin 1998, Bowler et al. 2008). They are found both in marine and freshwater environments and are physiologically robust organisms which can withstand a variety of external stresses like salinity, temperature fluctuations (Kudo et al. 2000), nutrient deprivation (McKay et al. 1997), fluctuating light intensities (Falkowski and LaRoche 1991) and silica deprivation (Wilhelm et al. 2006). Over 100,000 species contained in this taxonomic group contribute to approximately one-fifth of the global primary production thereby making a very strong impact on global biogeochemical cycles (Falciatore and Bowler 2002, Wilhelm et al. 2006). These characteristics make diatoms a popular object of research among marine ecologists. In addition diatoms have been in the focus of applied research in recent years to obtain high value products like lipids to obtain biodiesel (Dunahay et al. 1996) or omega-3-fattyacids (Barclay et al. 1994). The very intricate and species specific silica cell wall patterning in diatoms has caught up interest in the fields of material science research and nanotechnology in recent years and great efforts are being made to understand the biosilica forming machinery (Lopez et al. 2005, Kröger and Poulsen 2008). Concerning photosynthesis research, the two diatoms *Thallasiosira pseudonana* and *P. tricornutum* have been vastly used owing to the availability of their complete genome

----

sequences and a huge compilation of expressed sequence tag (EST) databases (Armbrust 2004, Bowler et al. 2008, Maheswari et al. 2009). Several research groups have contributed to the understanding of the process of photosynthesis in diatoms – regarding genes involved in the process, light harvesting antenna proteins, photo-protection, photosystems and other important aspects of photosynthesis.

1.2 Overview of oxygenic photosynthesis in higher plants

The conversion of light energy into chemical energy in the form of sugar is called photosynthesis. Oxygenic photosynthetic organisms use water as the electron donor and oxygen is released as a byproduct and this reaction sustains the majority of life in the biosphere. Oxygenic photosynthesis is defined by the basic chemical equation:

$$6\,CO_2 \;+\; 12\,H_2O \;\xrightarrow{\text{light}}\; C_6H_{12}O_6 \;+\; 6O_2 \;+\; 6H_2O$$

$6\,CO_2$ (carbon dioxide) + $12\,H_2O$ (water) → $C_6H_{12}O_6$ (sugar) + $6O_2$ (oxygen) + $6H_2O$ (water)
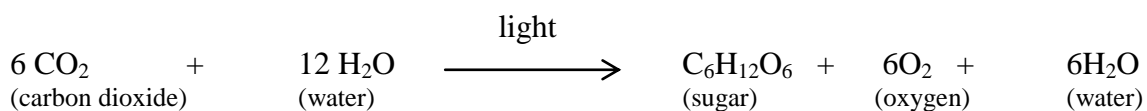
The schematic organization of thylakoid membranes in higher plants is shown in figure 1. These are differentiated into stacked grana thylakoids and unstacked stroma thylakoids. The space contained within the membranous system of thylakoids is the 'thylakoid lumen' and that contained outside of the thylakoids but within the chloroplast envelope membranes is the 'stroma'.
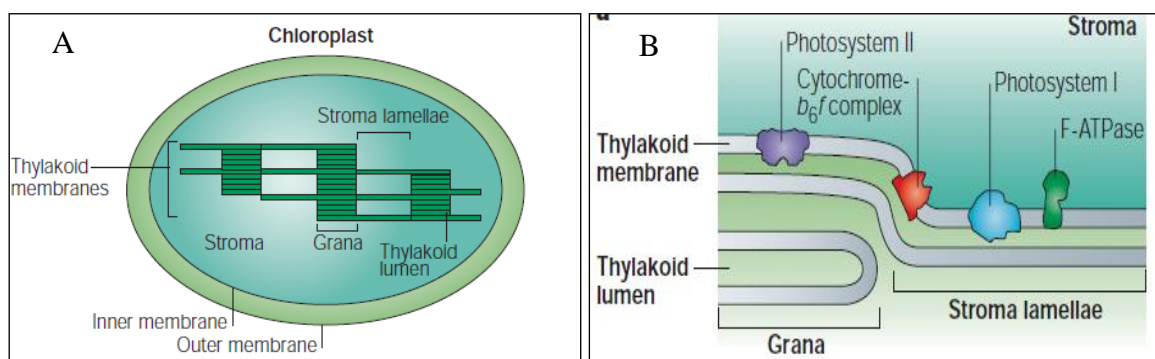
Figure 1: Schematic representations of photosynthetic apparatus. In panel A; ultrastructure of higher plant chloroplasts, B; distribution of the essential components of oxygenic photosynthesis in the thylakoid membranes of higher plants. Image taken from Nelson and Ben-Shem (2004).

Photosystem (PS) II and its associated light harvesting complexes i.e. LHCII are preferentially localized in the grana whereas PSI and its specifically associated complexes, the LHCI, are localized in the stromal thylakoids. ATPsynthase is located towards the stromal side of the lamellae and cytb$_6$f complex is localized mostly at the grana and the granal margins (Dekker and Boekema 2005).
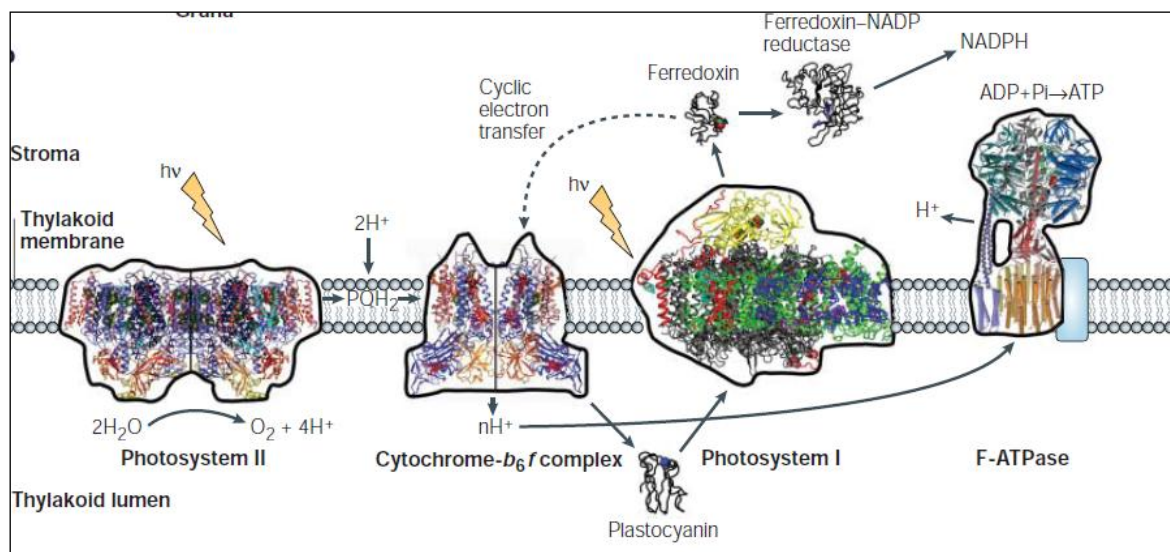
Figure 2: Scheme and apparatus of the light driven oxygenic photosynthesis. Four large membrane protein complexes along with soluble enzymes are essential to drive oxygenic photosynthesis. LHCII and LHCI are not indicated in the figure. Image taken from Nelson and Ben-Shem (2004).

1.3   Oxygenic photosynthesis

The main components of the apparatus of the oxygenic photosynthesis are the membrane intrinsic multi-protein complexes PSII and PSI, the cytb$_6$f complex and the F-type ATP synthase as indicated in figure 2. Primary (chlorophylls) and accessory pigments (carotenoids) absorb light energy at specific wavelengths. This light energy is transferred as excitation energy via several pigments to final energy acceptors i.e. reaction center (RC) chlorophylls. Charge separation at PSII occurs at the reaction center Chl *a* where an electron is transferred via a series of electron carriers until it reduces plastoquinone (PQ). This process is performed twice and after two protons are taken up from the stroma of the thylakoids the

plastoquinone is converted to plastoquinol. Plastoquinol diffuses into the thylakoid membrane and releases the electron at the $cytb_6f$ complex. This reduced $cytb_6f$ further reduces the PSI via plastocyanin (PC). Another quantum of light is needed to further drive the electron from the PSI-RC via ferredoxin and ferredoxin-NADP$^+$ reductase to generate NADPH. Electrons from a cluster of four manganese ions and cofactors replace the electrons ejected from the PSII-RC. Water is oxidized at the manganese cluster to generate oxygen and 4 protons and 4 electrons. 4 electrons reduce the manganese cluster to its original state and the photosynthetic chain then operates again to generate oxygen and reducing equivalents of NADPH. At every step of the redox reaction free energy is released, a part of which is utilized to pump protons across the photosynthetic membrane and create a proton motive force or a proton gradient which is utilized for the synthesis of the chemically utilizable form of energy i.e. Adenosine triphosphate (ATP) via the enzyme ATPsynthase. These energy and redox equivalents (ATP and NADPH) provide the driving fuel for the light-independent reactions or the so called 'dark' reactions. The dark reaction of the Calvin-Benson cycle fixes atmospheric carbon dioxide into chemically utilizable form such as three carbon sugars (Nelson and Ben-Shem 2004).

1.3.1   Photosystem I

Photosystem is a large monomeric multiprotein complex consisting of 12-14 subunits in higher plants. The core of PSI is a heterodimer formed by the proteins PsaA and PsaB which are together called the core proteins (CP1) each of which is an eleven trans-membrane helix protein. The core proteins bind a large amount of cofactors essential for the electron transport chain and also a large part of antenna chlorophylls. The subunits PsaC, D and E provide docking site for the binding of ferredoxin. PsaC also plays a role as a docking site for the two iron-sulfur clusters (Amunts and Nelson 2008, Amunts et al. 2010). In higher plants and green algae the N-terminal domain of the subunit PsaF provides a docking site for PC which

allows faster electron transfer than in case of cyanobacteria (Amunts and Nelson 2008). PsaF, G, J and K form a site for the docking of LHCI and H and L are postulated to form the docking site for LHCII during state transitions as well as functions related to maintaining the integrity of the complex (Nelson and Ben-Shem 2004).

1.3.2   Photosystem II

PSII is the essential core of oxygenic photosynthesis because it is the site of water splitting and oxygen evolution. It is composed of the highly homologous 5 transmembrane helix intrinsic core proteins; D1 (PsbA) and D2 (PsbD). D1 binds most of the cofactors responsible for electron transport and is more sensitive to photodamage than D2 (Ferreira et al. 2004). D2 has a function in photoprotection and binds lesser cofactors involved in charge separation (Hankamer et al. 1997, Ishikita et al. 2007). The proteins CP43 (PsbC) and CP47 (PsbB) are the intrinsic light harvesting antennae of PSII. Apart from light harvesting, CP43 and CP47 are involved in the assembly and stability of PSII. CP43 along with D1 is also involved in the correct positioning of the manganese cluster (Bricker and Frankel 2002). The PsbE and PsbF proteins form the α and β subunits of the cytb$_{559}$ heterodimer associated with D1 which is thought to play a photoprotective role by acting as either electron donor or acceptor under conditions where electron flow is not optimal (Hankamer et al. 1997). The small single transmembrane helix proteins PsbH, I, J, K, L, M, N and T are also intrinsic proteins of the PSII but their function is unclear. It is suggested that the subunits PsbL, M and T are involved in the dimerization of PSII (Loll et al. 2005). PsbJ provides such a conformation of PSII where LHCII can bind effectively (Suorsa et al. 2004). PsbW is a nuclear encoded intrinsic protein of the PSII which stabilizes coredimer of PSII (Shi et al. 2000). PsbS is a 4 transmembrane helix protein and has a high homology with LHCII. It plays a role in the qE dependant NPQ in higher plants. However, the exact mechanism of NPQ is unclear (Niyogi et al. 2005, Kereïche et al. 2010). Among the extrinsic proteins of PSII are the PsbO, P, Q,

and R. These are present on the luminal side of the core of PSII and are functionally related with the oxygen evolving center (OEC). PsbU and PsbV are cyanobacterial proteins that are absent in higher plant PSII and are the homologues of PsbP and PsbQ (Loll et al. 2005).

1.3.3   Light harvesting complexes

The LHCII is the specific antenna complex of the PSII in plants and accounts for approximately 30% of all proteins of the plant thylakoid membrane and binds at least 50% of the chlorophylls contained in the chloroplast (Thornber 1975). The Lhcb1, 2 and 3 form the major antenna which is trimeric and situated at the periphery of the PSII. It has been shown that the trimers are formed in all possible combinations within the subunits (Standfuss and Kühlbrandt 2004). Furthermore, the assembly of trimers of LHCII is a spontaneous process (Hobe et al. 1994). The subunits Lhcb4 (CP29), b5 (CP26) and b6 (CP24) form the minor antenna which are monomeric. The minor antennae mediate the energy transfer from LHCII to CP43 and CP47 or D1 and D2. In cases where Lhcb1 and b2 are absent, trimers of CP26 (Lhcb5) are formed which substitute for the loss of major LHCII and keep the organization of the PSII-LHCII intact (Ruban et al. 2003). The LHCI is the specific antenna of the PSI in higher plants and consist of subunits Lhca1, a2, a3 and a4. These 4 subunits form 2 heterodimers of a crescent shape and dock at PsaF side around PSI. The PSI supercomplex is monomeric in plants but trimeric in cyanobacteria (Nelson and Ben-Shem 2004).

1.4   Diatoms- cell structure, chloroplast organization and photosynthesis.

1.4.1   Cell structure and chloroplast organization

Depending upon the internal fold of symmetry, diatoms are either classified as the centrics - which possess a radial symmetry or the pennates - which possess a bi-lateral symmetry. Figure 3 shows schematic cross-section of a pennate diatom cell. Diatoms have the ability to generate an external wall; frustule; composed of amorphous silica. The frustule shows a Petri

dish like structure where the outer larger component of the cell wall is called the epitheca and smaller inner component the hypotheca. The raphe slit is the axis which imparts bilateral symmetry to the cell.
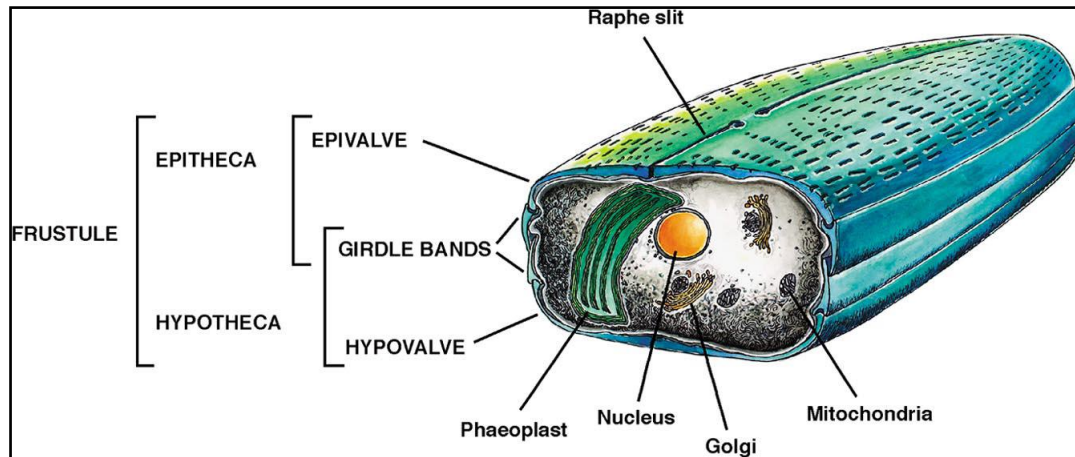
Figure 3: Schematic representation of the general structural features of a pennate diatom cell. Image taken from Falciatore and Bowler (2002).

In *P. tricornutum* the contribution of silica in the cell wall is highly reduced compared to other diatoms. It has been reported that amorphous silica is deposited in the loosely bound organic matrix (Lewin et al. 1958, Borowitzka and Volcani 1978) and thereby it possesses no significant robust cell morphology as demonstrated in figure 4.
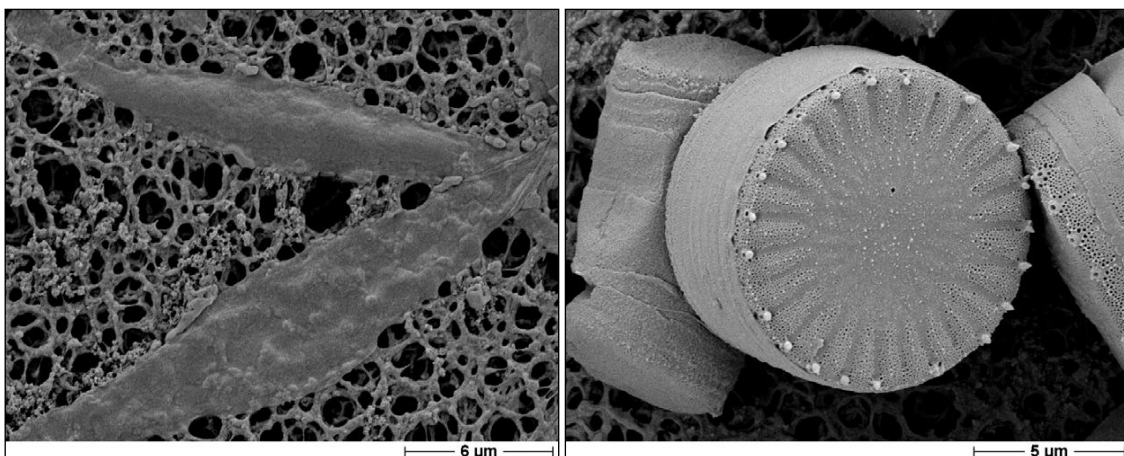
Figure 4: Scanning electron microscopy image of the pennate diatom *P. tricornutum* strain UTEX 646 (left) and centric diatom *C. meneghiniana* (right). Image taken from Barka F (2008).

The ultra structure of diatom cells shows either few small chloroplasts in case of centrics or a single large chloroplast in case of pennates (Lavaud J 2007). The remnants of the secondary endosymbiosis process are seen as the four membranes that surround the chloroplast instead of the only two chloroplast membranes in higher plants (Wilhelm et al. 2006). The outermost membrane of the chloroplasts is connected with the endoplasmic reticulum (Bouck 1965, Kilian and Kroth 2005).
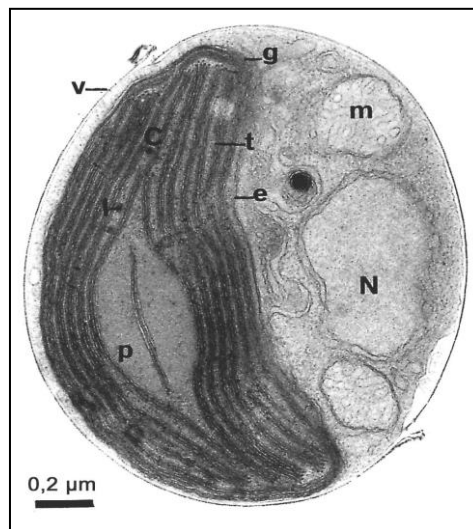
Figure 5: Electron micrograph of the diatom *Phaeodactylum tricornutum*. The nucleus is represented by (N), the mitochondria (m) and the cell-wall silica valves (v). Thylakoids (t) are arranged in three parallel bands surrounded by an inner 'girdle stack' of thylakoids (g). The chloroplast is surrounded by a four membrane envelope (e) and it contains one pyrenoid (p). Image taken from Lavaud J (2007).

The ultra structure of chloroplasts differs considerably as compared to those of higher plants. The thylakoid membranes in diatoms are not differentiated into granal and stromal lamellae, i.e. the granal stacking is absent. The thylakoid membranes are arranged into groups of three loosely stacked lamellae which span through the whole length of the chloroplast (Gibbs 1962, Pyszniak and Gibbs 1992). The thylakoid membranes within the chloroplast are surrounded by a so called girdle lamella, which also contains three loosely stacked thylakoid membranes (Murata et al. 1979, Pyszniak and Gibbs 1992).

In case of plant thylakoids, PSI and PSII can be spatially separated owing to the structural differentiation of the thylakoid membranes into stacked and unstacked grana. This spatial

distribution is not possible in case of the undifferentiated thylakoids of diatoms and PSI and PSII are rather homogenously distributed in the thylakoid membranes (Gibbs 1962).

1.4.2 Photosynthetic pigments in diatoms

Chl *a* acts as the central photosynthetic pigment in all oxygenic photosynthetic organisms. However there exist major differences between higher plants and diatoms in the further photosynthetic pigment content. The accessory chlorophyll i.e. Chl *b* in plants is replaced by Chl *c* in diatoms. Chl *c* does not possess an aliphatic phytol chain like that in Chl *b* which changes the absorption spectrum to produce a strong Soret band (absorption in blue region) and a weak band in the red region. Chl c_1 and c_2 exhibit small structural differences and are the dominant forms of Chl *c* which are present in diatoms (Larkum 2004). Additionally, the major carotenoid in case of higher plants which is lutein is replaced by fucoxanthin (Fx) in diatoms. Carotenoids exhibit intense absorption between 400 and 500 nm. Fx is a highly asymmetric molecule and possess an allene group on an ionone ring causing it to absorb light in a wide spectral range between 450 and 570 nm (Zigmantas et al. 2004). Photosynthetic organisms which use xanthophylls for photoprotection use either the violaxanthin (Vx) cycle or the diadinoxanthin (Ddx) cycle (figure 6). The violaxanthin cycle is present in case of higher plants, which operates in the pH dependent branch of the NPQ. Lohr and Wilhelm (1999) showed that this cycle is present in *P. tricornutum* as well. However it was suggested that the cycle operates in very minor amounts and predominantly under prolonged high light stress as compared to the Ddx cycle which is involved in the major NPQ component in diatoms. Additionally it was also shown that in *P. tricornutum*, Vx is the obligate precursor in the synthesis of the carotenoid Fx (Lohr and Wilhelm 2001).
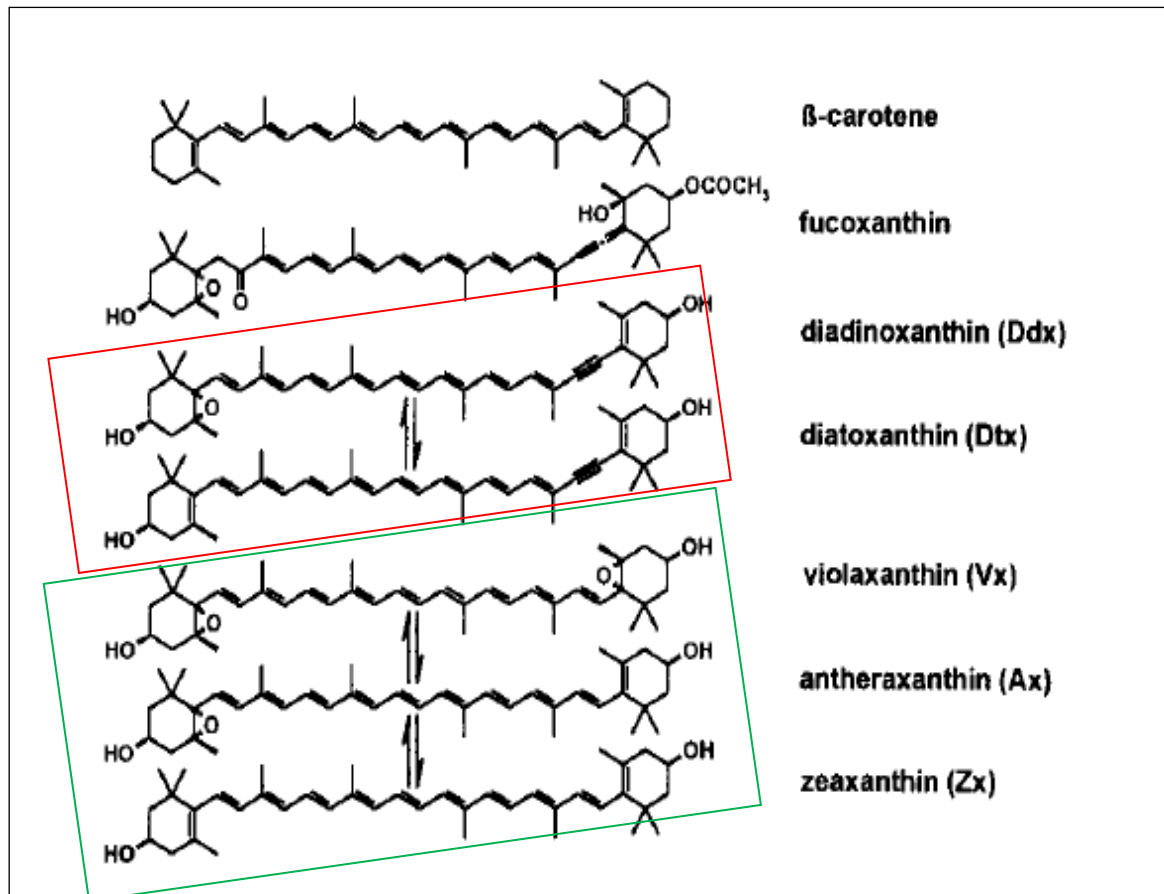
Figure 6: Molecular structures of the major carotenoids in diatoms. Outlined in red are the xanthophylls of the diadinoxanthin cycle and in green those taking part in the violaxanthin cycle. Arrows indicate enzymatic conversion among pigments during the xanthophyll cycles. Image adapted from Lohr and Wilhelm (1999).

1.4.3 Light harvesting and photoprotection

Owing to the presence of Fx as the major carotenoid and Chl *c* as the accessory chlorophyll, the light harvesting complexes in diatoms are known as the Fucoxanthin Chlorophyll a/c binding proteins (Bhaya and Grossman 1993). Fx is the main carotenoid coordinated in the Fcps and its binding to the protein backbone leads to a bathochromic (red) shift and absorption between 470 nm and 550 nm. This absorption property in the blue-green region is peculiar for diatoms since they can utilize the 'green gap' of the absorption spectrum that higher plants cannot and is attributed to one of the reasons why diatoms survive in oceans where the major available wavelength of light in the euphotic zone is blue light.

The Fcps are membrane intrinsic proteins which belong to the LHC superfamily which is encoded by a conserved multigene family (Bhaya and Grossman 1993, Green and Pichersky 1994, Green and Durnford 1996).
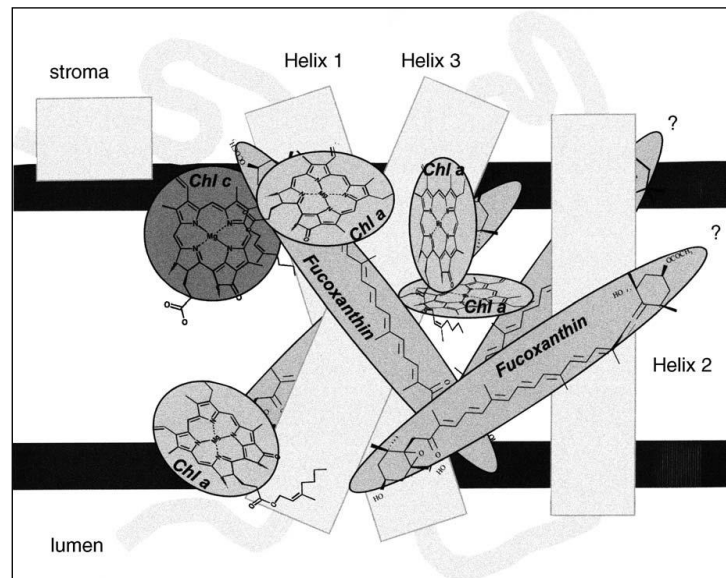
Figure 7: Hypothetical model of the arrangement of pigments on the Fcp polypeptide backbone. '?' denotes that the positions assigned to the 2 fucoxanthins are not experimentally proven and are only hypothetical. Image taken from Wilhelm et al. (2006).

The predicted structure of Fcps is highly related to the structure of higher plant LHCII and modeling based on the structure of LHCII from *P. sativum* suggested that the helix 1 and helix 3 are conserved whereas the helix 2 is rather non-conserved (Eppard and Rhiel 1998). The amount of carotenoids in proportion to Chl is very large in diatoms as compared to that in plants. In LHCII the Chl *a*: Lutein ratio is 4:1 (Liu et al. 2004) whereas in diatom Fcps this ratio was calculated to be Chl *a*: Fx :: 1:1 (Papagiannakis et al. 2005). Figure 7 shows the hypothetical tertiary structure of Fcps which takes into account spectroscopic characterizations and stoichiometric ratios of pigments (Papagiannakis et al. 2005, Wilhelm et al. 2006). The most recent reports based on Resonance Raman Spectroscopy with Fcps of *C.meneghiniana* estimated the presence of at least 6 Fx molecules per Fcp monomer (Premvardhan et al. 2009) and the ratio of Chl *a*: Fx: Chl c_2 has been updated to 8:8:2 based

1 Introduction

----

on further measurements and sequence analyses (Premvardhan et al. 2010). The purification

of Fcps in the reports from Papagiannakis and Premvardhan were based on different

procedures. The results of the former (Papagiannakis et al. 2005) were based on studies

where Fcps were purified by the very gentle purification procedure of sucrose density

gradient and the stoichiometry of 4 Fx: 4 Chl *a*: 1 Chl c_2 was obtained for a mixed Fcp

population after normalization to one Chl c_2. The stoichiometries of pigments per monomer

of Fcp in Premvardhan et al. (2009) were based on studies where Fcps were highly purified

by the slightly harsher procedure of IEX chromatography which could have lead to the loss of

peripheral pigments. However the latter study rules out the possibility of underestimation of

pigments due to slight impurities and also points out the presence of two structurally different

Chl c_2 molecules per Fcp monomer (Premvardhan et al. 2010).

The hydrophilic loop regions between the membrane spanning regions (MSRs) are shortened

in case of Fcps in comparison with the LHCs of higher plants thereby making them more

hydrophobic than plant LHCs. All known Fcps have a molecular weight between 17–23 kDa

(Fawley and Grossman 1986; Caron and Brown 1987) and are classified into three major

groups based on sequence analyses. Group I represents the classical light harvesting proteins

also named Lhcf group of proteins which are denoted by numbers in *C. cryptica* or

C.meneghiniana which include Fcp1-3 and Fcp5 and the proteins Lhcf1-17 from *P.*

tricornutum (Durnford et al. 1996; Eppard et al. 2000; Bowler et al. 2008). Group II proteins

are the red algae related Lhcr proteins which are represented by Lhcr1-14 in *Thalassiosira*

pseudonana and *P. tricornutum*, respectively (Armbrust 2004; Bowler et al. 2008). It was

shown recently that in *C.meneghiniana*, the Lhcr related protein, Fcp4, acts as a PSI specific

antenna (Veith et al. 2009). Group III is represented by proteins similar to LI818 type of

proteins which are light-inducible proteins found in green algae. They are named as the Lhcx

type of proteins in the databases of *P. tricornutum* and *T. pseudonana*. Homologues of these

are proposed to function in light protection (Richard et al. 2000; Zhu and Green 2008; Peers et al. 2009). Participation of the Lhcx type of proteins in NPQ was established recently in case of *T. pseudonana* (Zhu and Green 2010). (For detailed annotation of Fcps please refer Appendix I). Lhcx type of proteins are thought to overtake the role of PsbS protein; which is active in the NPQ mechanism in higher plants; but not found in the genome of diatoms (Zhu and Green 2008; Armbrust 2004; Bowler et al. 2008).

Increasing amounts of information about the biochemistry of Fcps has been available in recent years. Büchel proved presence of trimeric (FCPa) and the concomitant higher oligomeric (FCPb) Fcp complexes in the centric diatom *C.meneghiniana* (2003). Beer and coworkers dissected the polypeptide composition of these complexes and found that the FCPa trimeric complex was composed mainly of 18kDa subunits encoded by the *fcp2* gene and minor amounts of a 19kDa polypeptide which was the product of *fcp6* gene (2006). The FCPb higher oligomeric complex was homogenously composed of 19kDa polypeptides thought to be encoded by *fcp5* gene. The *fcp6* gene product in FCPa trimer was shown to be up regulated under high light and to bind higher amounts of xanthophyll diatoxanthin (Dtx) under these conditions. A higher amount of diatoxanthin was shown to correlate with a decrease in the fluorescence yield of FCPa (Gundermann and Büchel 2008).

Guglielmi and coworkers reported the presence of a Fcp trimer and a subpopulation within this trimer in case of *P. tricornutum*. One subpopulation was more stable and enriched in the carotenoid Fx while the other was stable and enriched in Ddx. The identities of Fcps contained in these two subpopulations were not revealed (2005). Lepetit isolated a higher oligomeric Fcp complex by mild solubilisation of thylakoids and a trimeric Fcp complex using a relatively harsh solubilisation of thylakoids of *P. tricornutum*. Using mass spectrometry, Lhcf1-5 and Lhcf11 (also named FcpA-F, Appendix I) were detected in the

13

trimeric Fcp population. However specific subpopulations of trimers could not be purified further and identified (2007).

The xanthophyll cycle pigments and their role in excess light response has been researched vastly in the past few years. The existence of three different pools of Ddx in *C.meneghiniana* was shown recently (Lepetit et al. 2010). One pool was associated with the whole pool of Fcp proteins, the second pool was also protein bound and supposed to be associated with Lhcrs associated with PSI (shown in case *P. tricornutum*) and the third pool of Ddx was synthesized in case of high light exposure and associated with the nonbilayer lipid monogalactosyldiacylglycerol (MGDG) shield around Fcps. Several ideas were put forward suggesting different roles of Ddx associated with different proteins. For e.g. It was put forth that the Ddx bound to Lhcr proteins associated with PSI might play a role in photoprotection via detoxification of triplet state Chl *a* and reactive oxygen species. The Ddx present in the MGDG shield might work as an antioxidant and Dtx in this shield could possibly scavenge oxygen (Lepetit et al. 2010). Concerning lipids associated with Fcps it has been shown that the amount of MGDG is essential for the function of the enzyme diadinoxanthin deepoxidase (DDE) which converts Ddx into Dtx upon high light stress. Further the activity of DDE was found to be reduced in the presence of the negatively charged lipid sulfoquinovosyl diacylglycerol (SQDG) (Goss et al. 2009). It was also indicated that in case of the centric diatom *C.meneghiniana*, the pure Fcp population is associated with MGDG and put forward that in case of *P. tricornutum* the pure Fcps are additionally associated with phosphatidylcholine (PC) (Goss et al. 2007; Goss et al. 2009; Goss and Jakob 2010).

1.4.4 Interaction of Fcps with photosystems

From the sequence homology of Fcps with LHCII of higher plants it is considered that they act as the light harvesting antenna of the PSII also in case of diatoms. However there are no reports available so far regarding the purification of a PSII-FCP supercomplex in diatoms

where the identity of the light harvesting proteins could be demonstrated. The isolation of PSII from the marine centric diatom *Chaetoceros gracilis* which were still associated with Fcps was shown in one report (Nagao et al. 2007). But even after using a very mild procedure of freeze-thaw induced breakage of cells and differential centrifugation assisted purification of protein complexes, the Fcps were found loosely bound to PSII and their identity was not further revealed. The isolation of a functional PSII-Fcp supercomplex from diatoms remains a challenging task to date.

The existence of distinct Fcps associated with PSI and PSII in case of the cryptophyte *Rhodomonas* was shown without revealing the identity of these Fcps (Bathke et al. 1999). After phylogenetic analyses it was suggested that Fcp4 could most probably represent a candidate associated with PSI whereas Fcp2, 3 and 5 could be the specific antenna proteins of PSII in *C.cryptica* (Eppard et al. 2000). However after using sucrose density gradient for separation of PSI-Fcp and PSII-Fcp complexes and their biochemical analysis, Fcp2 and 4 were shown to be associated with both photosystem I and II in *C. cryptica* (Brakemann et al. 2006). Thus there is a wide debate about the existence of specific antenna proteins for PSI and PSII in diatoms and is currently widely assumed that at least some Fcp proteins are shared by both PSI and PSII. This does not rule out the possibility that distinct photosystem specific Fcps could exist (Büchel 2003; Brakemann et al. 2006; Lepetit et al. 2011). A highly pure PSI-Fcp complex monomeric in nature could be purified from *C. gracilis* (Ikeda et al. 2008). Similarly, using ion-exchange chromatography a PSI-Fcp complex was purified from *P. tricornutum*; however the Fcps were not identified further. It was shown using electron microscopy of single particles of these supercomplexes that PSI in case of *P. tricornutum* is monomeric like in higher plants but different from that in cyanobacteria where it is trimeric (Veith and Büchel 2007). Similar studies were also carried out in case of centric diatom *C.meneghiniana* where a PSI-Fcp supercomplex was isolated using two rounds of sucrose

density gradient centrifugation and usage of mild detergents each time. Fcp4 which is a Lhcr type of protein was identified associated with PSI and functional in excitation energy transfer (Veith et al. 2009). In another study it was shown using sucrose density gradient ultracentrifugation followed by tandem mass spectrometry that several Lhcr proteins associate with PSI in *P. tricornutum* (Lepetit et al. 2010). Additionally also one Lhcf type of protein viz. Lhcf3/4 was found to be associated with PSI in the same organism. Thus apart from the specific association of Fcp4 with PSI, there is no evidence which suggests that only a certain family of proteins are associated with PSI or PSII in diatoms. The use of different methods like the mild sucrose density gradient centrifugation in some cases and the harsh procedure of ion exchange chromatography in others along with the usage of different detergents can be one of the biggest reasons for the discrepancy of results from each working group to the other. The presence of specific antenna systems for PSI and PSII in diatoms therefore remains a matter of debate.

1.4.5   A short comparison between photosystems in higher plants and in diatoms

In spite of the similarity between the components of electron transport chain of higher plants and diatoms there exist several differences at the level of PSI and PSII. In higher plants the PsbO, P, Q and R are the extrinsic proteins of PSII responsible for the function of the OEC. In diatoms there are proteins like PsbU, PsbV and Psb31 which are homologous of PsbP and Q take up the similar function (Enami et al. 2008). The PSII intrinsic protein PsbS which is known to have a function regulation of NPQ via the energy dependant quenching qE is absent in algal genome (Armbrust 2004; Bowler et al. 2008). In case of diatoms the mobile electron carrier between cytochromeb_6f and PSI is cytochrome *c* and not plastocyanin as in higher plants. The PSI core of diatoms contains, PsaA and B and additionally PsaL, PsaE and PsaM. PsaM is thought to be the component necessary for trimerisation of PSI. In spite of this, it

----

could be shown that the PSI in *P. tricornutum* was monomeric and the similarity between

PsaM in plants and diatoms was only 50% (Veith and Büchel 2007).

1.4.6 Life cycle of diatoms

The predominant cycle of cell life in diatoms is the vegetative state and the cell division

follows asexual- mitotic way (figure 8) where the parent cells first enlarges and the hypotheca

and epitheca are pushed away while the nucleus divides mitotically.
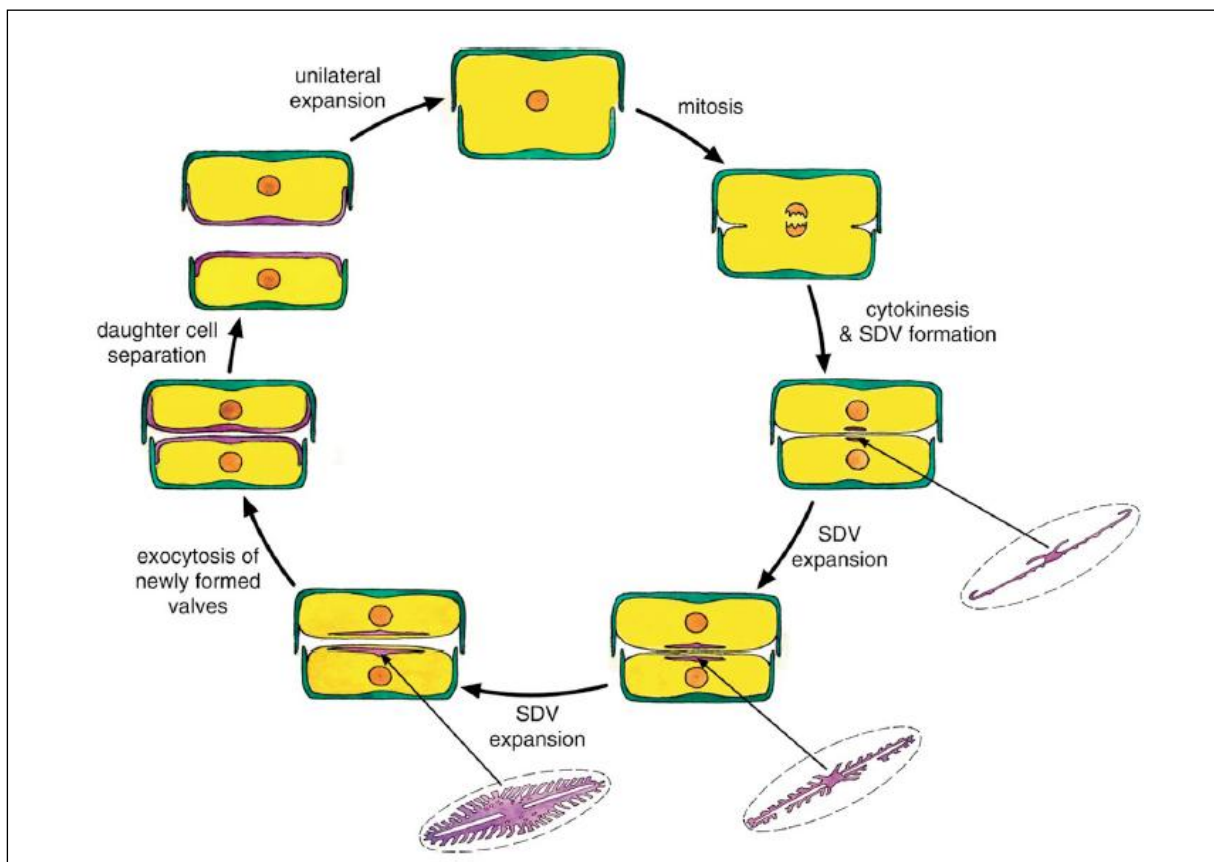
Figure 8: Schematic representation of the asexual cell division and the formation of a hypotheca in daughter cells in a pennate diatom. Image taken from Falciatore and Bowler (2002).

The plasma membrane invaginates and the protoplast divides into two. Each valve of the

parent cell becomes the epitheca of the daughter cell which generates its new hypotheca. The

generation of the hypotheca follows after the creation of a silica deposition vesicle (SDV)

between nucleus and plasma membrane. A new hypotheca if formed within the SDV by

transport of silica, polysaccharides and proteins into it and this hypotheca is exocytosed after

----

which the daughter cells separate. It is obvious that the daughter cells so formed are smaller in size owing to the inheritance of the unequal sized epitheca and hypotheca of the parent. Once the cell size decreases to 30-40% of maximum diameter a sexual cycle begins which allows the cells to regain the original size. Male and female gametes of the sexual cycle combine to create a diploid auxospore; which is a cell larger than either parent. The auxospore proceeds via asexual pathway as described before (Falciatore and Bowler 2002). The process of cell division was reported to be similar also in centric diatoms (Pickett-Heaps et al. 1980).

1.5   Transgenic diatoms

The availability of complete genomes of two diatoms: the centric *T. pseudonana* [http://genome.jgi-psf.org/Thaps3/Thaps3.home.html] and the pennate *P. tricornutum* [http://genome.jgi-psf.org/Phatr2/Phatr2.home.html] and the huge repertoire of ESTs (Maheswari et al. 2009) provide the possibility of unraveling highly complex processes at the whole genome level. Genetic transformation systems for a few diatoms have been established so far. Dunahay first described the transformation of *C. cryptica* and *Navicula saprophila* and tried to enhance lipid biosynthesis in *C. cryptica* by introducing multiple copies of *acetyl CoA carboxylase* gene (Dunahay et al. 1996). Apt and coworkers described the stable genetic transformation of *P. tricornutum* using *sh ble* as a selectable marker the product of which provides resistance to the antibiotic zeocin (1996). The usage of nonselectable reporter genes like the firefly *luciferase* gene was described for the transformation of *P. tricornutum* (Falciatore et al. 1999). The heterologous expression of cell wall and membrane proteins in *Cylindrotheca fusiformis* was described by Fischer and coworkers (1999). The use of a general transformation vector pPha-T1, backbone of which is shown in figure 9, for *P. tricornutum* has greatly simplified genetic manipulation of this organism (Zaslavskaia et al. 2000).This vector; pPha-T1; offers the advantage that the transformants can be selected using

the antibiotic zeocin. Further there is a multiple cloning site under the control of the fcpA

promoter which simplifies the expression of heterologous genes.
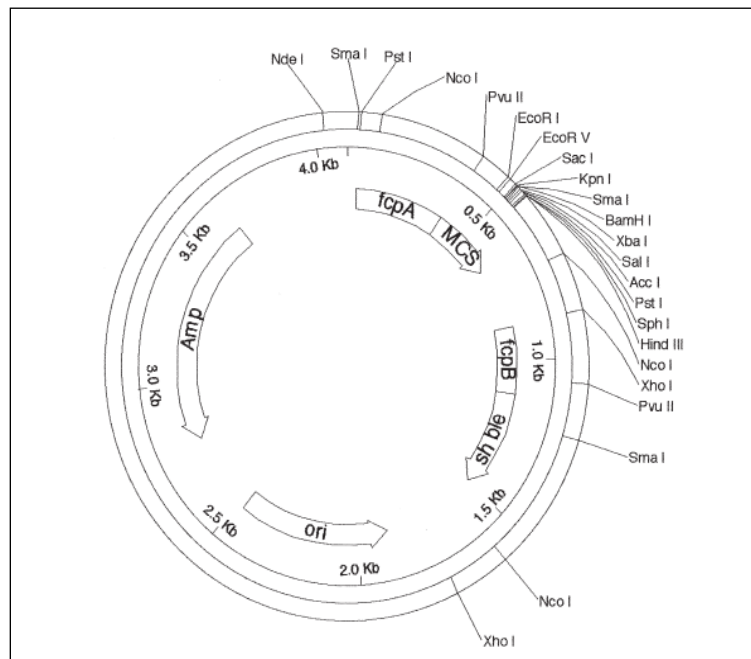
Figure 9: Schematic representation of the general transformation vector of *P. tricornutum*; pPha-T1 (Zaslavskaia et al. 2000). MCS denotes the multiple cloning site, sh ble indicates the region encoding resistance to the antibiotic zeocin, ori is the origin of replication in *E. coli*, Amp is region encoding resistance to ampicillin and fcpA and fcpB are the promoters which control expression of the respective downstream genes.

Diatoms grow mainly as diploid vegetative cells as described before and the sexual cycle

cannot be controlled in culture (Apt et al. 1996). In case of *P. tricornutum* there is no

evidence so far of a sexual cycle (de Riso et al. 2009). Further there is no proof of

homologous recombination in diatoms which makes targeted gene disruption unlikely

(Falciatore and Bowler 2002; de Riso et al. 2009). For this reason it is possible to express

additional genes but always with a simultaneous expression of the endogenous genes. Recent

reports have also shown that knockdown mutants can be generated in *P. tricornutum* using

the interference RNA (RNAi) approach. Also targeted gene silencing is possible by

introduction of constructs which contain antisense or inverted repeat containing RNAs (de

Riso et al. 2009). Apt and coworkers showed using the pre-sequence of the gamma subunit of

plastid ATP synthase of *P. tricornutum* that engineering of a His-tag to the C-terminus of the protein does not affect its transport into the plastid (Apt et al. 2002). Detailed work has been carried out to reveal the importance of a specific signal and transit sequence in *P. tricornutum* for correct transport of the nucleus encoded proteins into the chloroplasts which are surrounded by 4 membranes. Several presequence:GFP fusion proteins were created with modifications in the signal and transit motif and expressed in *P. tricornutum* and it was proved that a the presence of phenylalanine residue at the N-terminus of the transit peptide along with a cleavable signal peptide is necessary for the transport of proteins into the plastid membrane (Gruber et al. 2007).

In summary, there is sufficient information available concerning the transformation of diatoms in particular of *P. tricornutum*. This opens up several possibilities of studying biochemical processes that were limited due to lack of genetic knowledge.

----

2   Aims of this work

Although a wide amount of information regarding light harvesting complexes in diatoms is available, existence of specific complexes has neither been shown nor is data concerning crystallization of Fcps available. Additionally the existence of photosystem specific antenna proteins in diatoms is widely debated. Based on this background, the aims of this work were:

1) **To make an efficient and reproducible protocol for purifying specific Fcp complex; viz. His-tagged FcpA; from the whole pool of Fcps in *P. tricornutum*.**- The high degree of similarity in molecular weights and possibly also pigmentation among all Fcps has been the reason why no specific Fcp or Fcp complex could be purified in the native state until date. This problem was addressed by creating a mutant expressing an additional His-tagged FcpA along with all endogenous Fcps and purifying specifically the His-tagged FcpA via affinity chromatography.

2) **Biochemical characterization of the recombinant FcpA protein**- $FcpA_{His}$ and a highly pure WT Fcp pool were characterized for spectroscopic properties, pigment binding, oligomeric status, pigment interactions. Additionally identification of the binding partners of $FcpA_{His}$ was carried out.

3) **To investigate the association of FcpA with photosystems in *P. tricornutum***- There is a wide debate about existence of photosystem specific antenna system in diatoms. Using very mild solubilisation of thylakoids and protein purification methods PSI and PSII supercomplexes were isolated and characterized.

4) **To crystallize the FcpA$_{His}$ in 2 dimensions**- One of the biggest bottlenecks towards the crystallization of Fcps is the inhomogeneity of preparation. This question can be addressed only when a homogenous preparation of specific Fcp can be achieved for e.g. like in case of recombinant FcpA which can be specifically purified using affinity chromatography.

----

3   Materials and methods

All materials used in this study were of technical grade unless mentioned otherwise.

3.1   Construction of a *P. tricornutum* mutant expressing recombinant His-tagged FcpA

A transgenic strain of *P. tricornutum* expressing a His-tagged FcpA protein was constructed by Dr. M. Schmidt, University of Frankfurt in collaboration with the working group of Prof. Kroth at the University of Konstanz. This is described very briefly in this section to help the reader understand the observations in the thesis better.

The complete nucleotide sequence for *fcpA* is deposited at EMBL – EBI database with gene ID number Z24768 also found in the US Department of Energy's Joint Genome Institute *P. tricornutum* genome database with Protein ID 18049. Using the genomic DNA from wildtype (WT) cells (UTEX culture collection, strain 646) and the following oligonucleotide primers the coding region of the *fcpA* gene was amplified by PCR:

(F) 5'-ga(gatatc)attcaagatgaaatttgc-3' and

(R) 5'-a(gtcgac)ttaatggtgatggtgatggtgaggaaggatag-3'.

Primer (F) inherently contained an EcoRV restriction site whereas the reverse primer (R) was designed to introduce a SalI restriction site and to simultaneously generate a fragment encoding a His-tag at the 3' terminus of the gene. The restriction sites within the primers are indicated in parentheses while the underlined sequence codes for six histidine residues. This insert was introduced in the multiple cloning site of the transformation vector pPha-T1 (Genbank accession number AF219942). The resulting plasmid pPha-T1-FcpA$_{His}$ carries a His-tagged *fcpA* gene under the control of the native fcpA promoter (Fig. 10). It was allowed to amplify in *E. coli* under ampicillin pressure. Plasmid DNA was isolated and used for transformation of WT cells.

WT cells plated on Artificial Seawater medium (ASP) agar (Provasoli et al. 1957) were bombarded using biolistic PDS-1000/He Particle delivery system (Bio-Rad laboratories,

----

Hercules, CA) fitted with a 1350 psi rupture disc. 1 μg plasmid DNA was coated onto M17

tungsten particles (Bio-Rad) and used for bombardment. Bombarded cells were illuminated

continuously for 24 hours at 40 μE m^{-2}s^{-1} before plating them on ASP agar plates

supplemented with 75 μg ml^{-1} zeocin to select possible transformants. Clones which could

survive repeated zeocin selection were screened for expression of the His-tagged recombinant

protein at mRNA level (courtesy Dr. M. Schmidt, University of Frankfurt). The recombinant

clones now contained one or more copies of the His-tagged *fcpA* gene along with a

background of all other WT *fcp* genes. The presence of the His-tagged gene within these

clones was again confirmed by PCR and also by sequencing (courtesy Dr. M. Schmidt). The

clone FcpA1.2 was observed to have the highest expression level and was chosen for further

work. It was cultured and sub-cultured regularly in ASP medium containing zeocin under low

light conditions for a period of 6 months before attempts were made to isolate the

recombinant protein.
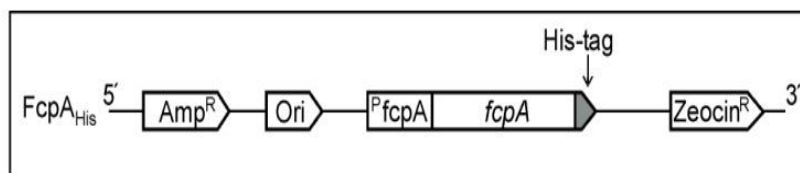
Figure 10: Scheme of the His-tagged *fcpA* gene under the control of the fcpA promoter (^{P}fcpA) and position of the hexa-histidine tag in the constructed plasmid pPha-T1-FcpA$_{His}$. The sequence encoding a six histidine residue was inserted at the 3' end of the coding region of the *fcpA* gene. The transformation vector pPha-T1 carries a gene for Ampicillin (Amp) resistance and the origin of replication (Ori) in *E. coli* upstream of the *fcpA* gene and for Zeocin resistance downstream of the *fcpA* gene. Image taken from Joshi-Deo et al. (2010).

3.2 Biological Material

Table 1: Source and use of strains of *P. tricornutum* used in this study.

Material	Source	Used in this study
Phaeodactylum tricornutum 646	UTEX culture collection	As Wildtype (WT)
Phaeodactylum tricornutum A1.2 (also noted as FcpA1.2)	University of Frankfurt, (Dr. M. Schmidt)	Mutant expressing His-tagged FcpA

3.3 Culture Conditions

P. tricornutum Böhlin WT (UTEX culture collection, strain 646) and the mutant were grown in ASP medium for 10 days at 18°C under constant aeration by bubbling sterile air at a light intensity of 40 μE $m^{-2}s^{-1}$ under a 16/8 hrs light/dark cycle. Cells were maintained as stock cultures in ASP medium on shakers for 21 days at 120 rpm following which they were transferred to fresh medium.

Table 2: Composition of the ASP medium, pH 7.7

Chemical	Concentration	Trace element	Concentration
NaCl	86 mM	$CaCl_2$	2.72 mM
Tris	4 mM	Na_2-EDTA	0.092 mM
KCl	21mM	$FeCl_3$	0.012 mM
$MgSO_4$	8.1 mM	$MnCl_2$	0.02 mM
$NaNO_3$	11.8 mM	$ZnCl_2$	0.002 mM
K_2HPO_4	0.58 mM	$CoCl_2$	50 pM
H_3BO_3	0.16 mM	Na_2MoO_4	25 pM
pH adjusted with H_2SO_4 to 7.7 and trace elements were added		$CuCl_2$	22.5 pM
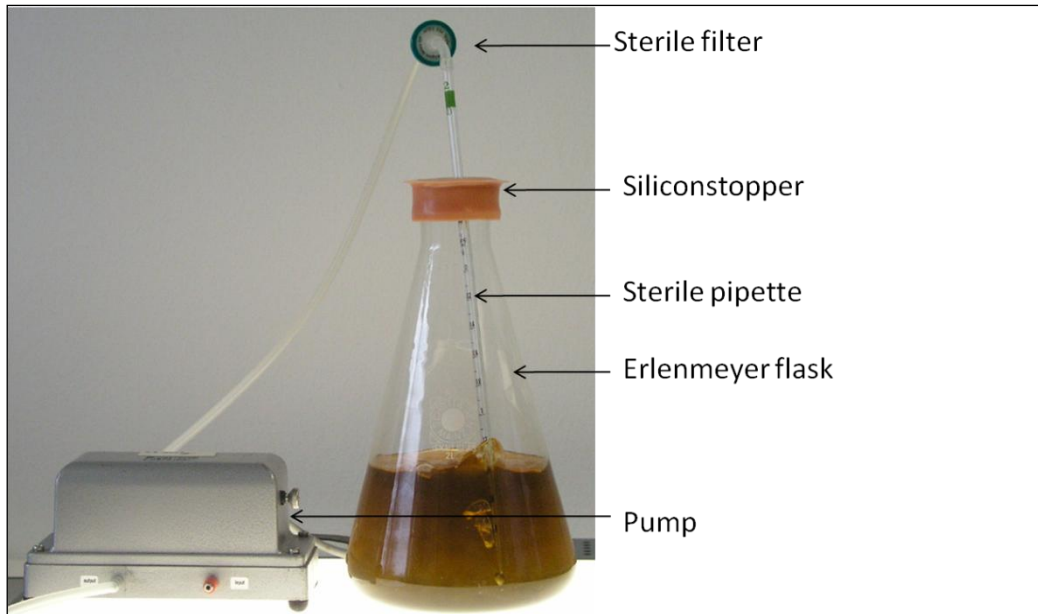
Figure 11: Cultivation of cells of *P. tricornutum* using bubbling culture. Image adapted from Barka F (2008).

3.4 Comparison of WT and mutant

3.4.1 Growth Curve

Growth curves were plotted with three independent cultures which were counted for several days using a Thoma cell counting chamber. Cells in the 4 diagonal squares of the chamber were counted including those on the outer borders of the squares. The number of cells were calculated accordingly:

Cells (million/ml) = x*4*15626, where

X= cells counted in the 4 diagonal squares

4= to obtain total number of cells in 16 squares

15625= counting chamber factor to obtain number of cells /ml.

3.4.2 High Performance Liquid Chromatography (HPLC)

HPLC deals with the separation of analytes which are pumped by a mobile phase over a separating stationary phase. Depending upon the physical properties like polarity, the analytes

bind to the stationary phase and upon the strength of interaction with the stationary phase, the analytes exhibit a different retention time as they are eluted by the mobile phase. As the analytes separate, their absorption spectra can be measured by a diode array detector (Hitachi) and the analyte pigment can be identified. Using a software (EZ Chrome-ELITE) the area under the peaks at a specific wavelength can be integrated using the extinction coefficient to obtain the absolute amount of separated component in the analyte. In this study a reversed phase HPLC-column (MERCK LiChrosorb, RP-18) was used and the HPLC apparatus was from VWR (Elite LaChrome / Hitachi). The mobile phase solvents used were as follows:

Solvent (A): 80 % Methanol + 1mM Tris (pH 7.1)

Solvent (B): 60 % Methanol + 40 % Acetone

Solvent (C): 20 % Methanol

Solvent (D): 80 % Methanol.

The column was equilibrated with solvent A for at least 10 min before any run. Concentration of solvent A was set to 100% during the first 7 min and then reduced to 90% while simultaneously introducing 10% solvent B. Concentration of solvent B was increased to 100% in the following 10 min and kept constant for another 10 min after which solvent A was introduced again at 100% for the next 4 min. The column was washed with 100% solvent C and 100% solvent D for 15 min each after the run. For quantification in pmol/µl peak areas were multiplied with the following pigment specific calibration factors calculated at specific wavelengths (kindly estimated by K. Gundermann) 3.1126×10^{-5} (Chl a at 432 nm), 1.5084×10^{-5} (Chl c at 450 nm), 1.8701×10^{-5} (diadinoxanthin at 450 nm), 2.4696×10^{-5} (diatoxanthin at 445 nm), 2.3933×10^{-5} (fucoxanthin at 450 nm), 2.5102×10^{-5} (β-carotene at 450 nm).

3.4.2.1 Preparation of whole cells for HPLC

Cells in the early stationary phase were pelleted at 5000 rpm (Hereaus, Biofuge Primo R) and lyophilized (Alpha 1-4, LSC-Christ). They were then suspended in extraction solution (1:2 :: cell volume: extraction volume) composed of 90% methanol buffered with 1mM Tris-HCl (pH, 7.5), and disrupted mechanically in the presence of glass beads by a homogenization pistil followed by sonication (Elma) for 30 s. Cells were then allowed to stand on ice for 1 min. This process was repeated 10 times after which the cell extract was spun at 13,000 rpm for 15 min and the supernatant in which the pigments were extracted was applied to the reverse phase HPLC column.

3.4.2.2 Preparation of protein samples for HPLC

From 5 μl of sample (~ 0.3 μg Chl ml^{-1}) pigments were extracted in 45 μl chilled methanol by centrifugation at 13,000 rpm for 10 min and the supernatant was used for measurement.

3.4.3 Transmission Electron Microscopy (TEM)

For comparing the ultra structure of cells using transmission electron microscopy (TEM), a series of processes like embedding, sectioning and staining of cells had to be carried out before imaging with the electron microscope. These processes are described in these subsections.

3.4.3.1 Fixation

Cells in the early stationary phase were harvested in 50 ml sterile falcon tubes by gentle centrifugation (1000 *g*, 5 min at RT) and these were resuspended in ca. 40 ml of fixative solution (table 3) for about 1 hr. Fixation was allowed to take place by letting the lids of the falcon tubes slightly open under a fume hood for 1 hr. During this step the falcons were shaken occasionally to allow fixation of all cells evenly. Fixed cells were pelleted by spinning

3 Materials and Methods

----

at 1000 *g* for 5 min and were washed twice with 10 ml of wash buffer III (table 3). Washed cells were pelleted again for further treatment.

3.4.3.2   Osmation

Twice the amount of osmator (table 3) as the cell pellet (after fixation section 3.4.3.1) was taken and cells were allowed to stand in this solution for at least 3 hrs with occasional shaking under a fume hood. Osmated cells were washed twice with wash buffer III as during the fixation step.

3.4.3.3   Dehydration

Osmated cells were dehydrated using increasing concentrations of denatured ethanol (30%, 50%, 70%, 90% and 100%) followed by 100% pure ethanol. Each dehydration step was allowed to occur at least for 20 minutes. Dehydrated cells were transferred in Eppendorf cups and were then incubated overnight in a mixture of propylene oxide: embedding resin (1:1) letting the lid of the Eppendorf cup open. Embedding medium used here was low viscosity agar resin. Completely dehydrated cells were centrifuged to obtain a firm pellet and were allowed to mix evenly with 2-3 drops of embedding resin and then allowed to stand in a dessicator for 2 hrs with the lid of the Eppendorf open. Few drops of resin were added again to the eppendorf cup and desiccation was carried out like the previous step.

3.4.3.4   Embedding

Desiccated cells in resin were injected onto a rubber bed and allowed to harden at 60˚C for about 48 hrs. After hardening, cells embedded in resin were obtained which were ready for sectioning.

Table 3: Buffers and solutions used for embedding of *Phaeodactylum tricornutum* cells.

Solution	Component	Concentration
Fixative	Glutaraldehyde	2.5% in cell culture medium
Wash Buffer III (pH 7.2)	Sodium Cacodylate	0.05M
	Sucrose	0.4M
Osmator	Osmiumtetroxide	2%
Dehydrant	Ethanol	30%, 50%, 70%, 90% and absolute

3.4.3.5 Sectioning of cells using a microtome

Ultrathin sections were cut using a diamond knife (Diatome) in a microtome (Reichert Ultracut S, Leica). Sections which appeared silver-grey in colour corresponded to a thickness between 45-60 nm (table 4) and were chosen. These were collected onto copper grids coated with thin film made of pioloform.

Table 4: Estimation of the thickness of ultrathin sections depending on interference colours.

Interference colour	Thickness of section(nm)
Grey	< 60
Silver	60-90
Gold	90-150
Purple	150-190
Blue	190-240

The sections were double-contrasted with uranylacetate and lead citrate and made ready for viewing under the microscope. For this purpose, the grids with samples were fixed in a gridholder and incubated for 10 – 15 min in 7% uranylacetate solution. This grid holder was then dipped into 50% and then 25% methanol solutions followed by ddH$_2$O. Each wash

30

----

lasted about 2 min. Excess water was dried off by a filter paper. Contrast was achieved by incubating the gridblock in leadcitrate (Reynolds 1963) for 8 min. Excess lead citrate was washed off by rinsing the grid block two times in ddH_2O. Grids were allowed to dry at least 1 hour before viewing under the TEM (Philips CM-12).

Images of whole cells were taken using a Philips CM-12 electron microscope with a lanthanumhexaborate (LaB_6) filament at 80 kV and a magnification of 40,000*x with a CCD camera (Gatan Erlangshen ES5W).

3.5   Isolation of Thylakoid Membranes

Cells were harvested by centrifugation at 5000 rpm for 15 min (HiCen 21C, Herolab) from 10 day old bubbling cultures (early stationary phase, cell count: $\sim 35*10^6$ ml^{-1} and at a Chl *a* concentration of approximately 10 - 15 mg l^{-1}) within one hour after the onset of light. If thylakoid preparation was not undertaken immediately, the harvested cells were frozen and stored at -20˚C. Harvested cells were resuspended in homogenization buffer (table 5) and broken by 6 repeated French Press cycles (Polytec/Thermo) at a cell pressure of 20,000 i.e. gauge pressure 1,280 pounds per square inch (psi). The cell lysate was spun for 2 min; 3000 *g* at 4 ˚C (Biofuge primo R, Heraeus) to avoid contamination with unbroken cells. The pellet was resuspended in homogenization buffer and centrifuged again at 2 min; 3000 *g* at 4 ˚C. The supernatants from both centrifugation steps were collected and ultracentrifuged (Sorvall Discovery 90 SE ultra-centrifuge, rotor: T-865) for 40 min at 206,000 *g*. The pelleted thylakoid membranes were resuspended in washing buffer I (table 6) and ultracentrifuged (Sorvall Discovery 90 SE ultra-centrifuge, rotor: T-865) once again for 40 min at 163,000 *g*. The pellet of thylakoid membranes was resuspended in washing buffer I and the chlorophyll content was determined (Jeffrey and Humphrey 1975). Thylakoids were frozen in liquid nitrogen and stored at -20˚C in aliquots of 0.5mg Chl *a*.

<div align="center">**Table 5: Composition of Homogenization Buffer, pH 7.4**</div>

HEPES	10 mM
KCl	2 mM
EDTA	5 mM
After adjustment of pH,	
Sorbitol	1M

<div align="center">**Table 6: Composition of Wash Buffer I, pH 7.4**</div>

HEPES	10 mM
KCl	2 mM

3.6   Chlorophyll determination

For estimating the chlorophyll content of whole cells, cells were broken as mentioned in (section 3.4.2.1) and pigments were extracted in 1ml of 90% acetone by centrifuging the samples for 10 min at 13,000 rpm. The chlorophyll content of protein samples was determined by extracting pigments using 90 % acetone in a dilution of 1:1000. Subsequently the samples were spun in a pre-cooled tabletop centrifuge at 13,000 rpm for 5 min and the supernatant was measured against 90 % acetone as reference. Concentrations of Chl *a* and Chl *c* were calculated with the following equations as described by (Jeffrey and Humphrey 1975).

Chl *a* [mg/l] = 11.47 x $(E_{664}-E_{750})$ − 0.40 x $(E_{630}-E_{750})$

Chl *c* [mg/l] = 24.34 x $(E_{630}-E_{750})$ − 3.73 x $(E_{664}-E_{750})$

3.7 Isolation and purification of protein complexes

3.7.1 Sucrose Density Gradient Ultracentrifugation:

Various types of sucrose density gradients differing in solubilisation conditions and gradient layers will be mentioned in further sections. These types are summarized here in a tabular form.

Table 7: Concentration of detergent used for solubilisation and types of sucrose density gradients used in this study.

Gradient type	Solubilisation	Det:Chl *a*	Gradient steps % sucrose in Wash Buffer I[1]
I	ß-DDM, 15 mM	30:1	5,7.5,10, 12.5, 15, 17.5, 25
II	ß-DDM, 15 mM	20:1	5, 10, 12.5, 15, 25
III	ß-DDM, 10 mM	17.5:1	5, 10, 12.5, 15, 25

3.7.1.1 Sucrose Density gradient Type I: for purification of FcpA$_{His}$ and WT Fcp pool

Thylakoids were solubilised with 15mM β-dodecyl maltoside (β-DDM) for 20 min under constant shaking on ice in wash buffer I. The solubilised membranes were separated from unsolubilised material by centrifugation in a table top centrifuge for 5 min at 13,000 rpm and the supernatant was loaded onto a discontinuous sucrose density gradient and ultracentrifuged at 141,000 g (Rotor: Beckmann SW28) for 22 hours at 4˚C. The sucrose gradient consisted of steps of sucrose solutions made in washing buffer I supplemented with 0.03% β-DDM (table 6). The brown fraction localized between 10% and 12.5% sucrose was presumably Fcp pool owing to the absorption by the carotenoid fucoxanthin. This band was harvested carefully to avoid any contamination with the green photosystems fraction which was localized at the interface of the 15% sucrose and 17.5% sucrose density bands. The green fraction was

---

[1] Wash buffer I was supplemented with 0.03% DDM

discarded. Fcp fractions were then concentrated in concentration devices with 30 kDa cutoff (Amicon) and were frozen under liquid nitrogen and stored at -80˚C until further purification.

3.7.1.2 Sucrose Density Gradient Ultracentrifugation type II and type III: for purification of supercomplexes

Thylakoids were solubilised either with 15mM β-DDM (Det: Chl *a* :: 20) or 10mM β-DDM (Det: Chl *a* ::17.5) for 20 min in wash buffer I under constant shaking on ice. Solubilised membranes were centrifuged in a table top centrifuge at 4˚C for 5 min at 13,000 rpm and the supernatant was loaded on a discontinuous gradient (table 7). Ultracentrifugation was carried out for 20 hours at 27,000 rpm in Beckmann Rotor SW-28 or Thermo rotor AH-629. Green fractions were harvested carefully with a syringe. These fractions were then concentrated in Amicon concentration devices with 10 kDa cutoff and the chlorophyll content of the fractions was estimated. These were then loaded on an anion exchange column to allow separation between photosystems, supercomplexes and free light harvesting complexes.

3.7.2 Ion Exchange

Veith and Büchel (2007) developed a protocol in case of *P. tricornutum* to separate free Fcps, PSI and PSII from one another. One of the important goals of the present study was to investigate if the light harvesting antenna protein FcpA in *P. tricornutum* is specifically bound to PSI or PSII. The protocol established previously (Veith and Büchel 2007) was modified here slightly to obtain a highly pure and intact PSI-Fcp and PSII-Fcp complex. An XK 16 column (Amersham Biosciences) was self-packed with ~22 ml of DEAE (Toyopearl 650D, TOSOH) connected to an Äkta Purifier P-900 (Amersham Bioscience). The resin was pre-equilibrated with 5 column volumes of buffer B1a (table 8). The concentrated green photosystem(s) fractions that were obtained using sucrose density gradient type II or III (section 3.7.1.2) were adjusted with B1a buffer to 2 ml end volume (~ 300 µg Chl *a* in total)

----

then applied to the column using a super loop. A flat salt gradient was used to elute PS supercomplexes and free light harvesting proteins. The harvested fractions were immediately analyzed spectroscopically and then concentrated and stored at -80˚C for further investigations.

3.7.3   Gel filtration

Analytical and preparative gel filtration was carried out to determine the oligomeric status of the purified proteins and/or to post-purify the proteins (if needed) respectively.

Samples were applied to a self-packed analytical gel filtration column (Superdex 200, GE Healthcare) or to a self-packed preparative gel filtration column (HW-55F Toyopearl, TOSOH) connected to an ÄKTA purifier P-900 (Amersham Biosciences). Every time the column was equilibrated with at least 4 CV of B1 buffer and 2 CV of B1a buffer. Flow-rate was maintained at 0.5 ml min^{-1} during the run and absorbance of the eluates was analyzed at 437 nm, 280 nm and 675 nm. The columns were calibrated with FCPa and FCPb complexes from *C.meneghiniana* (courtesy: K. Gundermann, University of Frankfurt) since their oligomeric status and molecular weights were previously established allowing their use as molecular weight markers (Büchel 2003; Beer et al. 2006). The major peak fractions were collected and concentrated in concentration devices. Fractions were analyzed by spectroscopy and then frozen in liquid nitrogen and stored at -80˚ C until further use.

Table 8: Composition of buffer B1, pH7.4

Tris-HCl	25 mM
KCl	2 mM

Table 9: Composition of buffer B1a, pH 7.4

Tris-HCl	25 mM
KCl	15 mM
ß-DDM	0.6 mM

Table 10: Composition of buffer B1a with NaCl, pH 7.4

Tris-HCl	25 mM
KCl	15 mM
NaCl	750 mM
ß-DDM	0.6 mM

3.7.4   Immobilized Metal Affinity Chromatography (IMAC)

3.7.4.1   Column packing

A simple laboratory glass column was filled with 5 ml of slurry of Chelating Sepharose Fast Flow material (Amersham, GE Healthcare).The column was then washed with double distilled water until traces of 20% ethanol were completely removed. For Ni^{+2} loading onto the chelating sepharose, an equal column volume of 0.2 M $NiCl_2$ was used. Ni^{+2} ions which were not bound to the sepharose were washed away using 1 column volume of acidic buffer (table 11) and at least 5 column volumes of double distilled water to remove acidic contents on the column. The resin was pre-equilibrated with regeneration buffer (table 12) to activate the Ni^{+2}. Column equilibration was done with binding buffer (table 13). This material was then ready for use to purify His tagged protein and could be used 5-6 times before the material had to be freshly loaded with nickel.

3.7.4.2 Purification of His-tagged FcpA

In case of the mutant, the concentrated Fcp band from the sucrose density gradient type I was applied to a self-packed Nickel- Nitrilo Triacetate resin (Ni-NTA) column pre-equilibrated with binding buffer and allowed to incubate for 1 hour at 4˚C. The column was washed with washing buffer II (table 14) at 0.5 ml min^{-1} flow-rate until the absorbance at 672 nm was less than 0.005 absorbance units. His-tagged FcpA was subsequently eluted using elution buffer (table 15) in 0.5ml aliquots, which were concentrated using 30 kDa cutoff microcon concentration devices (Amicon).

Table 11: Composition of acidic buffer used for IMAC, pH 4.0

NaCl	1 M
Sodium-acetate	0.02 M

Table 12: Composition of regeneration buffer for IMAC

Guanidine-HCl	6 M
Sodium-acetate	0.2 M

Table 13: Composition of binding buffer used in IMAC, pH 7.4

Phosphate buffer	25 mM
KCl	150 mM
Imidazole	5 mM
ß-DDM	0.6 mM

Table 14: Composition of washing buffer II used in IMAC, pH 7.4

Phosphate buffer	25 mM
KCl	50 mM
ß-DDM	0.6 mM

Table 15: Composition of elution buffer used in IMAC, pH 7.4

Phosphate buffer	25 mM
KCl	15 mM
Imidazole	400 mM
ß-DDM	0.6 mM

3.8 Sodium dodecyl sulfate-polyacrylamide gel electrophoresis (SDS-PAGE)

3.8.1 Tris-Tricine gels

TrisTricine gels were cast according to Schaegger and van Jagow using 1 mm Biometra-Minigel set-up (Biometra) (Schaegger and von Jagow 1987). Samples were directly denatured in 1/4 volume Rotiload (Roth) compared to sample volume for 15-20 min at room temperature (RT). Current was set to 15 mA in the stacking gel and 30 mA in the separating gel.

Table 16: Components for casting 2 mini gels.

Chemical component	Separating gel (15%)	Stacking gel (4%)
Urea	5.4 g	-
3X Gel Buffer	5 ml	2.5 ml
Acrylamide	5.78 ml	0.77 ml
Bisacrylamide	0.51 ml	52.25µl
Fill with ddH$_2$O to	15 ml	7.5 ml
10% APS(fresh)	45 µl	75 µl
TEMED	4.5 µl	7.5 µl

Table 17: Composition of the 3X gel buffer used in Tris-Tricine gels

Tris	3M
SDS	0.3% (w/v)

Table 18: Composition of the cathode buffer used for running gel electrophoresis

Tris	0.1M
Tricine	0.1M
SDS	0.1% (w/v)

Table 19: Composition of the anode buffer used for running gel electrophoresis

Tris	0.2M

3.8.2 Gels using PDA as cross linker

To achieve a higher degree of resolution in the low molecular weight range, another gel system was adopted which utilized piperzinediacrylamide (PDA) as the crosslinker instead of bisacrylamide.

Table 20: AA-PDA solution

PDA	0.2g
30%Acrylamide	25 ml

Table 21: Components for casting 2 mini PDA gels.

Chemical component	Separating gel (12.5%)	Stacking gel (4%)
ddH$_2$O	9.9 ml	6.8 ml
AA-PDA solution	8.3 ml	1.7 ml
1.5 M Tris-HCl (pH 8.8)	6.3 ml	-
1.5 M Tris-HCl (pH 6.8)	-	1.25 ml
10% SDS	0.25 ml	0.1 ml
TEMED	10 µl	10 µl
Mix well and then add TEMED	250 µl	100 µl

As molecular weight (MW) markers either the Roti-Mark Prestained (Roth) or a self-made prestained molecular weight marker (Dr. M. Schmidt, University of Frankfurt) were used.

40

3 Materials and Methods

Table 22: Molecular weight protein markers Roti-Mark Prestained (Roth) and a self-made prestained protein standard.

Prestained marker SM0441 (Roth)		Home-made marker	
Protein	MW (kDa)	Protein	MW (kDa)
ß-galactosidase	112.7	BSA	69
BSA	74.5	Ovalbumin	45
Ovalbumin	53.2	Carbonic anhydrase	30
Carbonic anhydrase	32.3	Trypsin inhibitor	20
ß-Lactoglobulin	21.5	Lysozyme	14
Lysozyme	9	Aprotinin	6

3.8.3   Coomassie staining

Gels were incubated at least 12 hrs in staining solution containing 0.25 % Coomassie Blue G (Serva) 10 % acetic acid. De-staining was performed in 10 % acetic acid for several hours until band patterns with sufficient resolution were obtained.

3.8.4   Silver staining

Protocols used for silver staining of gels are summarized in a tabular form below. It must be noted that the modified protocol of Heukeshoven and Dernick (1988) which utilizes formaldehyde as cross linker is used when the bands from a silver stained gel are used for mass spectrometric analyses due to the reason that formaldehyde is a weaker cross linker than glutaraldehyde and this allows easier elution of bands from gel .

Table 23: Composition of buffers used for silver staining.

Silverstaining (Heukeshoven and Dernick, 1988)			Silver staining followed by Mass Spectrometry		
Solution	Component	Duration	Solution	Component	Duration
Fixing	30% EtOH 10% Acetic acid	30 min to O/N	Fixing	40% EtOH, 10% Acetic acid	30 min
Incubation	0.5M Na-acetate 8mM Sodiumthiosulfate 30%EtOH 0.5%Glutaraldehyde	1 hour to O/N	Incubation	30% EtOH, 0.2% Sodiumthiosulfate 0.5M Sodium acetate	30 min to O/N
Washing	ddH$_2$O	3* 5min	Washing	ddH$_2$O	3* 5min
Silvering	0.2% Silvernitrate 0.02% Formaldehyde	20 min	Silvering	0.1% Silvernitrate 0.02% Formaldehylde	40 min
Development	2.5% Sodiumcarbonate 0.02% Formaldehyde	As needed	Development	2.5% Sodiumcarbonate 0.01% Formaldehyde	As needed
Stopping	1% Glycine	5 min	Stopping	0.05M Na$_2$EDTA	5 min
Washing	ddH$_2$O		Washing	ddH$_2$O	

3.9 Protein transfer & Immunodetection

3.9.1 Western Blot

Unstained gels were incubated in cathode buffer I (table 26) for 15 min. Six pieces of 3mm chromatographic Whatman filter papers (Schleicher and Schüll) and a PVDF membrane (Roth) with a similar size as the gel were prepared. Two filter papers were equilibrated in anode buffer I (table 24) and layered below one filter paper equilibrated in anode buffer II (table 25). The PVDF membrane (Roth) was activated in methanol for 10 s, transferred to distilled water for 2 min and then incubated in anode buffer II shortly. The gel was layered on

42

top of the PVDF membrane and three filter papers equilibrated in cathode buffer I were arranged on top of this arrangement. Transfer was carried out for 1 hr at 1.5 mA cm^{-2} in a semi-dry transfer cell (Bio-Rad Trans-blot SD).
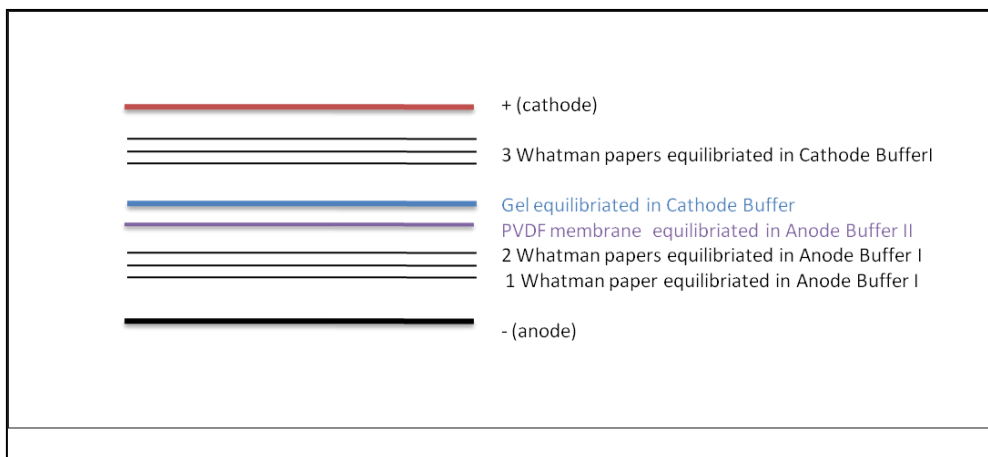
Figure 12: Scheme of assembly on western blotting apparatus

Table 24: Composition of anode buffer I, pH 10.4

Tris-HCl	0.3M
Methanol	10%

Table 25: Composition of anode buffer II, pH 10.1

Tris-HCl	25 mM
Methanol	10%

Table 26: Composition of cathode buffer I, pH 9.0

Tris-HCl	25 mM
Glycine	40 mM
Methanol	10%

3.9.2   Immunodetection

After proteins were transferred onto PVDF, the membranes were incubated on a shaker for 1 hr at room temperature or up to several hours at 4°C in blocking solution consisting of 5 % milk powder in PBS. After incubation with the first antibody solution (table 29) the membrane was washed thrice for 5 min in PBST (table 27) and then incubated in the secondary antibody solution. The membrane was then washed off of excess antibody by washing thrice for 5 min in PBST. For visualization of signals the membrane was incubated for 1 min in 20 ml of ECL solutions (table 28). The peroxidase induced luminescence was detected using an x-ray film (Amersham Hyperfilm ECL, GE Healthcare) in a dark chamber. Exposition time varied in between several seconds and to 5 min depending on quality of the antibodies and quantity of the protein samples. X-ray films were treated in developing (Roentgen, Tetenal) and fixing solution (Adefofix, Adefo) according to the manufacturer's instructions and the reaction was stopped using 2% acetic acid.

Table 27: Composition of PBS

NaCl	137 mM
KCl	2.7 mM
Na2HPO4	4.3 mM
KH2PO4	1.4 mM
PBS in Tween (PBST)= PBS + 0.1% Tween-20	

Table 28: Composition and usage of ECL solutions for detecting protein-HRP coupled antibody reaction.

Enhanced Chemiluminescence (ECL) Solutions		Amount in a 20 ml reaction tube
Luminol in DMSO	250 mM	200 µl
p-Coumaric acid	90 mM	89 µl
Tris-HCl (pH 8.5)	1M	2 ml
Volume was made up to 20 ml with ddH$_2$0		
H$_2$O$_2$	1.4 mM	6.1 µl

Table 29: Specifications of antibodies used in this study.

Antibody	Directed against	Dilution	Diluted in	Incubation (min)	Source
α-cm-Fcp	All Fcp polypeptides of *C.meneghiniana*	1:5000	PBS	60	AK Büchel, Frankfurt
α-cc-Fcp	All Fcp polypeptides *C. cryptica*	1:1000	PBS	60	E. Rhiel, Oldenburg
α-Hisα-HRP monoclonal	6x Histidine residues as epitope	1:2000	PBST+5% milk powder	60	Sigma
α-D2	Higher plant PSII RC protein PsbB	1:2000	PBS	60	B. Godde, Bochum
α-CP1	Higher plant PSI RC protein PsaA and PsaB	1:1000	PBS	60	J.Feierabend, Frankfurt
HRP-Goat-α-rabbit	HRP conjugated 2° Antibody	1:10000	PBS	45	Calbiochem

----

3.10 Spectroscopy

3.10.1 Absorbance spectra

Absorbance spectra were recorded with a spectrophotometer (Jasco V550) using a band pass of 1 nm and 1 cm optical path length at room temperature. Samples were adjusted to an absorbance of ~0.03 at the Qy band of Chl *a*, which corresponded to a Chl *a* concentration of ~0.3 µg ml^{-1}.

3.10.2 Fluorescence spectra

Fluorescence spectra were recorded at room temperature in a fluorescence spectrometer (Jasco FP6500) with a band pass of 3 nm both on the excitation and emission side and at 0.1 nm or 0.5 nm data pitch. Emission spectra were recorded between 600 nm to 800 nm when the samples were illuminated at λex = 465 nm, λex = 440 nm and λex = 530 nm to preferentially excite Chl *c*, Chl *a* and Fx, respectively. Excitation spectra were recorded at λem = 675 nm upon excitation from λex = 400 nm to 600 nm. A rhodamine-B spectrum was used as a reference for the correction at the excitation side and the photomultiplier was corrected using a calibrated lamp spectrum.

3.10.3 Circular dichroism (CD) spectra

CD spectra were measured at room temperature using 1 cm optical path length, 2 nm bandwidth and a 2 s response time in the range of 370 nm to 750 nm in a CD spectrometer (Jasco 810). Concentration of the samples was adjusted to ~ 5 µg ml^{-1} of Chl *a*. Five spectra were recorded sequentially in each case to improve the signal-to-noise ratio.

3.11 Mass Spectrometry:

This work was carried out in collaboration with Prof. Dr. M. Mittag at the University of Jena. The band of interest was cut out from a silver stained gel. A tryptic digest and nano LC-ESI-

----

MS/MS analysis of the peptides were carried out according to (Veith et al. 2009) without changes.

3.12 Structural characterization of the FcpA$_{His}$ complex: 2D crystallization

Membrane proteins can be isolated in the native state by solubilizing the membrane using suitable detergents. Above the critical micellar concentration (cmc), the detergent spontaneously forms micellar structures where the hydrophobic chains point inwards towards the interior and the hydrophilic groups are in contact with solution. In case the solution contains both lipids and detergent the hydrophobic areas of lipids and membrane proteins are embedded and stabilized in the hydrophobic interiors of detergent micelles. The detergent which is not the natural part of a thylakoid membrane can be removed either by dialysis or by adsorption using bio-beads. Upon detergent removal the lipids try to assemble into bilayers in the form of vesicles, sheets or tubes. Membrane proteins try to insert into the bilayer and stabilize themselves by shielding off from solution or aggregate due to hydrophobic forces of interaction. The formation of micellar structures as well as of ordered structures like bilayers, vesicles, etc. is driven by a net gain in entropy due to which assemblies of membrane proteins and lipids form readily and remain as such quite stable. Mobility of lipids and proteins in such assemblies is restricted only in 2D directions and specific contacts between protein-proteins and protein-lipids cause the protein to arrange itself in an ordered manner in 2 dimensional space (Kühlbrandt 1992).
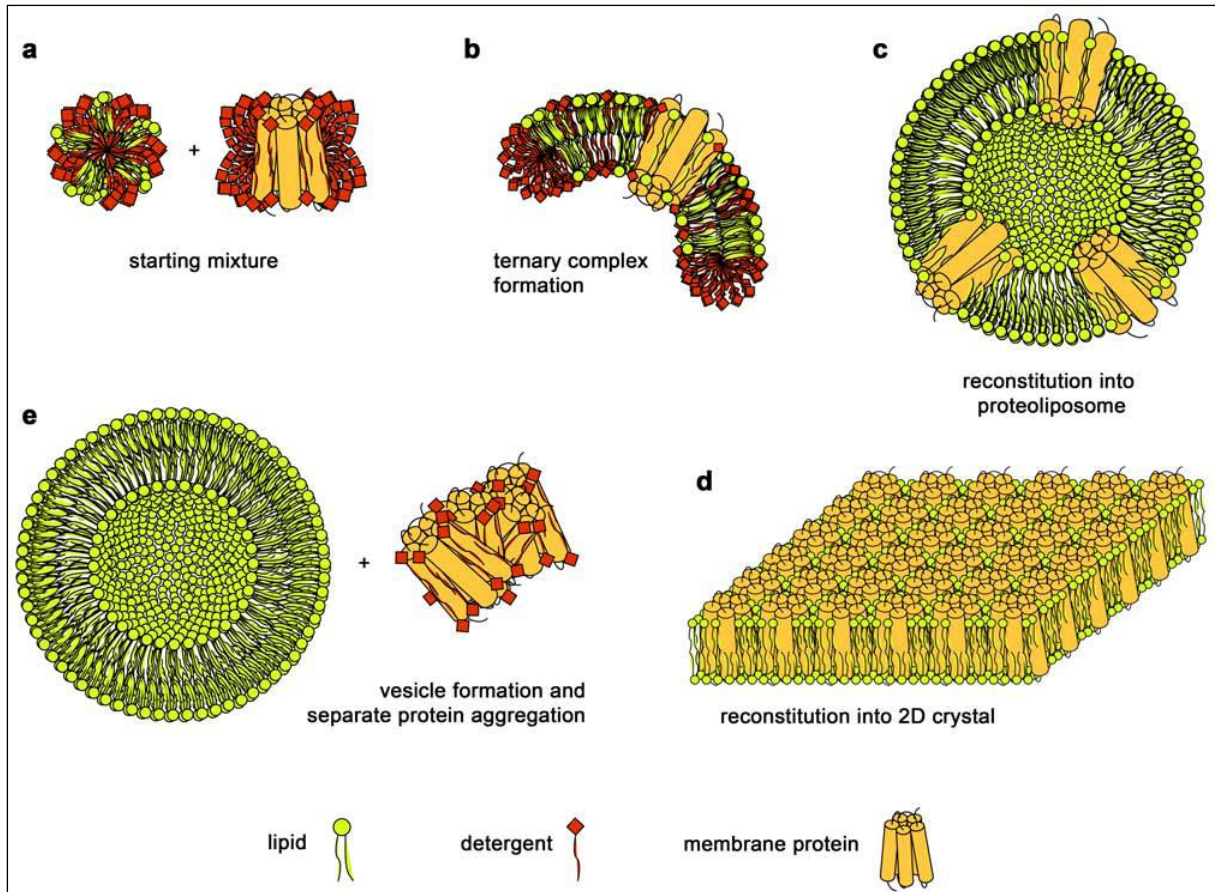
Figure 13: Two-dimensional crystallization and reconstitution into proteoliposomes of membrane proteins. a; Components of the starting mixture for detergent mediated reconstitution, b; ideally, ternary micelles are formed upon equilibration in the starting mixture. After subsequent detergent removal different structures in the assay mixture are formed, c; at a higher lipid-to-protein ratio (LPR) the membrane protein is reconstituted into proteoliposomes, d; at a sufficiently low LPR 2D crystals can assemble, e; in unfavorable circumstances the ternary micelles do not form or vesicle formation and protein aggregation occur temporally separated at different concentrations of the free detergent. Image taken from Kaufmann T (2006).

When a suitable condition concerning the right lipid, the ambient lipid to protein ratio (LPR),

salt and precipitant is reached, 2D crystals are formed which can assume several shapes as

shown in figure 14.
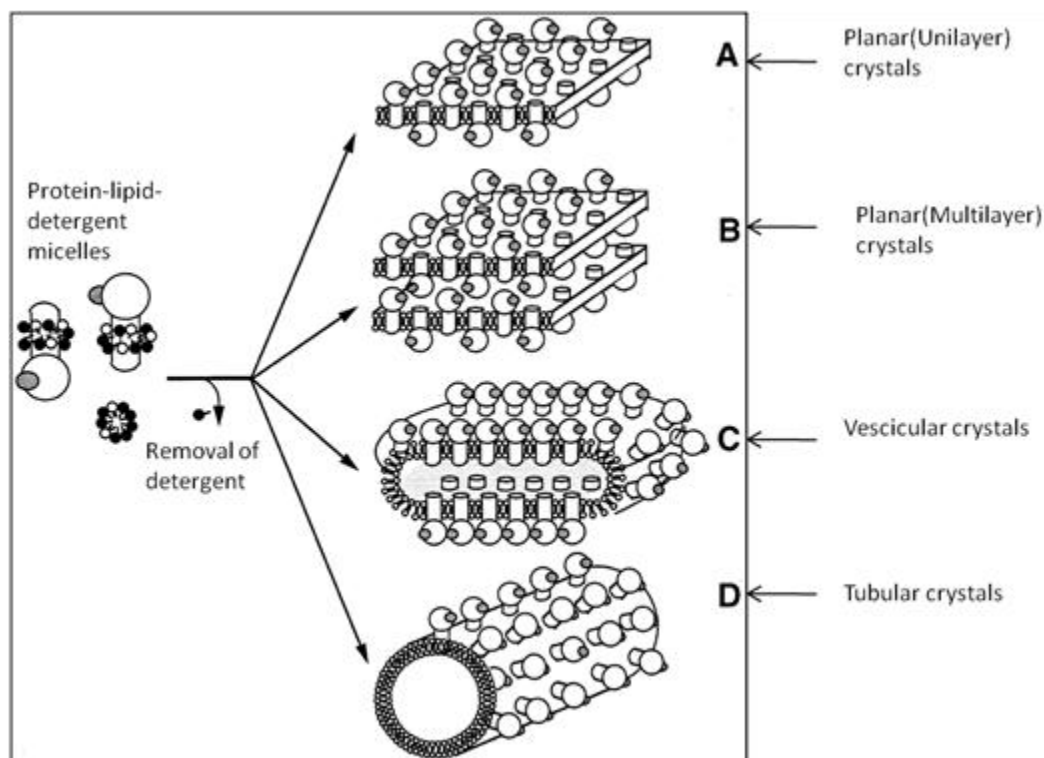
Figure 14: The several shapes in which 2D crystals can be formed after detergent removal. Image adapted from Rigaud et al. (2000).

FcpA$_{His}$ was purified via Ni-NTA (section 3.7.4.2) and concentrated to 0.078 mg Chl a ml^{-1} (i.e. ~ 0.34 mg protein ml^{-1} if it is assumed that 5 Chl molecules are bound on each polypeptide backbone and that the estimated molecular weight of FcpA$_{His}$ is 18.9kDa [Calculated according to the PhD thesis of Anja Beer 2010, University of Frankfurt]. After concentration the protein was stored in aliquots of 50 µl at -80°C and used as desired. Repeated freeze-thaw cycles of the same aliquot of purified protein were avoided. Various combinations of lipids like MGDG, DGDG, MGDG and PC (Larodan Fine Chemicals, Sweden) and salts like KCl, NaCl, MgCl$_2$, LiCl$_2$, KAc, AlCl$_3$, ZnCl$_2$, CaCl$_2$ and CuCl$_2$ were used in different LPRs. The starting conditions for crystallization of FCPa from *C.meneghiniana* were used as a reference for setting up initial trials in this study (Beer A 2010). Dialysis buttons (Hampton Research, USA) with 15µl volume were used for the purpose of detergent removal. Protein, lipid, salts and buffer were mixed in an Eppendorf cup to achieve desired LPRs and salt concentrations. These mixtures were subjected to 3x freeze-

----

thaw cycles of liquid N_2 and room temperature and then inserted in the dialysis button. A

dialysis membrane (VWR) with 14kDa cutoff was activated by immersing in boiling water

for 15 min and then applied onto the button and fixed with an O-ring with utmost care to

avoid air bubbles getting trapped between sample and membrane.
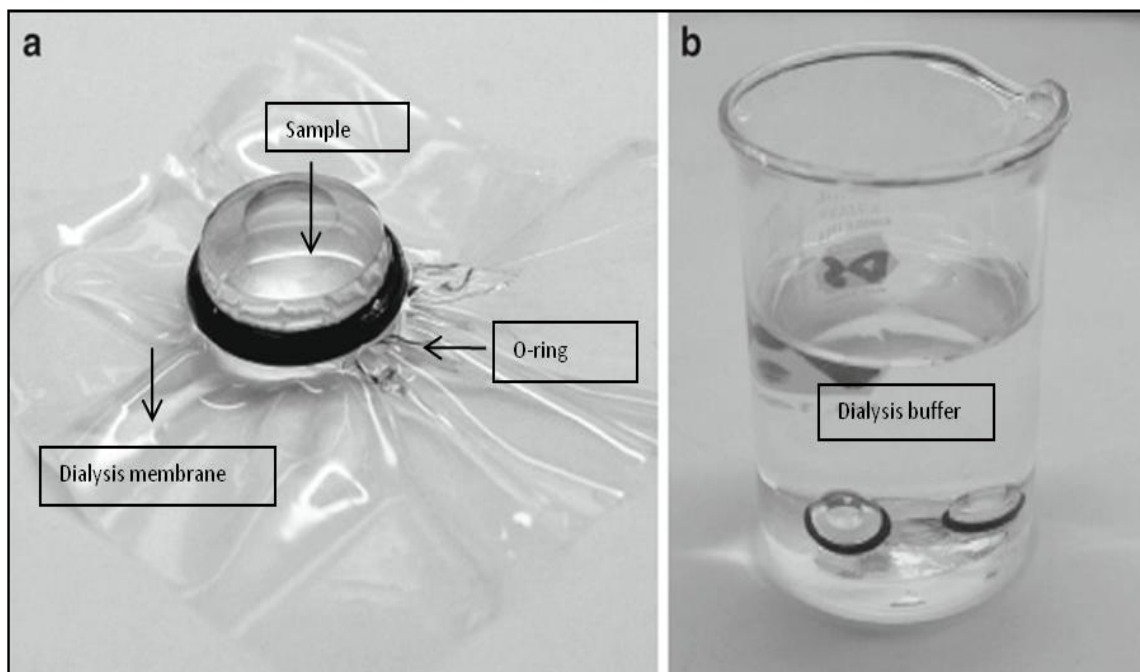
Figure 15: Representative assembly of dialysis buttons used for removal of detergent from lipid-protein-detergent mix. A; dialysis button with membrane, B; dialysis buttons immersed in the dialysis buffer. Adapted from Lacapere J J (2010).

3.12.1 Preparation of samples for screening of crystals using electron microscope

A freshly cleaved piece of mica (Plano, Wetzlar) was placed on filter paper in a glass Petri

dish and set into the vacuum cell of the carbon coater 208 (Cressington). To coat with carbon

two pulses of 4 V for 5 s each were applied after the vacuum reached a pressure of at least 5 x

10^{-5} mbar. The coated mica was dried for at least 1 day and then used to apply the carbon film

to new copper mesh grids (Agar Scientific 400 square mesh, copper 3.05 mm). The grids

were placed onto a flat holder lying below the surface of distilled water in a small self-made

50 ml tank. The mica was carefully pushed under water so that the carbon film floated on the

surface. By releasing the water in the tank using the attached syringe, the carbon was settled

----

flat on the grids. The plain carbon grids were removed from the holder, dried and stored. To make the carbon grids hydrophilic they were glow discharged (Cressington power unit 208) by applying an electric field for 7 s. with a current of 5 mA using a vacuum with a pressure of approximately 0.02 mbar.

Samples were removed from the dialysis button using a pipette tip by gently piercing a hole in the dialysis membrane attached to the button. This sample was allowed to rest at 20˚C for 1 day and characteristics like colour and clarity of the sample were noted. 4 µl of sample was placed on a recently prepared grid. After 45 s incubation, specimen was negatively stained for 45 s with filtered 2 % uranyl acetate (Plano). Images were taken in the low-dose mode at 120kV acceleration as described in section 3.4.3.5.

4   Results

4.1   Comparison of wildtype and mutant

Sections under 4.1 deal with the comparison of the cultures of the WT and the mutant based on parameters of growth, pigment content and ultra structure.

4.1.1   Growth curve

Cells were maintained as stocks in flasks on shakers and cultivated in large scales for protein purification by bubbling sterile air. By plotting growth curves the effect of cultivation of cells by shaking or by bubbling sterile air on cell numbers were analyzed and a point suitable for harvesting of cells was determined. In both cases the starting number of cells was 1 million ml^{-1}.
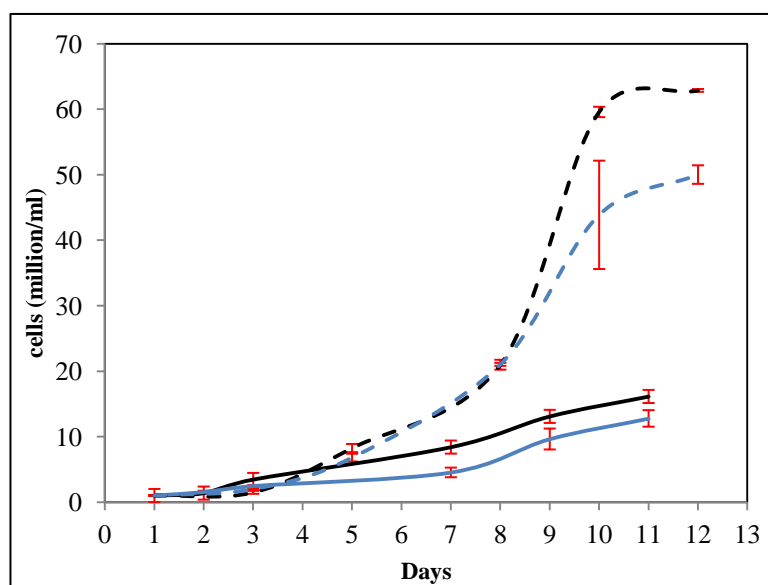
Figure 16: Growth curves of cultures under different growth conditions. WT cells grown by shaking (solid black line) or by bubbling (dashed black line) and mutant cells grown by shaking (solid blue line) and bubbling sterile air (dashed blue line). 3 independent cultures were analyzed in case of shaking cultures and 2 independent in case of bubbling cultures with sterile air and the values plotted are means and standard deviations of these values.

Table 30: Number of cells (million/ml) during various growth phases.

	WT (shaking)	**WT (bubbling)**	**Mutant (shaking)**	**Mutant (bubbling)**
Lag (7th day)	8.39±0.72	8.24±0.62	4.52±0.0.73	6.78±0.58
Log (9th day)	13.08±0.64	20.96±0.75	9.62±0.1.59	21.02±.22
Stationary (11th day)	16.12±0.2.46	59.56±0.79	12.76±0.1.26	43.85±8.27

The growth curves of both cultures grown either by shaking or bubbling sterile air showed a typical sigmoidal curve with a long lag phase until 6 days. The logarithmic phase lasted from the 7th until the 10th day after which the stationary phase started. Cells were counted for at least 30 days and in this time no death phase was observed (not shown). When cultures were grown on shakers the cell number multiplied by 16 times in case of WT and approximately 13 times for the mutant (table 30). When cultures were bubbled with air to create a better gaseous exchange the cell number multiplied by 60 times in case of WT and 43 times in case of the mutant (table 30) compared to the starting number of cells. Thus an active gas exchange led to a larger cell number and biomass in the same amount of days as compared to simple shaking cultivation without gas exchange. The mutant culture grew slightly slower than the WT under both culture conditions.

4.1.2   Colour of cultures
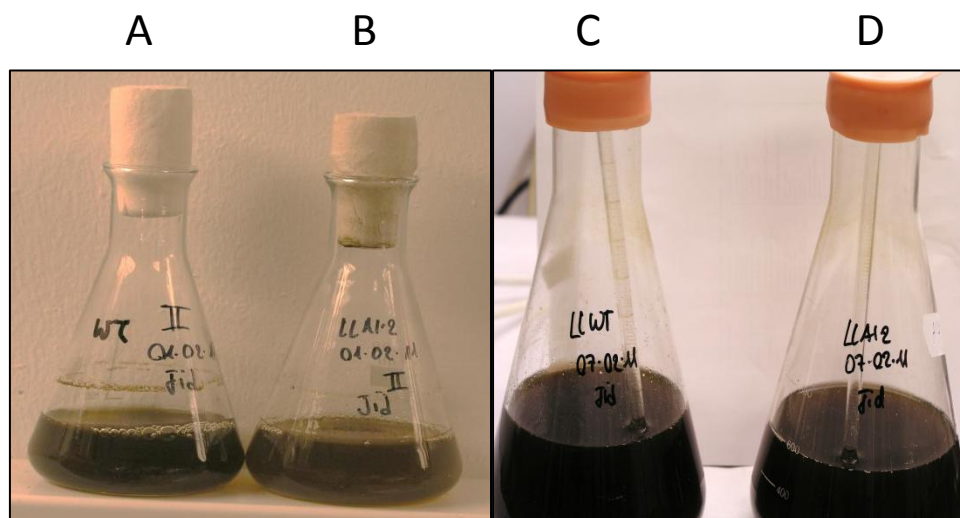
Figure 17: Colour of cultures after growth period of 10 days. A; WT shaking culture, B; mutant shaking culture, C; WT bubbling culture and D; mutant bubbling culture.

After 10 days the cultures grown using shaking cultures appeared pale brown in colour (figure 17A and B) whereas those after bubbling sterile air were dark brown to almost black in colour (figure 17C and D) and thick in consistency in spite of being inoculated with the same number of cells.

4.1.3   Chlorophyll concentration of whole cells

Table 31: Total chlorophyll concentration in cells at the end of the growth period (10 days). Values are means and standard deviations of 3 independent measurements.

Culture	Chl ($a+c$) µg/ml
WT (shaking)	9.3 ± 0.21
Mutant (shaking)	8.98 ± 0.78
WT (bubbling)	15.03 ± 1.13
Mutant (bubbling)	13.78 ± 0.64

It was clearly observed that cultures grown by bubbling sterile air had more Chl *a* content than the cultures that were grown without bubbling air on simple shakers. The amount of Chl *a* was comparable in both cultures when cultivated in the same manner.

It was clear from the growth curve and chlorophyll content calculations that cells grew very rapidly when gas exchange at the cell interface was provided by bubbling air. This method of cultivation of cells was therefore adopted during the further course of this study to obtain higher biomass.

4.1.4   Ultra structure of cells and chloroplasts
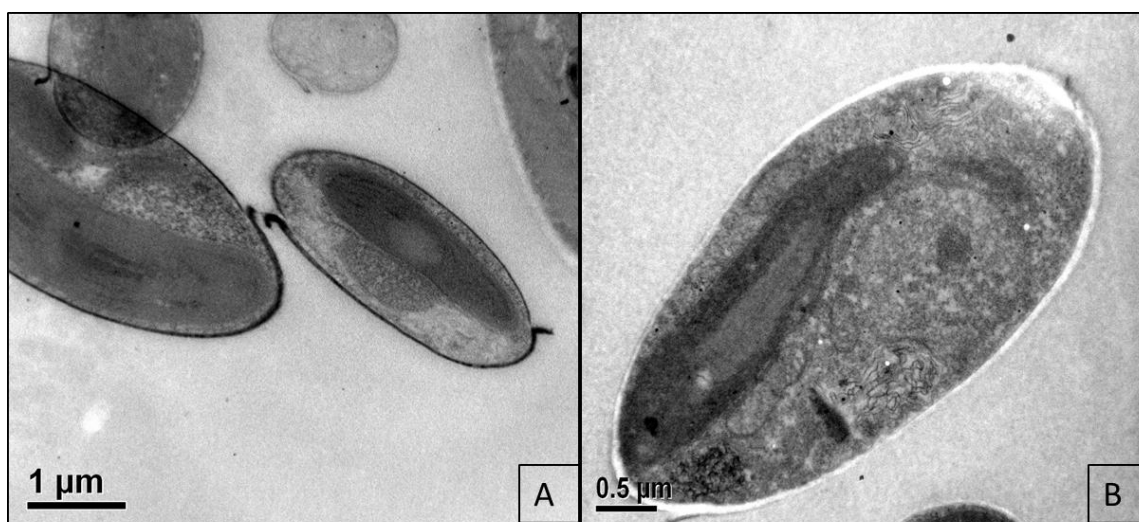
Figure 18: Ultra structure of whole cells of *P. tricornutum*. A; WT UTEX 646, B; Mutant FcpA1.2

Under a light microscope both cultures showed fusiform cells with no visible differences in overall shape. To gain a clearer image, ultrathin sections of cells were analyzed using TEM. The cells measured approximately 5 µm length and 2 µm in breadth in both WT and mutant. Both showed only 1 large chloroplast as reported by (Lavaud J 2007). Contrary to the reports of the reduction of silica cell wall in *P. tricornutum* (Lewin et al. 1958, Borowitzka and

Volcani 1978) the frustule retained a very clear Petri dish like shape in the cultures in spite of being grown in silica free medium.

The ultra structure of thylakoids was analyzed at a higher magnification to investigate the typical band structure of the thylakoid membranes and any structural effects due to the presence of His tagged Fcp.
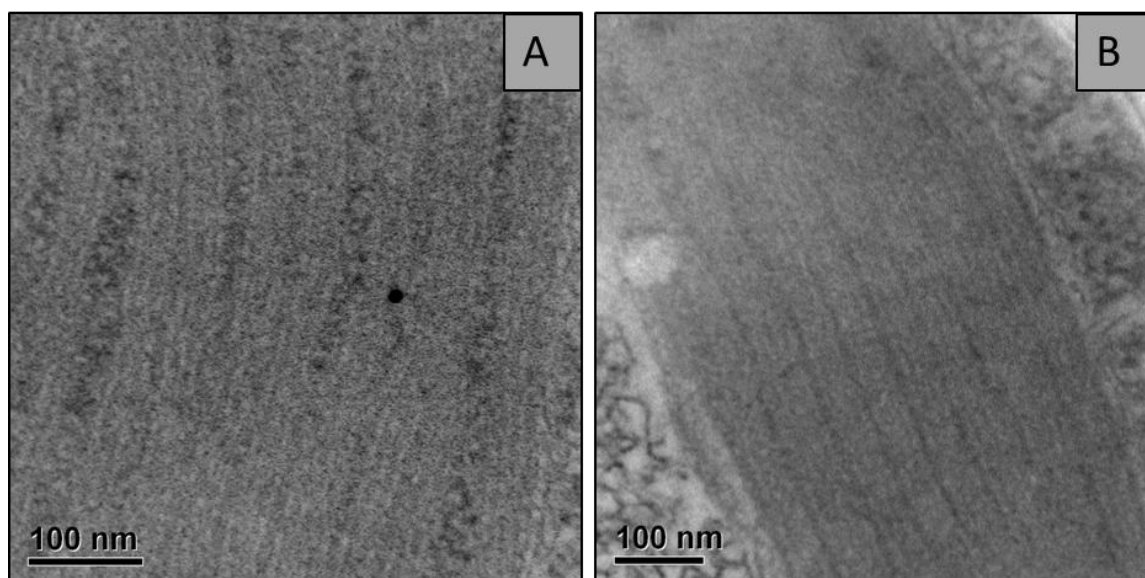
Figure 19: Ultra structure of the thylakoid membranes. A; WT UTEX 646, B; Mutant FcpA1.2

The ultra structure of thylakoids showed a typical three parallel band pattern for the thylakoid membranes of both cultures. The size of the bands was comparable in both cultures and there were no visible differences either in shape, size or organization of the thylakoids.

4.1.5 Pigment stoichiometries in whole cells and thylakoids

Pigment content was investigated in whole cells and in thylakoids to investigate effects of different culture conditions.

Table 32: Stoichiometries of pigments in whole cells harvested after bubbling with sterile air for 10 days and thylakoids prepared from these cells. The values depict means of at least 3 independent preparations and their standard deviations.

Mol/mol Chl *a*	Fx	Chl *c*	Ddx+Dtx	ß-carotene
WT cells	0.781±0.136	0.219±0.013	0.124±0.021	0.036±0.020
Mutant cells	0.806±0.052	0.231±0.030	0.120±0.008	0.033±0.026
WT thylakoids	1.369±0.184	0.362±0.053	0.167±0.033	0.017±0.007
Mutant thylakoids	1.457±0.186	0.389±0.044	0.238±0.138	0.0088

The pigment stoichiometries described in table 32 are graphically depicted below for better comparison.
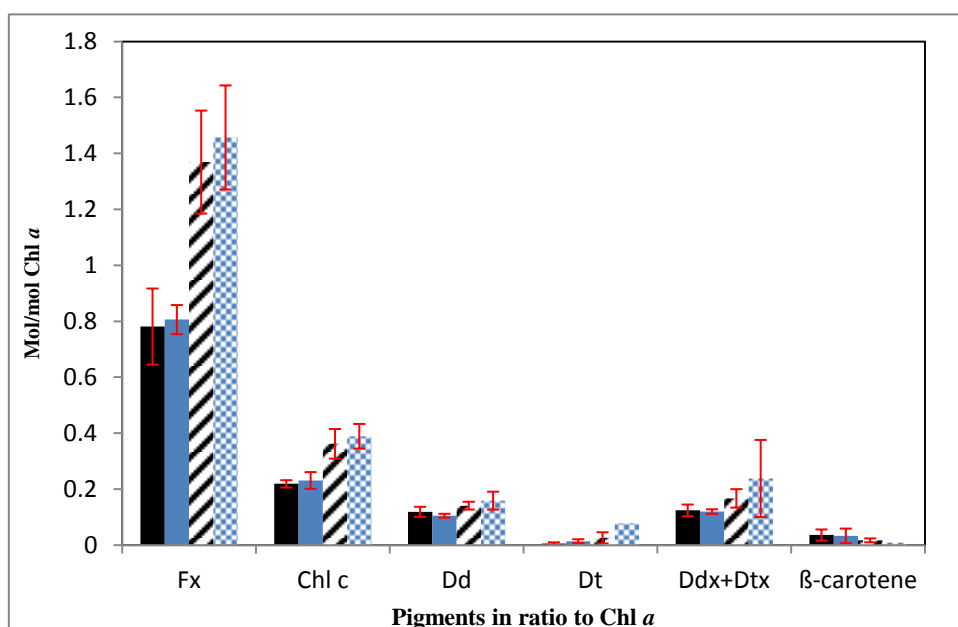
Figure 20: Pigment analysis of whole cells. WT (solid black bar), mutant cells (solid blue bar), WT thylakoids (black striped bar) and mutant thylakoids (blue checked bar) grown by bubbling cultures with sterile air. The pigments Fx, Chl *c*, Ddx, Dtx and ß-carotene were analyzed in comparison with Chl *a*.

The amount of Fx was 0.806 ± 0.05 mol/mol of Chl *a* in case of bubbling cultures and this was slightly higher than that in the WT where it was 0.78 ± 0.13 mol/mol of Chl *a*. The

values reported in literature for Fx (0.68 mol per mol Chl *a*) for similar cultures are slightly

lesser than values obtained in this work.

4.2   Purification of His-tagged FcpA and comparison with pure WT Fcp pool.
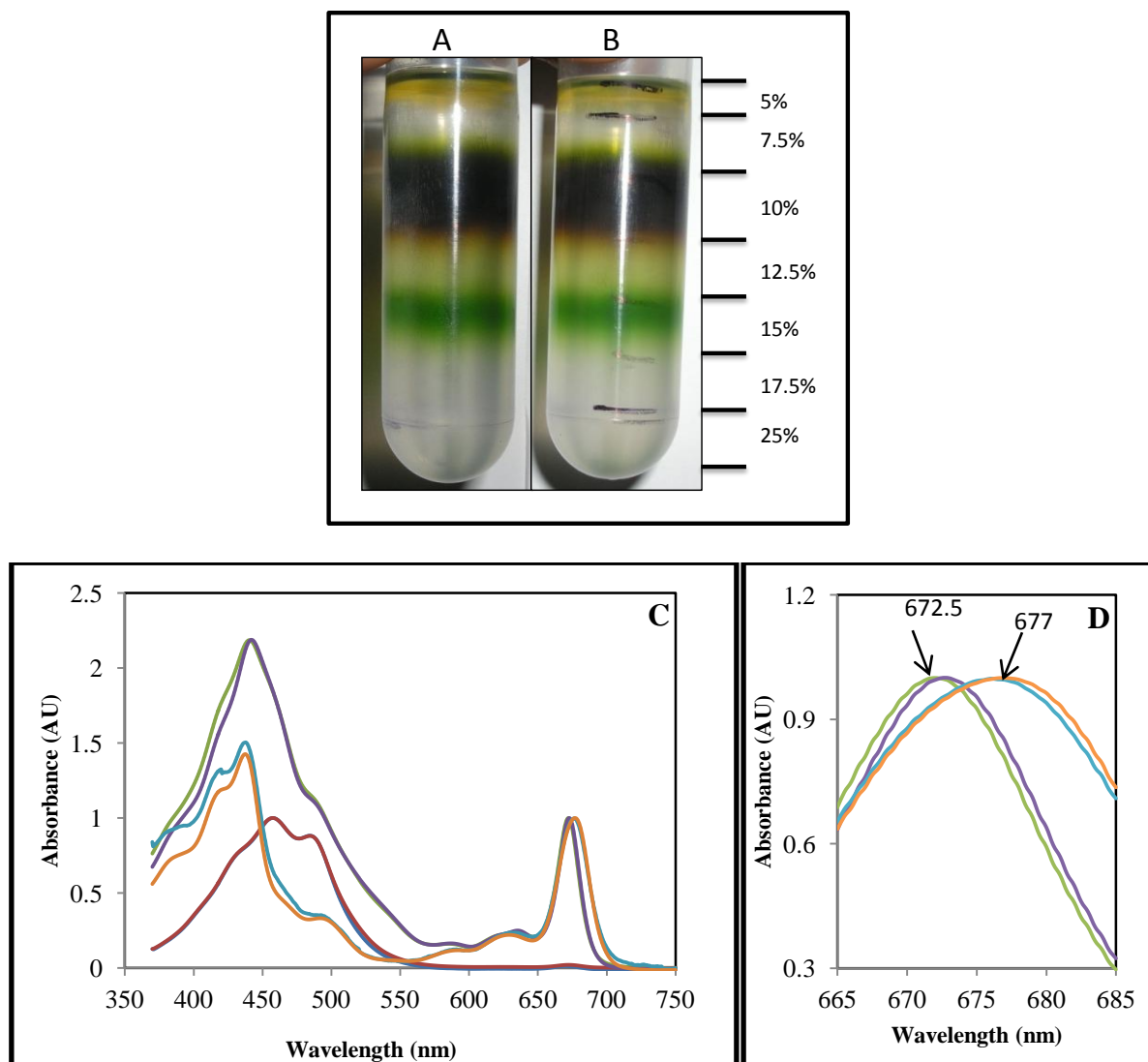
Figure 21: Separation of protein fractions using sucrose density gradient centrifugation. A; thylakoids of the WT, B; thylakoids of mutant, were solubilized with 15mM ß-DDM and loaded on a discontinuous sucrose gradient. C; the normalized absorption spectra of the 3 bands obtained after SDG. In blue and brown are the bands at 5% in WT and mutant respectively; in green and violet the bands at 10% in WT and mutant respectively; in azure and orange the band at 15% in WT and mutant respectively. D; the Qy maxima of the corresponding bands of absorption spectrum are zoomed.

Solubilisation of thylakoids with 15mM ß-DDM and subsequent separation on sucrose

density gradient, the pigment-protein complexes split into three distinctly coloured bands. A

golden-olive coloured band at 5%-7.5% sucrose gradient step corresponded to free pigment

----

(Fig. 21A and B) and was therefore discarded. A brown coloured band with Qy absorption

maxima (maximum absorption in the red region of spectrum) at 672.5 nm and Soret

maximum (maximum absorption in the blue region of the spectrum) at 442 nm was localized

at the 10% step which was presumed to be enriched in Fcps due to its spectral shape and due

to the absorption between 400-550 nm attributed to Fx (Guglielmi et al. 2005, Lepetit et al.

2007). The third green coloured band which localized at the 15% sucrose step appeared to be

a mixture of photosystem fractions owing to the red shift in its absorption maxima at 677 nm

(Veith T 2009). Analysis of the pigment stoichiometries of the brown bands is shown in

figure 22.
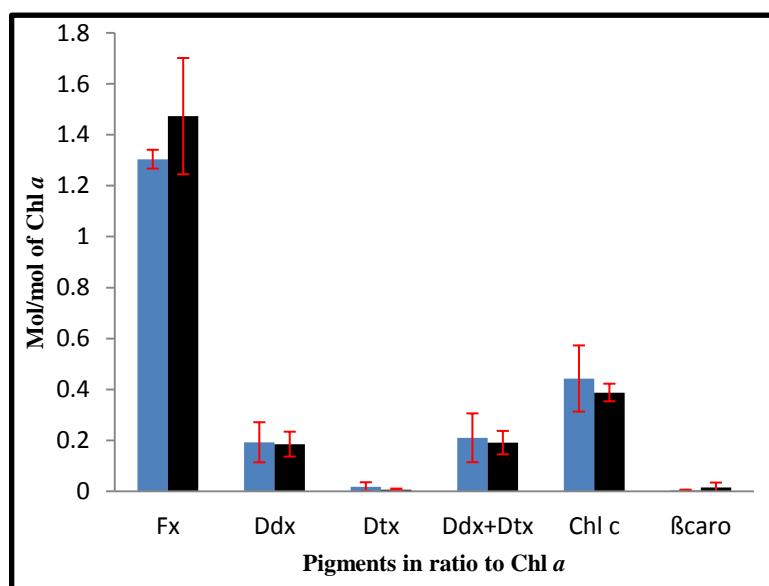
Figure 22: Pigment stoichiometries of the brown coloured bands after sucrose density gradient. WT; black bars, mutant; blue bars. Values represent means and standard deviations of at least 3 different preparations.

A high amount of Fx (1.3-1.5 mole) per mole of Chl *a* was observed both in the mutant and

the WT. The amounts of Chl *c* (0.38-0.44 mole) and diadinoxanthin (0.18-0.19) was also

similar in both cultures. Insignificant amount of ß-carotene in the brown bands indicated that

Fcps separated very well from the photosystem fractions.

4.2.1   Preparative gel filtration of FCP band of the WT from SDG

The Fcp band that was obtained from SDG was further purified using preparative gel filtration to get rid of any contamination from free pigment or other proteins.
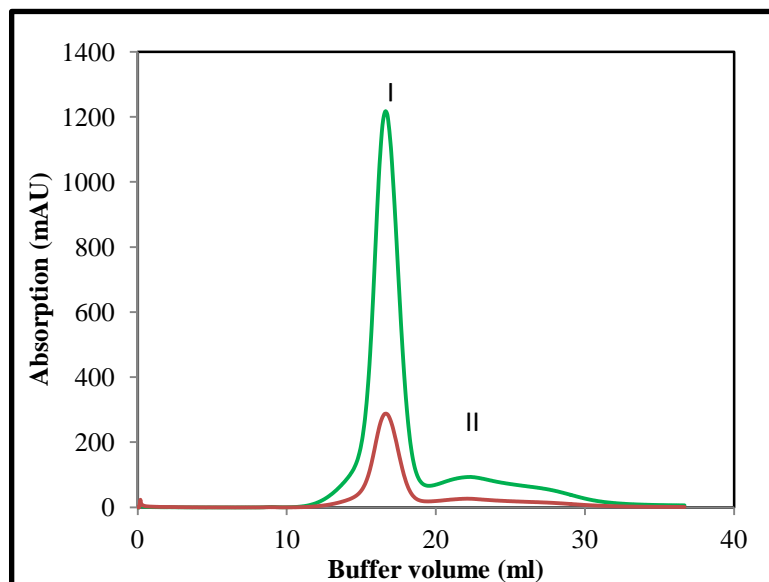
Figure 23: Preparative gel filtration of the WT Fcp fraction after sucrose density gradient. Brown Fcp band after SDG was loaded and elution was measured at 437nm (green) to trace Chl *a* and at 280 nm (brown) to trace proteins.
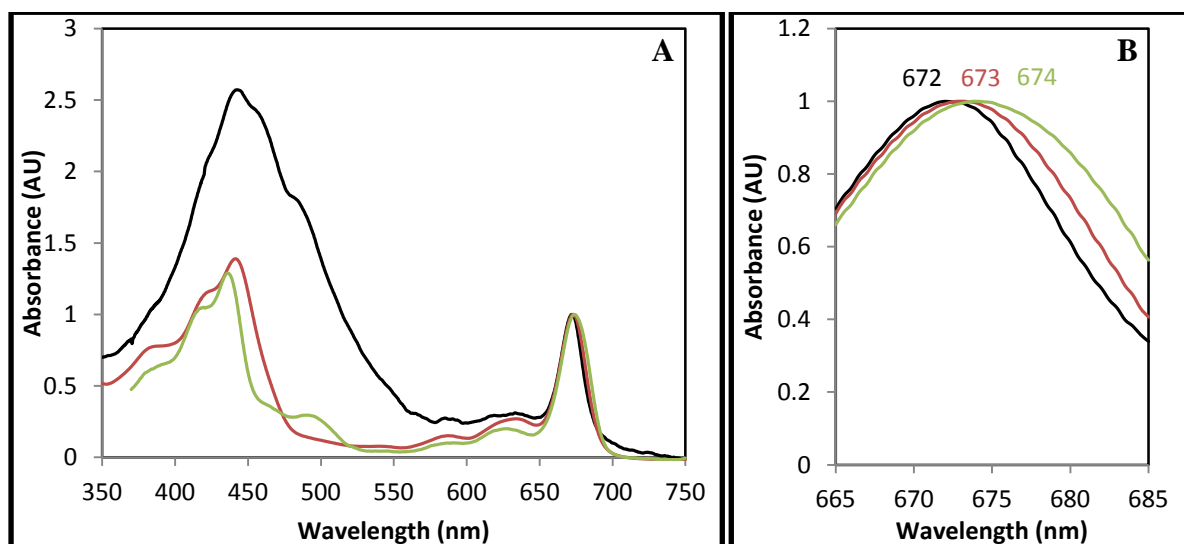
Figure 24: Absorption spectra of the main peaks of the preparative gel filtration of WT Fcps. In A, black denotes the absorption of peak I, brown the absorption of peak II and green the absorption of pure PSII for comparison. In panel B Qy maxima of the respective fractions of the absorption spectra are zoomed. (For purification of PSII see section 3.7.2.).

The gel filtration profile of the Fcp band purified from SDG in case of WT showed 2 peaks namely peak I and II (figure 23). The absorption spectrum of these peaks is shown in figure 24 where peak I resembled typical Fcp spectrum (Lepetit et al. 2007; Büchel 2003) with a Soret maximum of 441.5 nm and Qy max of 672 nm and peak II resembled absorption spectrum of either free Chl *a* or PSII (Fey et al. 2008). The latter hypothesis could be neglected since a shoulder between 470 nm and 500 nm corresponding to the absorption of β-carotene was missing. Thus peak II was attributed to be only free Chl *a*. i.e. free pigment with minor traces of PSII contamination.

4.2.2 Purification of FcpA$_{His}$
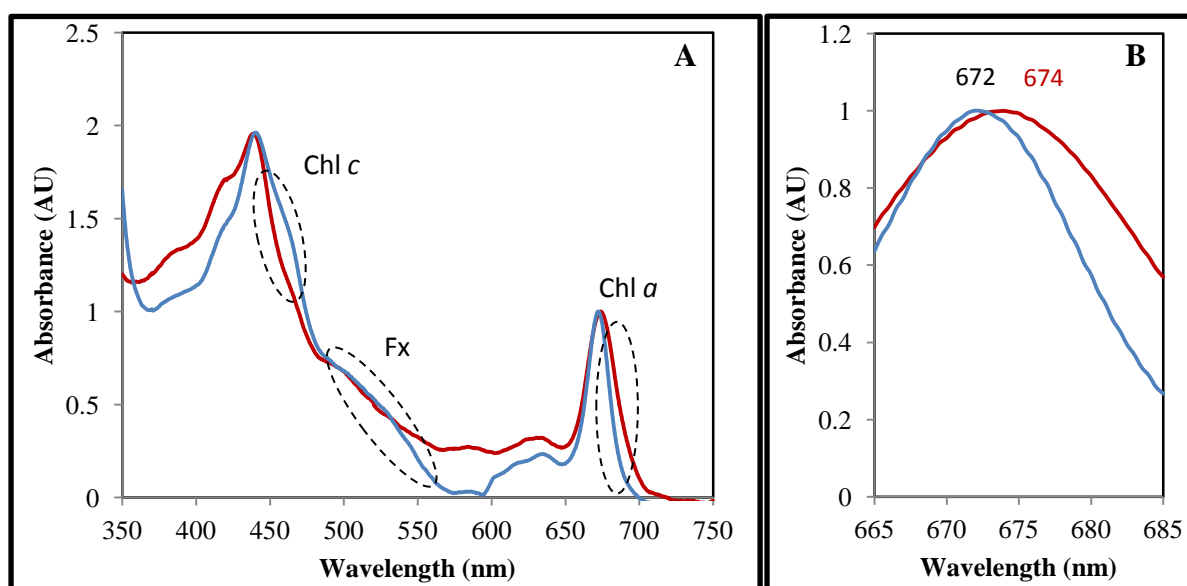
Figure 25: Comparison of absorption spectra of FcpA$_{His}$ with and without pre-purification on SDG. Panel A shows the comparison of absorption spectra when FcpA$_{His}$ was purified directly from thylakoids (brown) and when it was subjected to a pre-purification using SDG (blue). Panel B shows the Qy maxima of the respective samples.

A comparison was made in the spectral shapes when His-tagged FcpA was purified directly after solubilisation of thylakoids or after using a pre-purification step of SDG. Absorption spectra remained almost similar in both cases. But a detailed look at absorption maxima of Chl *a* and the broad carotenoid shoulder between 450-550 nm showed some significant differences. The Qy maximum of chlorophyll absorption was at 674 nm or at 672 nm when

----

FcpA$_{His}$ was purified from thylakoids directly or when subjected to a round of pre-purification, respectively. Additionally the peak in the red region corresponding to the absorbance of Chl *a* was broader as shown in figure 25 and this breadth and red shift indicate contamination with photosystems. The shoulders in the Soret region corresponding to the absorption of carotenoids and xanthophyll cycle pigments and at 460 nm due to absorption of Chl *c* were more pronounced after pre-purification of Fcps. Polypeptide analysis revelaed the presence of mainly PSI contamination when a SDG pre-purification step was not performed (data not shown). Additionally to check for unspecifically bound proteins on the IMAC column, WT thylakoids were solubilised exactly as the mutant thylakoids (Chl: det :: 1:30) and an affinity chromatography was carried out. Eluates from the column were found to be unspecifically bound PSI proteins (data not shown).

Due to the refinement of the absorption spectrum and the better quality of preparation after an additional step of pre-purification, SDG was performed before every round of purification of the recombinant protein.

Concerning pure FcpA$_{His}$, the absorption spectrum showed the Qy maximum at 672 nm and the Soret maximum at 440 nm. A very broad shoulder between 480 nm and 560 nm was indicative of the presence of the carotenoid Fx. A peak at 636 nm and a shoulder at 460 nm marked the presence of Chl *c* in the complex.

4.2.3   Yield of purification of FcpA$_{His}$

The recombinant FcpA$_{His}$ could be purified using the protocol established in this study within 48 hrs taking together the cell harvest, thylakoid preparation, sucrose density gradient centrifugation and affinity chromatography. From the total Chl *a* amount that was loaded on the column in the form of the Fcp band of SDG, only ~ 1.2-.1.5 % Chl *a* could be recovered after affinity chromatography. If the total amount of Chl *a* in the form of thylakoids was considered, only 0.2 % Chl *a* could be recovered after affinity chromatography.

4.2.4   Comparison of the purified Fcps of WT and FcpA$_{His}$

In the following section the WT Fcp pool purified using sucrose density gradient and subsequent gel filtration will be compared with the FcpA$_{His}$ specifically purified using IMAC.

4.2.4.1   Polypeptide composition of the FcpA$_{His}$ and the WT Fcp pool.

To prove that the protein purified via IMAC was indeed a His-tagged protein, polypeptide analysis was carried out. The predicted molecular mass of FcpA$_{His}$ is 18.9 kDa.
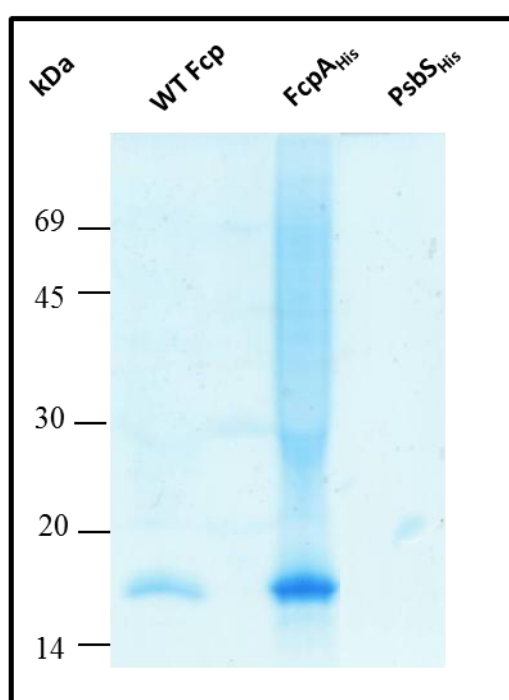
Figure 26: SDS-PAGE of the WT Fcp pool and FcpA$_{His}$. Molecular weight marker is indicated on the left. 0.5µg Chl *a* of WT Fcp and FcpA$_{His}$ and 0.75 µg of PsbS$_{His}$ were loaded.

A coomassie stained gel showed as expected a single prominent band around 19 kDa along with a slight smear in the FcpA$_{His}$ fraction. In spite of loading same concentrations of Chl *a* the FcpA$_{His}$ band appeared to contain more protein than the WT Fcp pool. Samples were also analyzed by immunoblots with antibodies either against the His - tag (α-His) or against all Fcps of *C.meneghiniana* (α-cmFcp) [Fig.27A and 27B respectively]. His-tagged PsbS protein from higher plants expressed in *E.coli* with a predicted molecular mass of 24 kDa was used

----

as a positive control for the anti-His antibody (courtesy K. Pieper, University of Frankfurt). In case where the blot was developed with α-cmFcp (Fig. 27B), signals were detected in the fractions from WT Fcp and also in the FcpA$_{His}$ fraction, confirming that the purified product consisted of Fcp polypeptides in each case. Only a single sharp signal was seen at 19 kDa in the FcpA$_{His}$ sample when developed with α-His (Fig. 27A) and none in the WT Fcp, confirming the presence of the His-tagged protein.
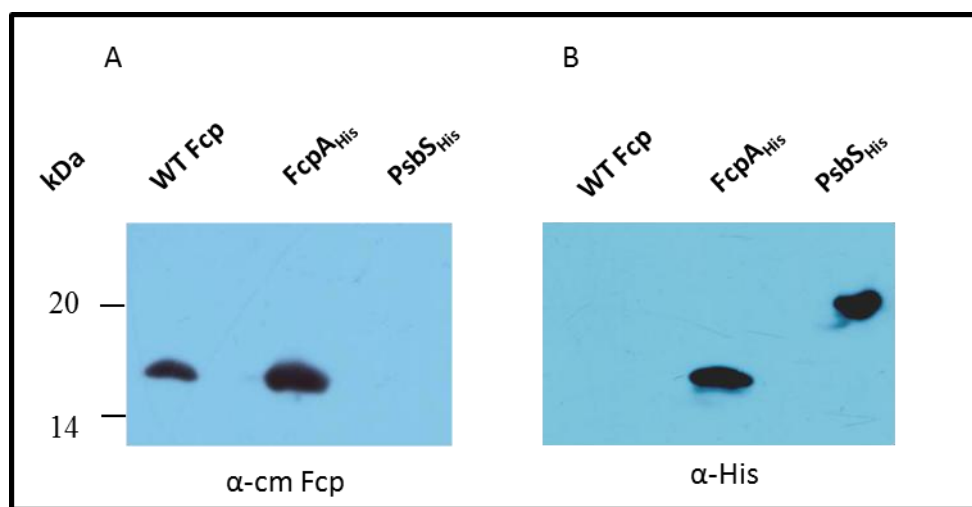
Figure 27: Western blot using antibody against all Fcp polypeptides of *C.meneghiniana* in panel A and using a monoclonal anti-His antibody in panel B. PsbS$_{His}$ was used as negative control for the Fcp antibody and as positive control for the anti-His antibody. 0.5 µg Chl *a* of WT Fcp and FcpA$_{His}$ and 0.75 µg of PsbS$_{His}$ were loaded.

4.2.4.2 Absorbance spectra
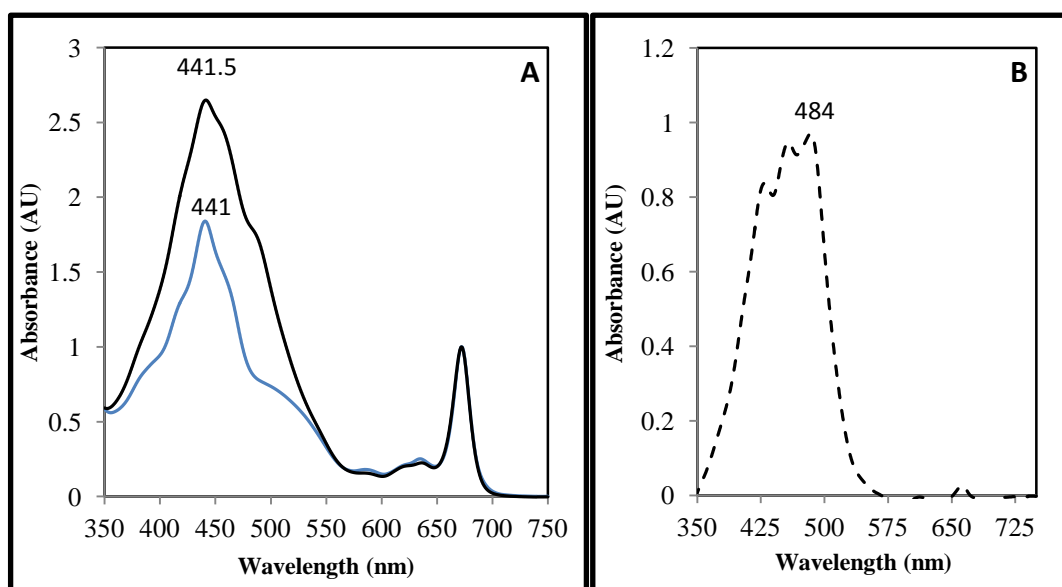
Figure 28: Absorption spectra of highly pure Fcp samples. Panel A; WT Fcp pool (black) and FcpA$_{His}$ (blue), panel B; a difference spectrum between the normalized absorbance of the WT Fcp pool and FcpA$_{His}$ is represented by a dashed line.

The spectral shapes were similar and absorption maxima of pure WT Fcp pool and FcpA$_{His}$ were both at 672 nm in the Qy region and Soret maxima at 441 nm for FcpA$_{His}$ and 441.5 nm for the WT Fcp. However the WT Fcp absorption spectrum showed a huge shoulder between 450-550 nm which was absent in the FcpA$_{His}$. A difference spectrum between the absorbance of the WT Fcp pool and that of FcpA$_{His}$ complex was found to be comparable to the absorption spectrum of pure carotenoids, Fx or XC cycle pigments (Goss et al. 2009, Lepetit et al. 2010). Pigment analyses were used to confirm the observations of the difference spectrum.

4.2.4.3 Pigment analysis

Table 33: Pigment stoichiometries of WT Fcp pool and FcpA$_{His}$. Values are means and standard deviations of at least 3 different preparations.

mol/mol Chl *a*	Fx	Chl *c*	Ddx+Dtx
WT Fcp	1.710 ± 0.137	0.369 ± 0.027	0.207 ± 0.020
FcpA$_{His}$	1.199 ± 0.090	0.376 ± 0.027	0.055 ± 0.04
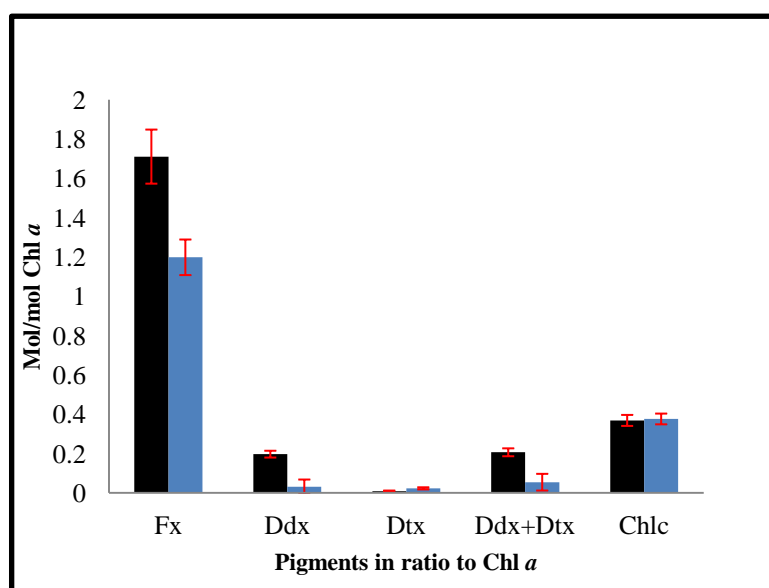
Figure 29: Graphical representation of the pigment stoichiometries of WT Fcp pool (black) and FcpA$_{His}$ (blue).

In both samples, the Chl *c* content was similar with $0.36\text{-}0.38\pm0.027$ mol per mol Chl *a* (Table 33). The Fx content in case of the His-tagged complex was about 1.2 mol per mol of Chl *a*, while in WT Fcp the content was about 1.5 times higher. This confirmed the earlier observation from absorption spectra that the WT Fcp pool bound more carotenoid Fx than the FcpA$_{His}$. Additionally WT Fcp pool bound approximately 4 times higher amount of Ddx+Dtx.

4.2.4.4 Oligomeric organisation
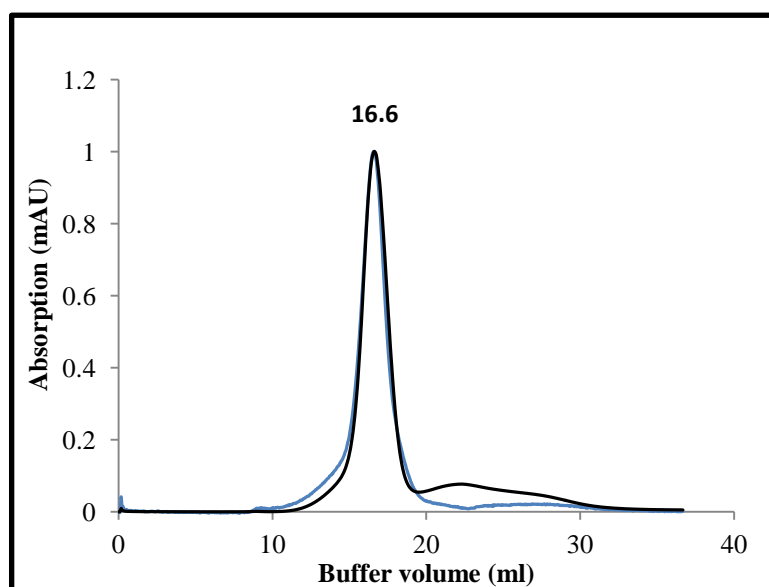
Figure 30: Analytical gel filtration of the WT Fcp pool (black) and FcpA$_{His}$ (blue). The absorption was measured at 437 nm.

WT Fcp purified from SDG and FcpA$_{His}$ were subjected to analytical gel filtration to investigate the oligomeric state as well as the homogeneity. Figure 30 shows the gel filtration profile of FcpA$_{His}$ where a single sharp peak was observed at 16.6 ml. An additional broad but minor peak was observed between 24 - 27 ml and spectroscopic investigations showed that the former peak was composed solely of Fcps and the latter was devoid of them. Absorption spectrum of the latter peak was comparable to that of free pigment was therefore discarded (data not shown). The WT Fcp fraction of *P. tricornutum* also eluted from the same column under identical conditions at 16.6 ml (figure 30). Trimeric FCPa complex from *C.meneghiniana* also eluted at 16.5 ml under identical conditions (K. Gundermann, University of Frankfurt, personal communication). The similarity in the elution volume thus related the oligomeric state of the trimeric FCPa complex from *C.meneghiniana* (Büchel 2003; Beer et al. 2006) and the isolated FcpA$_{His}$ complex along with the WT Fcp from *P. tricornutum*. Neither higher oligomers nor monomers were observed in the samples.

4.2.4.5 Polypeptide identification with mass spectrometry (MS)

MS was used to identify the polypeptides which built up the FcpA$_{His}$ containing complex. Trypsin digestion of the 19 kDa band which was identified in western blot as His-tagged Fcp followed by nano LC-ESI-MS/MS led to the identification of several peptide sequences. These were used to identify proteins within the database of *P. tricornutum*. Two Fcp proteins were unambiguously identified (Table 34). These were Lhcf1 (JGI protein ID: 18049) and Lhcf5 (JGI protein ID: 30648) from *P. tricornutum*, which are also annotated as FcpA and FcpE, respectively (refer Appendix I). Since the technique of MS is not a quantitative the contribution of the His-tagged FcpA in the complex could not be estimated at this point.

Table 34: Nano LC ESI MS/MS analysis of the FcpA$_{His}$ containing complex. JGI-Phatr2, Joint Genome Institute-vs2 of the *P. tricornutum* genome. z, charge. Xcorr, cross-correlation factor. Mo, oxidized Met. * indicates that the peptide is present in both models.

Protein ID (JGI-Phatr2)	Name	Identified peptides	z	Xcorr
18049	LhcF1(FcpA)	NNYLDFGWDTFSEDK	2	4.55
		NNYLDFGWDTFSEDKK	2	3.99
		DITGGEFVGDFR*	2	3.93
30648	LhcF5(FcpE)	NDFIDFGWDSFDEETK	2	4.04
		DITGGEFVGDFR*	2	3.93
		ISMoLAVAGYLVQENGIR	2	3.24

4.2.4.6 Spectroscopic characterization of FcpA$_{His}$ and the WT Fcp pool

Detailed spectroscopic investigations were made to analyze the intactness of the purified Fcp complexes. Comparisons were made between the WT Fcp pool, FcpA$_{His}$ purified using IMAC and post-purified using gel filtration.
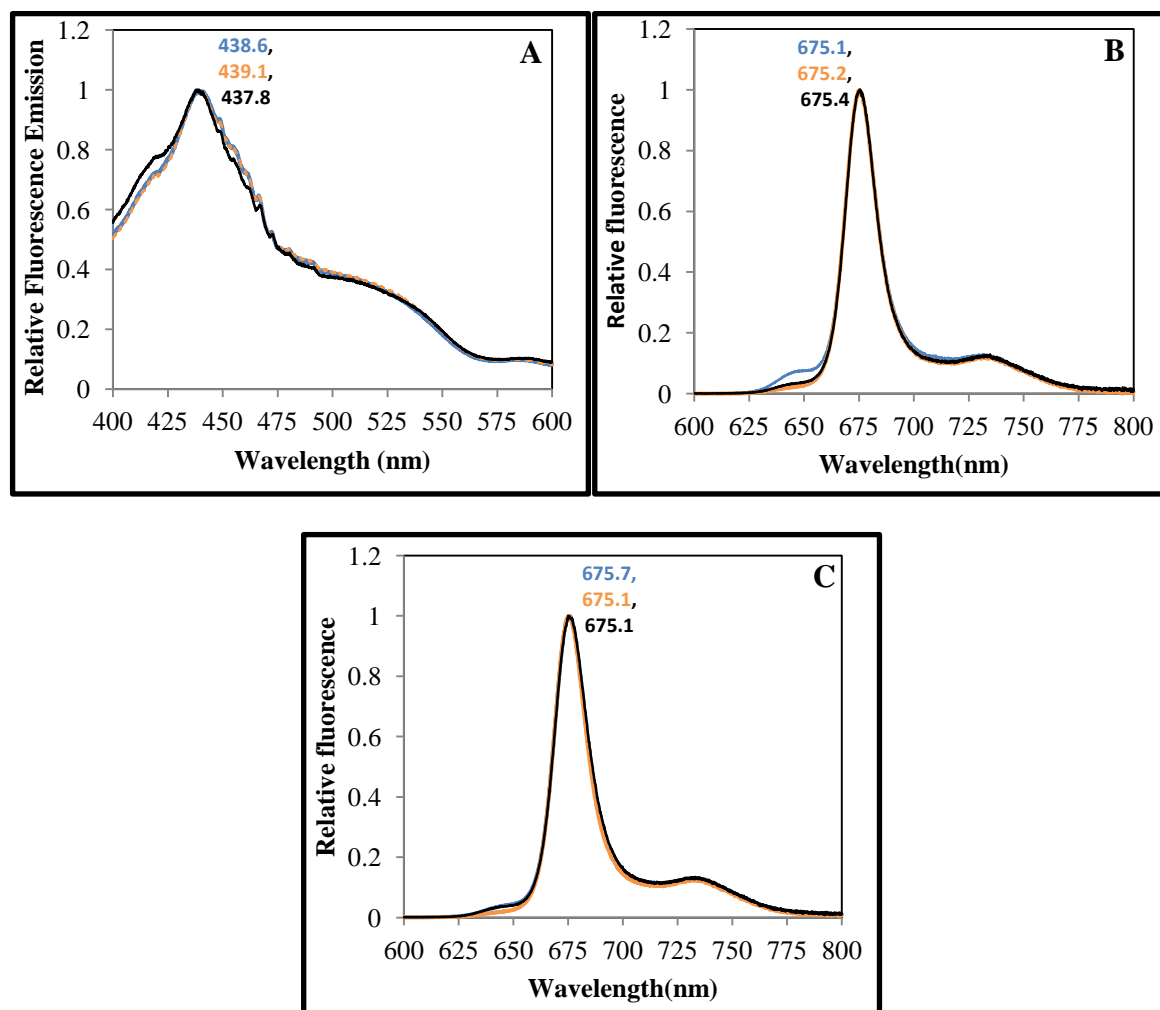
Figure 31: Spectroscopy of purified Fcps. A; normalized excitation spectra of WT Fcp (black), FcpA_{His} (blue) and FcpA_{His} post purified by gel filtration (orange). B; emission spectra when Chl *c* was excited at 465 nm, C; emission spectra when Fx was excited at 530nm. The fluorescence maxima are indicated in each case in respective colours.

In fluorescence excitation spectra as shown in figure 31A, samples were excited between 400 nm and 600 nm where pigments like Chl *c* and Fx are expected to absorb the incident energy. The intensity of the emitted fluorescence was measured at 675 nm since energetically coupled Chl *c* and Fx should transfer the excitation energy to Chl *a*, the final emitter, the emission maximum for which is 675nm. Fluorescence maxima around 438 nm in all cases as a result of excitation of Chl *a* was observed for all samples. Small shoulders around 460 nm indicated the energy transfer from Chl *c* to Chl *a* and a very broad shoulder between 475 and 550 nm indicated the transfer of excitation energy from the carotenoid Fx to Chl *a*. The excitation

spectra thus resembled the absorption spectra and further indicated that pigments were energetically coupled in the complex. Excitation spectra also showed that the additional pigments seen in absorbance spectra of the WT Fcp compared with FcpA$_{His}$ were not involved in the transfer of excitation energy to Chl *a.* (figure 31A). Thus, the additional pigments in the WT complexes as compared to the FcpA$_{His}$ (table 33) most probably represented a pool of pigments not properly working or not taking part in excitation energy transfer. Fluorescence emission spectra indicate the excitation energy transfer after specifically exciting pigments. Figure 31B indicates specific excitation of Chl *c* at 465 nm (Soret band of Chl *c*). Emitted fluorescence was measured between 600 and 800 nm. In case of all samples single peaks around 675 nm indicated that the energy was transferred to the end acceptor Chl *a.* Additionally a very small peak was observed around 640 nm in case of FcpA$_{His}$ which indicated the presence of some Chl *c* which was decoupled from the Fcps. However this peak was highly reduced when the FcpA$_{His}$ was post purified using gel filtration and also in the WT Fcp pool which was similarly purified. This indicated that the peak at 640 nm represented a pool of free Chl *c* independent of the Fcp complexes. The additional gel filtration in FcpA$_{His}$ was helpful to determine the oligomeric state and to confirm that the complex was extremely stable and functional even after multiple series of purification processes. Similar results were observed when Fx was excited specifically at 530 nm (figure 31C). The fluorescence maxima were around 675.5 nm in all three samples and the peak at 640 nm corresponding to decoupled Chl *c* was minimum.

Circular dichroism spectra were recorded to investigate arrangement of pigments on the polypeptide backbone.
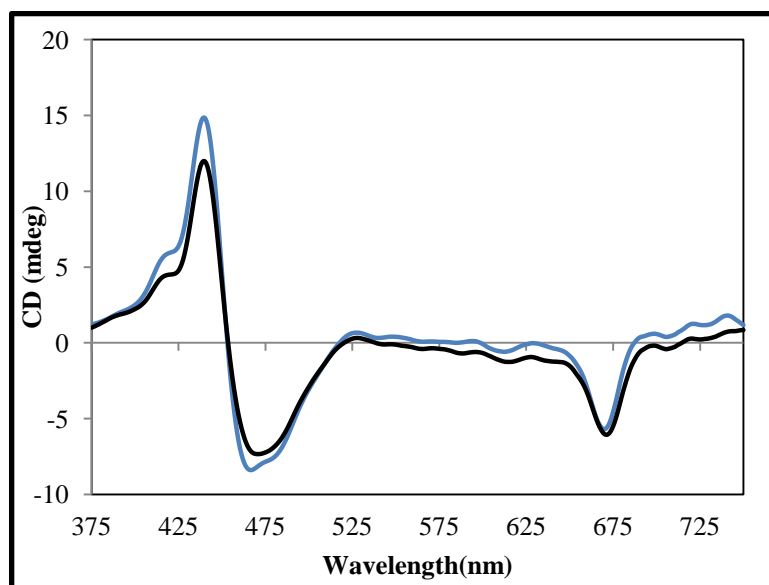
Figure 32: Circular dichroism spectra of pure Fcps. FcpA$_{His}$ (blue) and WT Fcp pool (black). Both samples were adjusted to a Chl *a* concentration of 5 μg ml^{-1} Chl *a*.

The CD spectra of both samples were observed to be very similar to each other (figure 32). They also resembled the previously reported CD spectra for trimeric Fcps from *P. tricornutum* (Lepetit et al. 2007) and also the trimeric FCPa and higher oligomeric FCPb complexes from *C.meneghiniana* (Büchel 2003) concerning the spectral structure. A prominent single negative band was observed at (-) 669 nm in case of FcpA$_{His}$ and at (-) 670 nm for the WT Fcps which was attributed to Chl *a*. This peak showed a 3 nm blue shift as compared to the Qy band of Chl *a* in the absorbance spectrum which might suggest the existence of a heterogeneous pool of Chl *a* in Fcps (Mimuro et al. 1990). This single band indicated that no Chl *a*–Chl *a* excitonic interactions exist in Fcps of *P. tricornutum*. Minor negative bands were observed at (-) 612 nm and (-) 615 nm for FcpA$_{His}$ and WT, respectively, corresponding either to the Qx absorbance of Chl *a* or to the Qy absorbance of Chl *c*. A huge split signal was observed in the Soret region at (-) 467 nm and (+) 440 nm for FcpA$_{His}$, resembling the spectral fingerprint observed earlier for Fcps in *P. tricornutum* (Lepetit et al. 2007). It clearly indicated the existence of a Chl *a* - carotenoid excitonic dimer.

4.3   Interaction of Fcps with photosystems in *P. tricornutum*

In the previous sections it was described that at least one of the main light harvesting antenna complexes in *P. tricornutum* is a trimer built of FcpA and FcpE proteins. In this study, special interest lay on the identification of either $FcpA_{His}$ or FcpE associated with either of the two photosystems in *P. tricornutum*. The methodology was to solubilize the thylakoids from the mutant in varying ratios of Chl *a* to the mild detergent β-DDM and thereby attempt to isolate PSI and PSII fractions still associated functionally with Fcps using ion exchange chromatography. $FcpA_{His}$ was to be identified by western blotting and other Fcps were supposed to be identified by mass spectrometry. Thylakoids were solubilized with either 10 mM β-DDM (Chl *a*: det :: 1:17.5) or 15 mM β-DDM (Chl *a* : det :: 1:20) and loaded on top of a discontinuous gradient. Three distinct bands were obtained on the sucrose gradient in each case (figure 33).
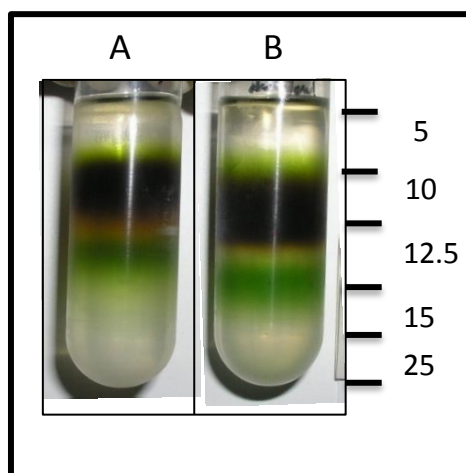
Figure 33: Separation of protein fractions on sucrose density gradient for subsequent purification of supercomplexes. A; thylakoids of the mutant were solubilized with 10 mM β-DDM (Chl: det :: 1: 17.5), B; thylakoids of the mutant were solubilized with 15mM β-DDM (Chl: det :: 1: 20).

Located within the 5% sucrose range was free pigment which was discarded. The Fcps were localized mainly between 10% and the interface of 12.5% and were identified using spectroscopy. However since the focus lay on the purification of photosystems, the Fcp band

72

was discarded too. A dark green band was observed at 12.5% or 15% sucrose density when

10mM β-DDM or 15mM β-DDM were used for solubilization respectively.

Absorption spectra of the green bands after sucrose density gradient centrifugation showed

that they were possibly a mixture of both the PSs (data not shown). To further separate the

two photosystems from each other, the green bands from SDG were loaded on an anion

exchanger.

4.3.1 Ion exchange chromatography of photosystems after solubilisation of thylakoids with 10mM β-DDM

Figure 34 indicates the ion exchange profile when the green band from SDG after

solubilisation of thylakoids with 10 mM β-DDM was applied to the column and different

proteins were eluted using sodium chloride.
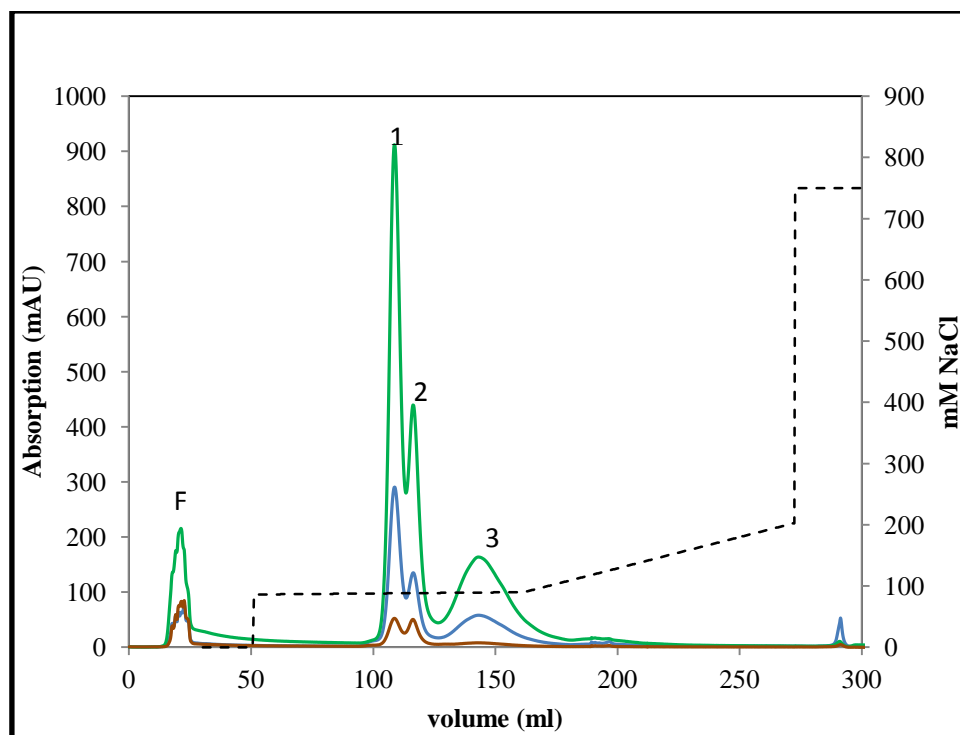
Figure 34: IEX profile of the green PS band obtained after SDG when the mutant thylakoids were solubilised using 10mM β-DDM. Absorption at 437 nm is shown in green, at 280 nm in blue and at 530 nm is shown in brown. Dashed black line represents the concentration of NaCl gradient used for elution.

Four prominent peaks were observed (figure 34) when thylakoids were solubilised with 10mM ß-DDM and the green band from SDG (figure 33 A) was subjected to IEX. The peaks are numbered in the order of elution F, 1, 2 and 3. Elution was controlled at three different wavelengths viz. 280 nm for proteins, 437 nm for Chl *a* and 530 nm for Fx. Peak F which was eluted before a salt gradient application was observed to be only free pigment since it did not show any absorption at 280 nm. It was not considered further. Eluate fractions 1-3 were green in colour. Fraction 1 showed the maximum absorption at 437 nm followed by fraction 2 and fraction 3. From the ratio of absorbance at 437 nm to 280 nm it was seen that fractions 1 and 2 contained approximately equal amount of protein per Chl. Fraction 1 and 2 showed a similar absorbance at 530nm which suggested that they both contained equal amount of Fx. It seemed likely that both fraction 1 and 2 represented photosystems associated with Fcps. Fraction 3 absorbed mainly at 437 nm and 280 nm but showed a highly reduced absorption at 530 nm implying that Fcps might not be bound to this fraction and it could be a pure photosystem fraction.

4.3.2 Ion exchange chromatography of photosystems after solubilisation of thylakoids with 15 mM β-DDM
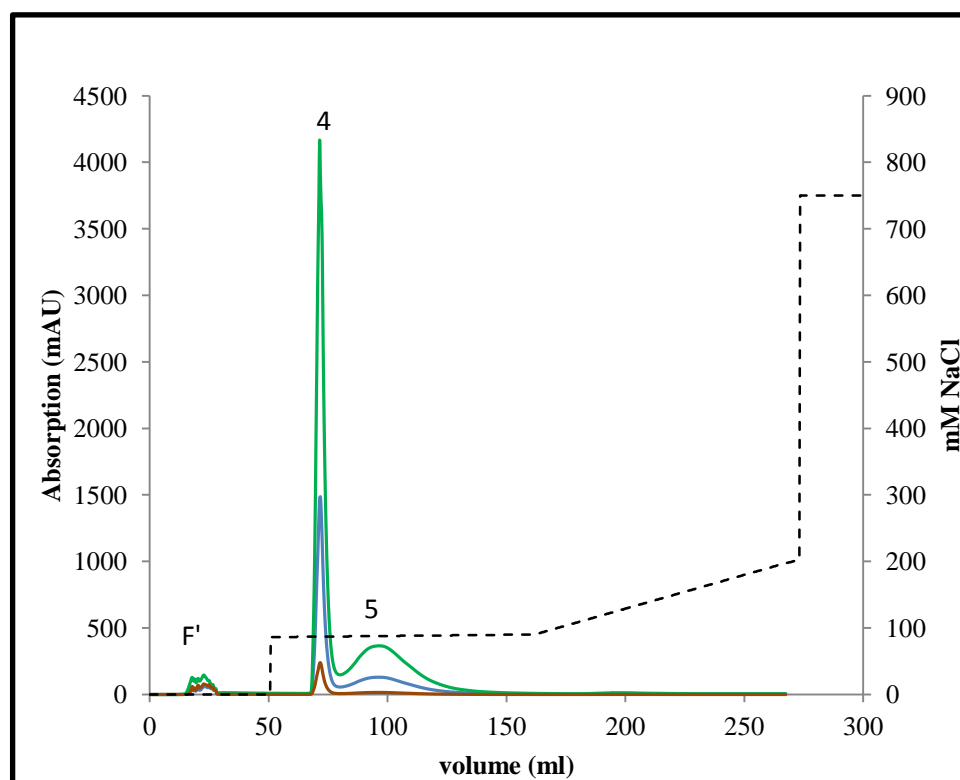
Figure 35: IEX of the green PS band obtained after SDG when mutant thylakoids were solubilised using 15mM β-DDM. Absorption at 437 nm is shown in green, at 280 nm in blue and at 530 nm is shown in brown. Dashed black line represents the concentration of NaCl gradient used for elution.

Similarly, when thylakoids were solubilised with 15mM ß-DDM and the green band from SDG (figure 33 B) was subjected to IEX, an elution profile shown in figure 35 was observed. In this case only three prominent peaks were observed and these were named peak F', 4 and 5. Peak F' was found to be free pigment and therefore discarded. Peak 4 showed an 8 fold higher absorption at 437 nm than peak 5. When the ratio of absorbance at 437 nm to 280 nm was considered then both peaks were found to contain almost the same amount of protein. Peak 4 showed higher absorption at 530 nm than peak 5.

4.3.3 Absorbance spectra of the peaks of ion exchange chromatographies

Absorbance spectra of the peaks 1-5 from the two different IEXs (refer figure 34 and 35) carried out in order to estimate the identity of the contents of these fractions.
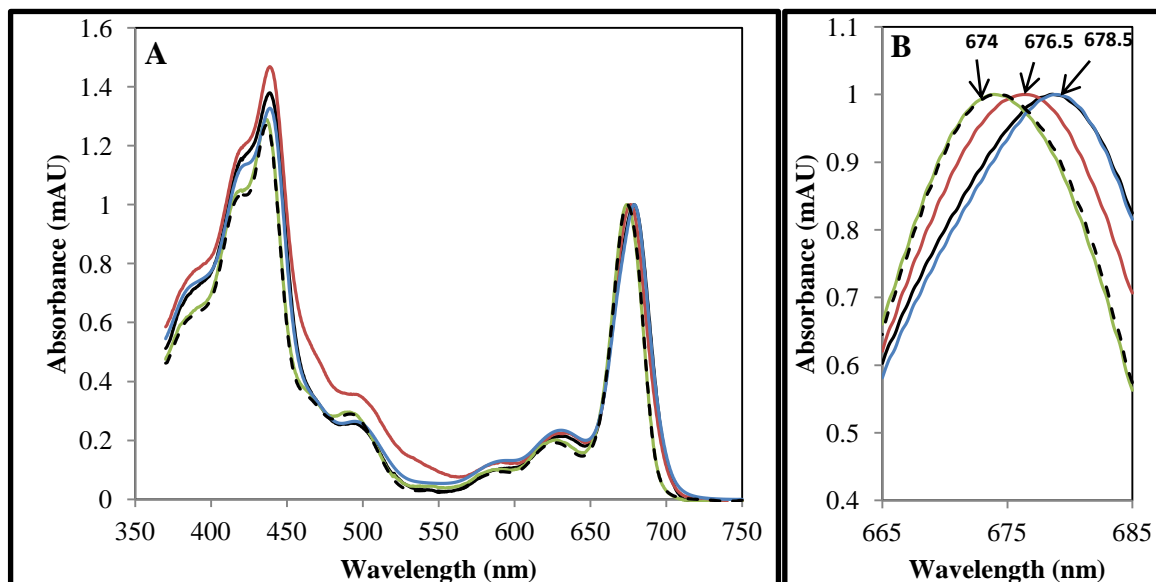
Figure 36: Absorbance spectra of peaks 1-5 from the two different IEXs. A; the absorbance spectrum of peak 1 (black), peak 2 (brown), peak 3 (green), peak 4 (blue) and peak 5 (dashed black line). B; the Qy maxima of the respective peaks from absorption spectra are zoomed. Peak 3 and 5 both showed Qy max at 674 nm and peak 1 and 4 both showed a Qy max at 678.5 nm. Peak 2 had a Qy max at 676.5 nm.

All peaks (1-5) showed a similar absorption spectrum shape. Peak 1 and peak 4 showed the maximum red shifted Qy_{max} at 678.5 nm. This was shown to be the Qy maximum in an absorption spectrum of pure PSI in *P. tricornutum* (Veith T 2009). Peak 2 showed slight blue shift and Qy_{max} at 676.5 nm. In addition a small shoulder around 480 nm- 550 nm was observed which is the region in which Fx absorbs. It seemed possible that this peak contained some Fcps along with a photosystem. Peak 3 and 5 showed the most blue shifted Qy_{max} at 674 nm. A blue shifted Qy_{max} of Chl between 673-675 nm is an indication of a pure PSII preparation in higher plants (Nagao et al. 2007, Enami et al. 2008). In all peaks except peak 2 the shoulder corresponding to Fx absorption was absent.

76

4 Results

4.3.4 Polypeptide analysis of the peaks of ion exchange chromatographies

SDS-PAGE gel was carried out using the samples of peaks 1-5 from the IEX to determine the components (Fig. 37). It could be seen that peak 1, 2 and 4 contained proteins characteristic of PSI. A double band was observed around 65 kDa which is the molecular mass of the core proteins of PSI – the PsaA and PsaB. A smeared band was also present at the same height in peak 3. In peak 5 this band was completely absent indicative that peak 5 was devoid of PSI. Furthermore there were clear single bands in peaks 1, 2 and 4 around 45 kDa and in peak 3 and 5 at lower heights around 40 kDa. In peaks 1, 2, 4 and 5 bands could be observed corresponding to molecular mass between 21 and 17 kDa which is the molecular mass of all Fcps (Fawley and Grossman 1986). These bands were most prominent in peaks 1, 2 and 4. No band corresponding to this weight was observed in peak 3.
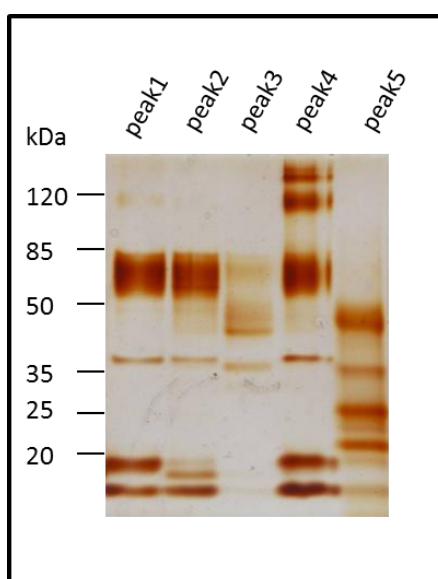
Figure 37: Polypeptide analysis of the five peaks obtained after the 2 different IEXs. (refer figures 33 and 34). Molecular weight marker is indicated on the left. Samples of the peaks 1, 2, 4 and 5 were loaded in 2 µg Chl *a* whereas sample from peak 3 was loaded at 0.75 µg Chl *a*.

It was thought that peak 5 could be PSII associated with some Fcps due to its typical band pattern between 40 and 15 kDa. Figure 38 shows western blot analysis which confirmed the identities of PSI, PSII and the also the presence of Fcps.
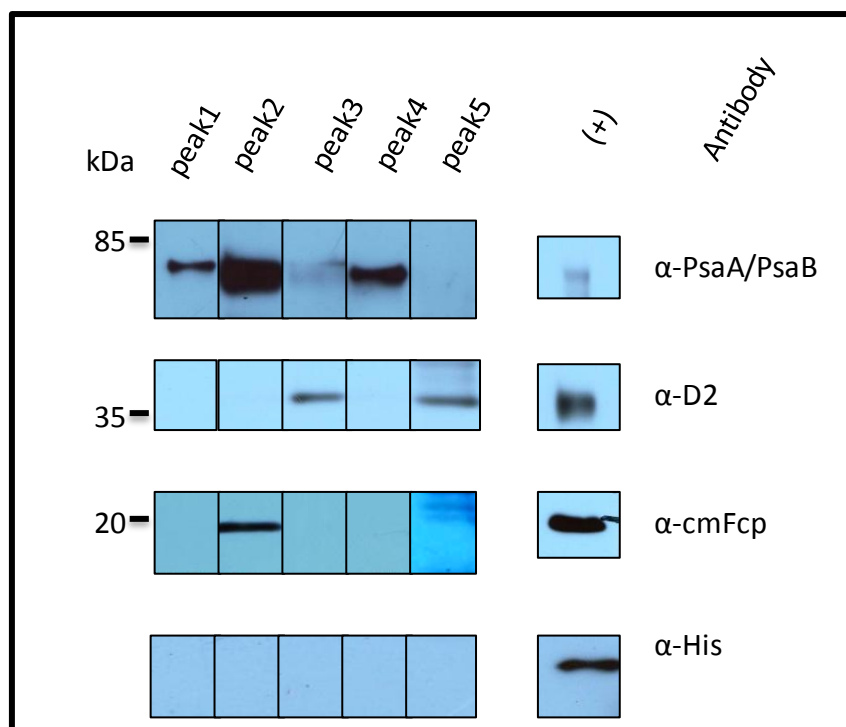
Figure 38: Western blot analysis of the peaks 1-5 obtained from the 2 different IEXs. Molecular weight marker is indicated on the left. Thylakoids of the WT UTEX 646 were used as (+) control for antibodies against PSI and PSII. Fcps purified from WT were used as (+) control against antibody against Fcps and a pure FcpA$_{His}$ was used as a (+) control for anti-His antibody.

Clear bands were obtained at around 65 kDa in peaks 1, 2 and 4 when a western blot was developed with an antibody against the core proteins of PSI. This indicated that all peaks except the 3rd and 5th contained some PSI constituent. Pale band in peak 3 seemed to be due to a slight contamination with PSI probes. When the blot was developed with antibody against the intrinsic core protein D2 (PsbD) single bands were obtained at the expected molecular weight (~ 35 kDa) in peak 3 and 5. Thus peak 3 and 5 were attributed to PSII. With an antibody against all Fcp polypeptides of *C.meneghiniana* a single sharp band was obtained around 18 kDa in peak 2 and a pale double band was obtained in peak 5 around 19 and 20 kDa. It was thus confirmed that peak 2 and peak 5 were PSI and PSII associated with Fcps respectively. It can be noted that the Fcp bands in PSI and PSII had different molecular weights. Therefore it could be presumed that the two photosystems bound different Fcps. Using an anti-His antibody no signals could be obtained in any of the samples. A mass

spectrometry analysis of the 18 kDa band in PSI sample and the 19 and 20 kDa band of the

PSII sample are listed in table 35 and 36, respectively.

Table 35: Nano LC ESI MS/MS analysis of the Fcps associated with PSI. JGI-Phatr2, Joint Genome Institute-vs2 of the *P. tricornutum* genome. z, charge; Xcorr, cross-correlation factor; Mo, oxidized Met. * indicates that the peptide is present in 3 out of 4 models and those marked with # are present in 2 models. Peptides reported here are those that were identified in two independent PSI preparations.

Protein ID (JGI-Phatr2)	Name	Identified peptides	z	Xcorr	Total no.of peptides
30648	Lhcf5 (FcpE)	NDFIDFGWDSFDEETK	2	4.316	35
		ISMoLAVAGYLVQENGIR	2	3.74	
		DITGGEFVGDFR*	2	3.22	
51230	Lhcf11 (FcpF)	NDYIDFGWDSFDEETQFK	2	3.251	2
18049	Lhcf1 (FcpA)	NNYLDFGWDTFSEDK#	2	2.765	1
		DITGGEFVGDFR*	2	3.01	
6686	Lhcf3 (FcpC)	DITGGEFVGDFR*	2	3.22	5
		NNYLDFGWDTFSEDK#	2	3.16	

Table 36: Nano LC ESI MS/MS analysis of the Fcps associated with PSII. z, charge; Xcorr, cross-correlation factor; Mo, oxidized Met. Peptides reported here are those that were identified in two independent PSI preparations.

Accession number	Name	Identified peptides	z	Xcorr	Total no.of peptides
118410982	D2	GIFDLIDDWLKK	2	3.98	2
193735613	CP43	SPSGEIIFGGETMoR	2	4.25	4

FcpE could be identified as the most predominantly present protein in the Fcps associated with PSI. Additionally also FcpA, C and F were found in traces in the Fcp band associated with PSI. Unfortunately no Fcps could be identified in the 2 faint bands of Fcps associated with PSII (peak 5) as found in Western blots. Instead only the intrinsic core protein D2 and the core antenna protein CP43 could be identified in PSII sample.

Additionally in the PSI sample, the core subunit PsaL could be identified using MS among the proteins lower in molecular weight than the Fcps (figure 37). It has been discussed that the separation of smaller subunits like PsaL, E, I, J and C by means of SDS-PAGE is not possible (Veith T 2009 and references therein) and also that the purification of a PSI complex containing all subunits especially the lower molecular weight subunits is relatively difficult. However since at least PsaL could be identified in this PSI-Fcp preparation it is reasonable to assume that this highly pure preparation retained most PSI subunits intact.

In summary a highly pure and intact PSI complex could be isolated and Fcps could be identified only associated with PSI and not tightly bound to PSII.

4.3.5 Spectroscopic analysis of PSI- Fcp complex

To confirm whether the Fcps bound to be PSI were intact in energy transfer further spectroscopic investigations were carried out with peak 2 of the IEX. Additionally the spectra were compared with those of highly pure WT Fcps (refer results section 4.2.1).
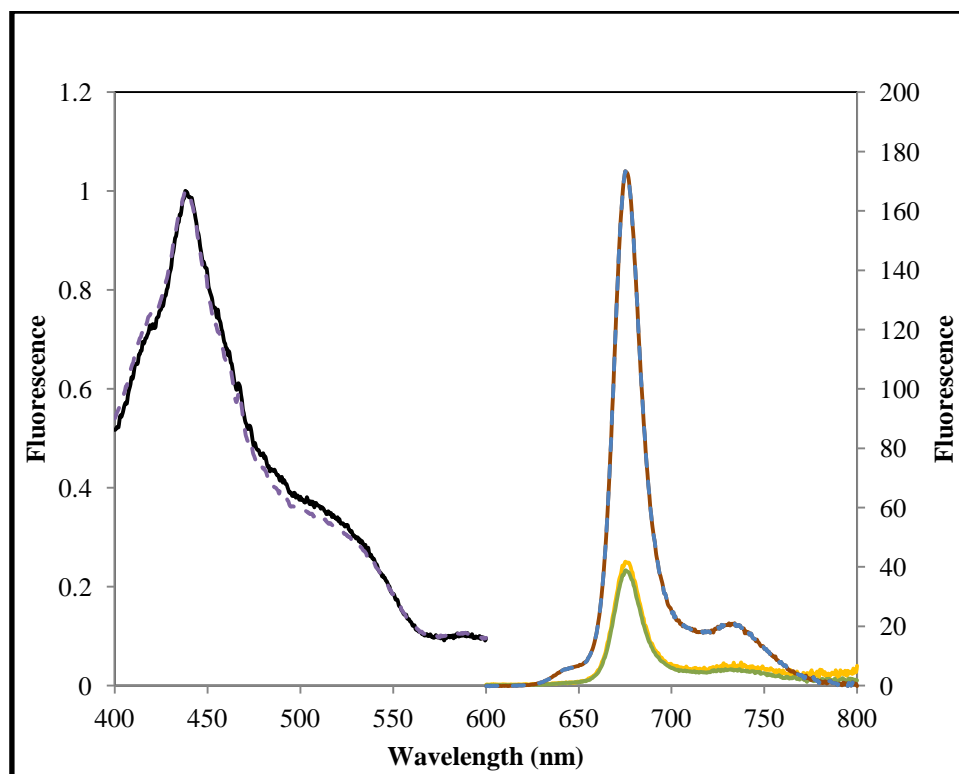
Figure 39: Room temperature spectroscopic analysis of the PSI-Fcp (refer figure 37). Solid black line and dashed purple line indicate normalized excitation spectrum of PSI-Fcp and of a reference WT Fcp pool, respectively. Samples were excited between 400 and 600 nm and fluorescence emission was measured at 675 nm. Emission spectra when PSI-Fcp (yellow) and WT Fcp pool (brown) was excited at 530 nm. Emission spectra when PSI-Fcp (green) and WT Fcp pool (blue) when the samples were excited at 465 nm respectively. WT Fcp pool samples were used as reference and adjusted to the same Chl *a* concentration as the peak 2 sample.

In the excitation spectrum of the PSI-Fcp containing samples it was clearly seen that the pigments Fx and Chl *c* transfer energy effectively to Chl *a*. The excitation spectrum was also compared with that of WT Fcp pool and it was seen that the spectral shapes were absolutely identical. PSI, due to its high quantum yield, is known to be a very strong fluorescence quencher and whereas Fcps do not quench fluorescence (Veith and Büchel 2007; Veith et al. 2009 and references therein). In case that the Fcps associated with PSI were functionally intact i.e. Chl *c* and Fx transferred energy to PSI, the fluorescence emission would be lower as compared to that of energetically intact free Fcps. When samples were excited at 530 nm (Fx) or 465 nm (Soret band of Chl *c*) and emission spectrum was measured the intensity of emission reduced to only 22.5% in PSI samples as compared to that in WT Fcp pool. At room

81

----

temperature the emission maximum was the same in both PSI-Fcp and free Fcps and at 675 nm and this finding was already reported (Veith T 2009). No shoulder was seen at 640 nm indicating that Chl *c* was not decoupled from the PSI-Fcp complex. Thus these measurements indicated that Fcps were intact in energy transfer and functionally associated with PSI. Since the complex was stable and functional in spite of undergoing several processes like French press breakage of cells, sucrose density gradient centrifugation and the harsh procedure of IEX, an additional gel filtration for confirming association Fcps with PSI and ruling out a co-elution was not necessary.

In conclusion it was possible to isolate a fully functional PSI-Fcp supercomplex using a modified protocol compared to that reported earlier (Veith and Büchel 2007). The Fcps that were bound to PS I were mainly FcpE polypeptides. In addition FcpA, C and F could also be identified associated to PSI. FcpE, A, C and F all belong to the Lhcf type of proteins. No Lhcr type of protein could be identified associated with PSI neither could Fcps be identified associated with PSII.

4.4   2D crystallization of FcpA$_{His}$

Using the technique of detergent dialysis, the FcpA$_{His}$ protein complex was tried to be crystallized in 2 dimensions for structural studies. A detailed lipid analysis of the FcpA$_{His}$ using thin layer chromatography was not successful owing to the extremely small amounts of protein that could be purified which had to be handled very economically. However an analysis of the lipid content of the WT Fcp showed the presence of MGDG only (data not shown). A large prescreen had to be set up to avoid missing a certain combination of lipid and LPR. Table 37 indicates the results of initial test conditions in which 3 lipid combinations were tested at 4 different LPRs at 2 different temperature ramps without the presence of any additives. 24 initial conditions were planned based on the pre-screen used for the 2D crystallization of FCPa trimer from *C.meneghiniana* (Beer A 2010)

Table 37: Overview of the pre-screen of crystallization conditions.

Protein	Detergent	Lipid	LPR (w/w)	Dialysis buffer	pH	Duration	characteristic	Colour	Remark
mg/ml									
0.2	0.2% NG	MGDG	10	25 ml of	7.4	25°C 1hr, 20°C 5 days	clear solution	yellow	**vescicles**
0.2	0.2% NG	MGDG	5	1mM Na-azide+	7.4	25°C 1hr, 20°C 5 days	clear solution	brown	aggregates
0.2	0.2% NG	MGDG	1	10mM Glycine+	7.4	25°C 1hr, 20°C 5 days	clear solution	brown	**vescicles**
0.2	0.2% NG	MGDG	0.5	10% Glycerol	7.4	25°C 1hr, 20°C 5 days	precipitate	brown	**vescicles**
0.2	0.2% NG	MGDG	10		7.4	37°C 1hr, 18°C 5 days	clear solution	green	none
0.2	0.2% NG	MGDG	5		7.4	37°C 1hr, 18°C 5 days	clear solution	green	aggregates
0.2	0.2% NG	MGDG	1		7.4	37°C 1hr, 18°C 5 days	precipitate	green	none
0.2	0.2% NG	MGDG	0.5		7.4	37°C 1hr, 18°C 5 days	precipitate	green	aggregates
0.2	0.2% NG	DGDG	10	25 ml of	7.4	25°C 1hr, 20°C 5 days	precipitate	enish-bro	aggregates
0.2	0.2% NG	DGDG	5	1mM Na-azide+	7.4	25°C 1hr, 20°C 5 days	precipitate	enish-bro	none
0.2	0.2% NG	DGDG	1	10mM Glycine+	7.4	25°C 1hr, 20°C 5 days	precipitate	brown	none
0.2	0.2% NG	DGDG	0.5	10% Glycerol	7.4	25°C 1hr, 20°C 5 days	precipitate	brown	**tube like structures**
0.2	0.2% NG	DGDG	10		7.4	37°C 1hr, 18°C 5 days	clear solution	green	none
0.2	0.2% NG	DGDG	5		7.4	37°C 1hr, 18°C 5 days	clear solution	brown	aggregates
0.2	0.2% NG	DGDG	1		7.4	37°C 1hr, 18°C 5 days	precipitate	yellow	none
0.2	0.2% NG	DGDG	0.5		7.4	37°C 1hr, 18°C 5 days	precipitate	yellow	aggregates
0.2	0.2% NG	MGDG+PC(2:1)	10	25 ml of	7.4	25°C 1hr, 20°C 5 days	precipitate	yellow	none
0.2	0.2% NG	MGDG+PC(2:1)	5	1mM Na-azide+	7.4	25°C 1hr, 20°C 5 days	precipitate	green	aggregates
0.2	0.2% NG	MGDG+PC(2:1)	1	10mM Glycine+	7.4	25°C 1hr, 20°C 5 days	precipitate	yellow	**vescicles**
0.2	0.2% NG	MGDG+PC(2:1)	0.5	10% Glycerol	7.4	25°C 1hr, 20°C 5 days	precipitate	yellow	**vescicles**
0.2	0.2% NG	MGDG+PC(2:1)	10		7.4	37°C 1hr, 18°C 5 days	precipitate	yellow	none
0.2	0.2% NG	MGDG+PC(2:1)	5		7.4	37°C 1hr, 18°C 5 days	precipitate	green	aggregates
0.2	0.2% NG	MGDG+PC(2:1)	1		7.4	37°C 1hr, 18°C 5 days	precipitate	green	aggregates
0.2	0.2% NG	MGDG+PC(2:1)	0.5		7.4	37°C 1hr, 18°C 5 days	precipitate	dark green	none

Small vesicles were mainly observed in the conditions where MGDG was used as the lipid and the LPR was 0.5 and 1. This was not surprising since pure Fcps are known to be associated with the nonbilayer lipid MGDG in case of *C.meneghiniana* (Goss et al. 2009; Lepetit et al. 2011; Lepetit et al. 2010). However small tube like structures were also observed when DGDG was used in the LPR of 0.5. No common point was reached where it could be safely concluded that a certain lipid leads to an organizational feature except that higher LPRs could be ruled out. From this data 72 further trials were conducted within the lower LPR range of 0.1-2.0 using again the three different lipid combinations and several additives to investigate if any crystal formation occurs. Following tables give an overview of

4 Results

----

the main screen of crystallization conditions along with the observations under the electron

microscope.

Table 38: Crystallisation screen using 3 lipid combinations, 6 LPRs and KAc and LiCl as additives.[2]

Protein	Detergent	Lipid	LPR(w/w)	Additives	Dialysis buffer	pH	Duration	characteristic	Colour	Remark
mg/ml										
0.2	0.2% NG	MGDG	0.1	350mM KAc,35mM LiCl	25 ml of	7.4	20°C, 3 weeks	clear solution	bright yellow	aggregates
0.2	0.2% NG	MGDG	0.5	350mM KAc,35mM LiCl	1mM Na-azide+	7.4	20°C, 3 weeks	precipitate	yellow	aggregates
0.2	0.2% NG	MGDG	0.75	350mM KAc,35mM LiCl	10mM Glycine+	7.4	20°C, 3 weeks	precipitate	yellow	aggregates
0.2	0.2% NG	MGDG	1	350mM KAc,35mM LiCl	10% Glycerol+	7.4	20°C, 3 weeks	precipitate	yellow	aggregates
0.2	0.2% NG	MGDG	1.5	350mM KAc,35mM LiCl	350mM Kac+	7.4	20°C, 3 weeks	precipitate	green	aggregates
0.2	0.2% NG	MGDG	2	350mM KAc,35mM LiCl	35mM LiCl	7.4	20°C, 3 weeks	precipitate	green	aggregates
0.2	0.2% NG	DGDG	0.1	350mM KAc,35mM LiCl	25 ml of	7.4	20°C, 3 weeks	milky	yellow	aggregates
0.2	0.2% NG	DGDG	0.5	350mM KAc,35mM LiCl	1mM Na-azide+	7.4	20°C, 3 weeks	NA	NA	aggregates
0.2	0.2% NG	DGDG	0.75	350mM KAc,35mM LiCl	10mM Glycine+	7.4	20°C, 3 weeks	clear solution	yellow	NA
0.2	0.2% NG	DGDG	1	350mM KAc,35mM LiCl	10% Glycerol+	7.4	20°C, 3 weeks	clear solution	brown	aggregates
0.2	0.2% NG	DGDG	1.5	350mM KAc,35mM LiCl	350mM Kac+	7.4	20°C, 3 weeks	precipitate	green	aggregates
0.2	0.2% NG	DGDG	2	350mM KAc,35mM LiCl	35mM LiCl	7.4	20°C, 3 weeks	clear solution	yellow	aggregates
0.2	0.2% NG	MGDG+PC*	0.1	350mM KAc,35mM LiCl	25 ml of	7.4	20°C, 3 weeks	precipitate	yellow	aggregates
0.2	0.2% NG	MGDG+PC	0.5	350mM KAc,35mM LiCl	1mM Na-azide+	7.4	20°C, 3 weeks	precipitate	NA	NA
0.2	0.2% NG	MGDG+PC	0.75	350mM KAc,35mM LiCl	10mM Glycine+	7.4	20°C, 3 weeks	precipitate	yellow	aggregates
0.2	0.2% NG	MGDG+PC	1	350mM KAc,35mM LiCl	10% Glycerol+	7.4	20°C, 3 weeks	precipitate	green	aggregates
0.2	0.2% NG	MGDG+PC	1.5	350mM KAc,35mM LiCl	350mM Kac+	7.4	20°C, 3 weeks	precipitate	green	NA
0.2	0.2% NG	MGDG+PC	2	350mM KAc,35mM LiCl	35mM LiCl	7.4	20°C, 3 weeks	precipitate	green	NA

No organization was observed when the additives potassium acetate and lithium chloride

were used.

---

[2] * MGDG:PC::2:1 in every trial set

Table 39: Crystallisation screen using 3 lipid combinations, 6 LPRs and MgCl₂ as additive.

Protein	Detergent	Lipid	LPR(w/w)	Additives	Dialysis buffer	pH	Duration	characteristic	Colour	Remark
mg/ml										
0.2	0.2% NG	MGDG	0.1	50mM MgCl₂	25 ml of	7.4	20°C, 3 weeks	clear solution	yellow	small vescicles
0.2	0.2% NG	MGDG	0.5	50mM MgCl₂	1mM Na-azide+	7.4	20°C, 3 weeks	clear solution	yellow	small vescicles
0.2	0.2% NG	MGDG	0.75	50mM MgCl₂	10mM Glycine+	7.4	20°C, 3 weeks	precipitate	brown	aggregates
0.2	0.2% NG	MGDG	1	50mM MgCl₂	10% Glycerol+	7.4	20°C, 3 weeks	precipitate	brown	tube
0.2	0.2% NG	MGDG	1.5	50mM MgCl₂	50mM MgCl₂	7.4	20°C, 3 weeks	clear solution	brown	aggregates
0.2	0.2% NG	MGDG	2	50mM MgCl₂		7.4	20°C, 3 weeks	precipitate	green	aggregates
0.2	0.2% NG	DGDG	0.1	50mM MgCl₂	25 ml of	7.4	20°C, 3 weeks	precipitate	green	NA
0.2	0.2% NG	DGDG	0.5	50mM MgCl₂	1mM Na-azide+	7.4	20°C, 3 weeks	precipitate	green	NA
0.2	0.2% NG	DGDG	0.75	50mM MgCl₂	10mM Glycine+	7.4	20°C, 3 weeks	precipitate	yellow	NA
0.2	0.2% NG	DGDG	1	50mM MgCl₂	10% Glycerol+	7.4	20°C, 3 weeks	precipitate	yellow	aggregates
0.2	0.2% NG	DGDG	1.5	50mM MgCl₂	50mM MgCl₂	7.4	20°C, 3 weeks	precipitate	green	NA
0.2	0.2% NG	DGDG	2	50mM MgCl₂		7.4	20°C, 3 weeks	clear solution	yellow	NA
0.2	0.2% NG	MGDG+PC*	0.1	50mM MgCl₂	25 ml of	7.4	20°C, 3 weeks	precipitate	green	NA
0.2	0.2% NG	MGDG+PC	0.5	50mM MgCl₂	1mM Na-azide+	7.4	20°C, 3 weeks	precipitate	yellow	aggregates
0.2	0.2% NG	MGDG+PC	0.75	50mM MgCl₂	10mM Glycine+	7.4	20°C, 3 weeks	precipitate	yellow	aggregates
0.2	0.2% NG	MGDG+PC	1	50mM MgCl₂	10% Glycerol+	7.4	20°C, 3 weeks	precipitate	yellow	aggregates
0.2	0.2% NG	MGDG+PC	1.5	50mM MgCl₂	50mM MgCl₂	7.4	20°C, 3 weeks	precipitate	yellow	aggregates
0.2	0.2% NG	MGDG+PC	2	50mM MgCl₂		7.4	20°C, 3 weeks	precipitate	yellow	aggregates

Small vesicles were observed when MgCl₂ salt was used in conditions where MGDG was present and the LPR was 0.1 and 0.5.

Table 40: Crystallisation screen using 3 lipid combinations, 6 LPRs and KCl as additive.

Protein	Detergent	Lipid	LPR(w/w)	Additives	Dialysis buffer	pH	Duration	characteristic	Colour	Remark
mg/ml										
0.2	0.2% NG	MGDG	0.1	250mM KCl	25 ml of	7.4	20°C, 3 weeks	clear solution	bright yellow	aggregates
0.2	0.2% NG	MGDG	0.5	250mM KCl	1mM Na-azide+	7.4	20°C, 3 weeks	precipitate	yellow	aggregates
0.2	0.2% NG	MGDG	0.75	250mM KCl	10mM Glycine+	7.4	20°C, 3 weeks	clear solution	yellow	aggregates
0.2	0.2% NG	MGDG	1	250mM KCl	10% Glycerol+	7.4	20°C, 3 weeks	NA	NA	NA
0.2	0.2% NG	MGDG	1.5	250mM KCl	250mM KCl	7.4	20°C, 3 weeks	clear solution	yellow	large vesicles
0.2	0.2% NG	MGDG	2	250mM KCl		7.4	20°C, 3 weeks	precipitate	brown	large sheets
0.2	0.2% NG	DGDG	0.1	250mM KCl	25 ml of	7.4	20°C, 3 weeks	precipitate	yellow	aggregates
0.2	0.2% NG	DGDG	0.5	250mM KCl	1mM Na-azide+	7.4	20°C, 3 weeks	precipitate	yellow	sheet
0.2	0.2% NG	DGDG	0.75	250mM KCl	10mM Glycine+	7.4	20°C, 3 weeks	NA	NA	NA
0.2	0.2% NG	DGDG	1	250mM KCl	10% Glycerol+	7.4	20°C, 3 weeks	clear solution	yellow	small vesicles
0.2	0.2% NG	DGDG	1.5	250mM KCl	250mM KCl	7.4	20°C, 3 weeks	precipitate	green	NA
0.2	0.2% NG	DGDG	2	250mM KCl		7.4	20°C, 3 weeks	precipitate	green	NA
0.2	0.2% NG	MGDG+PC*	0.1	250mM KCl	25 ml of	7.4	20°C, 3 weeks	clear solution	yellow	aggregates
0.2	0.2% NG	MGDG+PC	0.5	250mM KCl	1mM Na-azide+	7.4	20°C, 3 weeks	clear solution	yellow	aggregates
0.2	0.2% NG	MGDG+PC	0.75	250mM KCl	10mM Glycine+	7.4	20°C, 3 weeks	clear solution	yellow	aggregates
0.2	0.2% NG	MGDG+PC	1	250mM KCl	10% Glycerol+	7.4	20°C, 3 weeks	precipitate	yellow	aggregates
0.2	0.2% NG	MGDG+PC	1.5	250mM KCl	250mM KCl	7.4	20°C, 3 weeks	clear solution	yellow	aggregates
0.2	0.2% NG	MGDG+PC	2	250mM KCl		7.4	20°C, 3 weeks	precipitate	green	NA

Promising results were observed when KCl was used as an additive in presence of MGDG

and secondary detergent NG. At LPRs between 1.5 and 2.0 a strong tendency to organize into

vesicles or sheets was observed. Exemplary pictures of these are shown below (figure 40).

The size of vesicles and sheets was poor when DGDG was used.
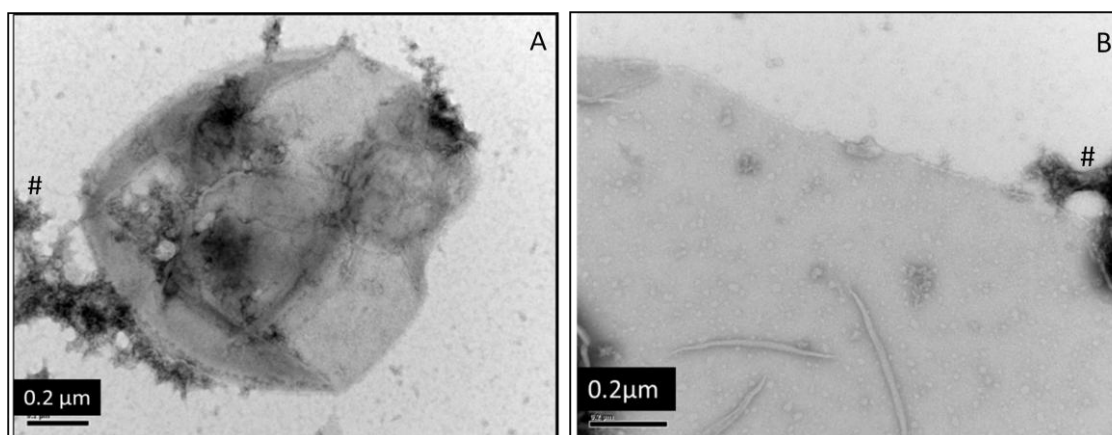
Figure 40: Different types of ordered structures obtained after dialysis as seen under the electron microscope after negative staining. Panel A; a collapsed vesicle when MGDG was used in the LPR of 1.5 and KCl was used as an additive in 250mM, panel B; a sheet when MGDG was used in LPR 2 and KCl was used as an additive in 250mM. # represents area where protein-lipid aggregates are seen. (Refer table 40).

Table 41: Crystallisation screen using 3 lipid combinations, 6 LPRs and NaCl as additive

Protein	Detergent	Lipid	LPR	Additives	Dialysis buffer	pH	Duration	characteristic	Colour	Remark
mg/ml										
0.2	0.2% NG	MGDG	0.1	250mM NaCl	25 ml of	7.4	20°C, 3 weeks	precipitate	green	aggregates
0.2	0.2% NG	MGDG	0.5	250mM NaCl	1mM Na-azide+	7.4	20°C, 3 weeks	clear solution	yellow	aggregates
0.2	0.2% NG	MGDG	0.75	250mM NaCl	10mM Glycine+	7.4	20°C, 3 weeks	clear solution	yellow	aggregates
0.2	0.2% NG	MGDG	1	250mM NaCl	10% Glycerol+	7.4	20°C, 3 weeks	NA	yellow	NA
0.2	0.2% NG	MGDG	1.5	250mM NaCl	250mM NaCl	7.4	20°C, 3 weeks	clear solution	yellow	vesicles
0.2	0.2% NG	MGDG	2	250mM NaCl		7.4	20°C, 3 weeks	precipitate	yellow	sheet
0.2	0.2% NG	DGDG	0.1	250mM NaCl	25 ml of	7.4	20°C, 3 weeks	NA	NA	NA
0.2	0.2% NG	DGDG	0.5	250mM NaCl	1mM Na-azide+	7.4	20°C, 3 weeks	precipitate	yellow	aggregates
0.2	0.2% NG	DGDG	0.75	250mM NaCl	10mM Glycine+	7.4	20°C, 3 weeks	clear solution	yellow	small vesicles
0.2	0.2% NG	DGDG	1	250mM NaCl	10% Glycerol+	7.4	20°C, 3 weeks	clear solution	yellow	small vesicles
0.2	0.2% NG	DGDG	1.5	250mM NaCl	250mM NaCl	7.4	20°C, 3 weeks	precipitate	green	NA
0.2	0.2% NG	DGDG	2	250mM NaCl		7.4	20°C, 3 weeks	precipitate	green	NA
0.2	0.2% NG	MGDG+PC*	0.1	250mM NaCl	25 ml of	7.4	20°C, 3 weeks	NA	NA	NA
0.2	0.2% NG	MGDG+PC	0.5	250mM NaCl	1mM Na-azide+	7.4	20°C, 3 weeks	NA	NA	NA
0.2	0.2% NG	MGDG+PC	0.75	250mM NaCl	10mM Glycine+	7.4	20°C, 3 weeks	NA	NA	NA
0.2	0.2% NG	MGDG+PC	1	250mM NaCl	10% Glycerol+	7.4	20°C, 3 weeks	NA	NA	NA
0.2	0.2% NG	MGDG+PC	1.5	250mM NaCl	250mM NaCl	7.4	20°C, 3 weeks	NA	NA	NA
0.2	0.2% NG	MGDG+PC	2	250mM NaCl		7.4	20°C, 3 weeks	NA	NA	NA

Using the additive NaCl no structural organization was observed. Thus from the results of the

several tested conditions (tables 38-41) it was clear that MGDG was the lipid of choice to be

used between the LPRs 1.5 and 2.0. It was also clear that the monovalent cation K^+ is needed

to observe any organization into vesicles or sheets. However since no results were obtained

when KAc was used it was clear that K^+ must be used in the form of KCl salt.

Further screening was thus conducted based on these reference points of using,

    i)   MGDG,

    ii)   LPR between 1.5 and 2.0,

    iii)   Primary additive KCl.

Details of this screen are outlined in table 42.

Table 42: Crystallisation screen using MGDG in 2 different LPRs using KCl as the primary additive.

Protein	Detergent	Lipid	LPR(w/w)	Additives	Dialysis buffer	pH	Duration	characteristic	Colour	Remark	Diffraction
mg/ml											
0.2	0.2% NG	MGDG	1	50 mM KCl	25 ml of	7.4	20°C, 3 weeks	precipitate	yellow	aggregates	none
0.2	0.2% NG	MGDG	1	100 mM KCl	1mM Na-azide+	7.4	20°C, 3 weeks	clear solution	yellow	aggregates	none
0.2	0.2% NG	MGDG	1	250 mM KCl	10mM Glycine+	7.4	20°C, 3 weeks	clear solution	yellow	large vescicles	poor
0.2	0.2% NG	MGDG	1	500 mM KCl	10% Glycerol+	7.4	20°C, 3 weeks	precipitate	brown	large vesicles	poor
					equimolar KCl						
0.2	0.2% NG	MGDG	2	50 mM KCl	25 ml of	7.4	20°C, 3 weeks	precipitate	yellow	aggregates	none
0.2	0.2% NG	MGDG	2	100 mM KCl	1mM Na-azide+	7.4	20°C, 3 weeks	precipitate	yellow	large vesicles	poor
0.2	0.2% NG	MGDG	2	250 mM KCl	10mM Glycine+	7.4	20°C, 3 weeks	precipitate	yellow	large vesicles	poor
0.2	0.2% NG	MGDG	2	500 mM KCl	10% Glycerol+	7.4	20°C, 3 weeks	precipitate	brown	large vesicles	poor
					equimolar KCl						
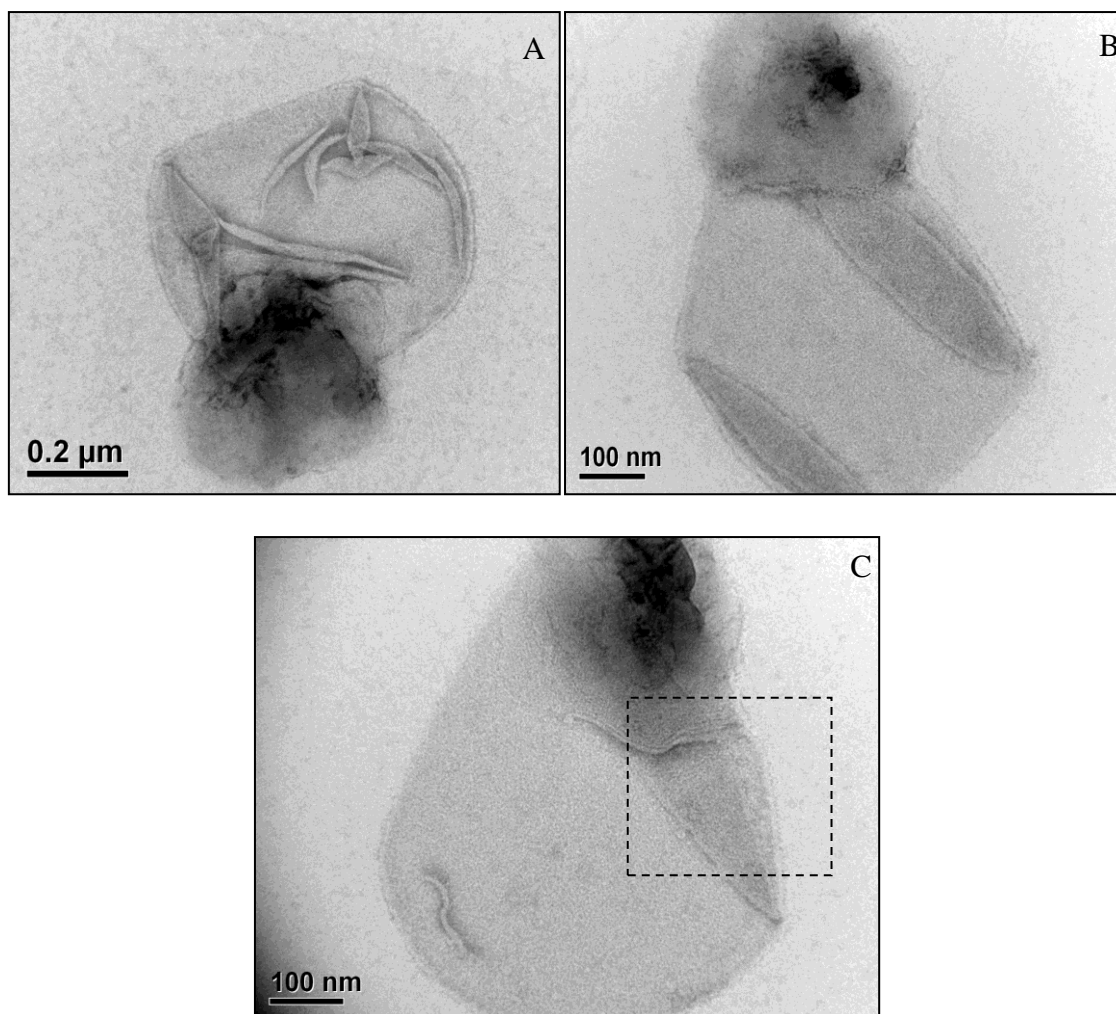
Figure 41: Vesicles obtained after crystallization using MGDG and KCl. In panel A after using KCl in 250 mM and LPR 1. In panel B after using 500 mM KCl and LPR 1 and in panel C after using KCl in 250 mM and LPR 2. Small crystalline patches were observed which are denoted by a box.

Table 43: Outlines the conditions tested for crystallization using KCl as the primary additive and several secondary additives.

Protein mg/ml	Detergent	Lipid	LPR(w/w)	Additives	2° additive	Dialysis buffer	pH	Duration	characteristic	Colour	Remark	Diffraction
0.2	0.2% NG	MGDG	1	250 mM KCl	2.5 mM CsCl	25 ml of	7.4	20°C, 3 weeks	precipitate	yellow	aggregates	none
0.2	0.2% NG	MGDG	2	250 mM KCl	2.5 mM CsCl	1mM Na-azide+	7.4	20°C, 3 weeks	clear solution	yellow	aggregates	none
						10mM Glycine+						
0.2	0.2% NG	MGDG	1	250 mM KCl	2.5 mM LiCl	10% Glycerol+	7.4	20°C, 3 weeks	clear solution	yellow	aggregates	none
0.2	0.2% NG	MGDG	2	250 mM KCl	2.5 mM LiCl	equimolar salts	7.4	20°C, 3 weeks	precipitate	brown	aggregates	none
						in all cases						
0.2	0.2% NG	MGDG	1	250 mM KCl	2.5 mM ZnCl$_2$		7.4	20°C, 3 weeks	precipitate	green	aggregates	none
0.2	0.2% NG	MGDG	2	250 mM KCl	2.5 mM ZnCl$_2$		7.4	20°C, 3 weeks	precipitate	green	aggregates	none
0.2	0.2% NG	MGDG	1	250 mM KCl	2.5 mM CaCl$_2$		7.4	20°C, 3 weeks	clear solution	yellow	aggregates	none
0.2	0.2% NG	MGDG	2	250 mM KCl	2.5 mM CaCl$_2$		7.4	20°C, 3 weeks	precipitate	brown	aggregates	none
0.2	0.2% NG	MGDG	1	250 mM KCl	2.5 mM CuCl$_2$		7.4	20°C, 3 weeks	precipitate	blue-green	aggregates	none
0.2	0.2% NG	MGDG	2	250 mM KCl	2.5 mM CuCl$_2$		7.4	20°C, 3 weeks	precipitate	blue-green	aggregates	none
0.2	0.2% NG	MGDG	1	250 mM KCl	2.5 mM AlCl$_3$		7.4	20°C, 3 weeks	clear solution	yellow	aggregates	none
0.2	0.2% NG	MGDG	2	250 mM KCl	2.5 mM AlCl$_3$		7.4	20°C, 3 weeks	precipitate	brown	aggregates	none

No vesicles were obtained after the trials were repeated with KCl as primary additive and monovalent, divalent or trivalent cations as secondary additives. Thus only poor quality vesicles as shown in figure 41 were obtained after ~ 120 trials. These results point out clearly towards certain conditions which show a propensity for organization into crystals namely potassium chloride as the only additive, MGDG as the lipid and low LPRs. More thorough investigations concerning secondary additive and detergent are needed to obtain high quality crystals of FcpA from *P. tricornutum*.

5 Discussion

----

5   Discussion

One of the biggest bottlenecks in Fcp research has been that single specific Fcps have not been purified owing to the similar molecular weights and hydrophobicity. In order to gain more information regarding structure it is necessary that Fcps be reconstituted into crystals. However this has not been possible with the heterogeneous pool of Fcps that have been purified so far (Büchel 2003, Beer et al. 2006, Lepetit et al. 2007). Furthermore there have been no clear evidences about the existence of photosystem specific antenna systems or otherwise in diatoms (Brakemann et al. 2006, Veith 2009, Lepetit et al. 2011).

A highly reproducible protocol was developed in this study to specifically purify His-tagged FcpA; a Fcp representative of the light harvesting type of proteins in diatoms; from the whole pool of Fcps in *P. tricornutum*. Comparative biochemical analyses were made with a highly pure WT Fcp pool purified using sucrose density gradient centrifugation followed by gel filtration chromatography. Several trials were also carried out to crystallize the FcpA$_{His}$ in 2 dimensions.

Investigation on the association of FcpA with photosystems was carried out using a modified protocol established by Veith and Büchel (2007). A combination of sucrose density gradient centrifugation and ion exchange chromatography was used here to isolate Fcps specifically and functionally associated with photosystem I.

5.1   His-tagged assisted purification of a specific Fcp protein complex.

P. tricornutum is the second diatom after *T. pseudonana* whose genome was fully sequenced and available for public use. Acquisition of genomic data of *P. tricornutum* began much earlier than the genome project and several EST sequences for *P. tricornutum* were known as early as in the year 2004 (Maheswari). Gene clusters encoding 6 Fcps (A-F) were identified which created the possibility of modifications at the genetic level (Bhaya and Grossman 1993). The highly challenging task of the transformation of *P. tricornutum* was successfully

----

reported using particle bombardment and the selectable reporter gene *sh ble* and reproducible protocols were made available for the same (Apt et al. 1996). A general transformation vector pPha-T1 became available which completed the repertoire of materials and methods needed for creation of recombinant strains of *P. tricornutum* for detailed biochemical studies (Zaslavskaia et al. 2000).

A *fcpA* gene carrying a fragment encoding a hexa-histidine tag on the 3' terminus could be created for the purpose of purification of a single Fcp. The modified gene also encoded the complete FcpA plastid targeting presequence with a conserved sequence at the predicted signal peptide cleavage site (Kilian and Kroth 2005, Gruber et al. 2007). It has been shown previously with the presequence of the γ-subunit of the *P. tricornutum* plastid ATP synthetase, that preproteins are also targeted correctly to the plastid when a His-tag is engineered to their C-terminus (Apt et al. 2002). Targeting of the $fcpA_{His}$ gene product to the thylakoid membranes should therefore have functioned analogously to the WT *fcp* gene products.

Using affinity chromatography, a $FcpA_{His}$ containing complex could be specifically purified thus proving that the strategy of his-tagging for purification of single fcp is functional. The yield of the procedure was very low and approximately 0.2% Chl *a* could be recovered in the form of the recombinant protein compared to the total amount of starting Chl *a* of the thylakoids. Expression of the recombinant gene was under the control of the native promoter of the gene in the transformed cell lines (Zaslavskaia et al. 2000) and this being a light regulated promoter this system did not allow an artificial overexpression of $FcpA_{His}$ (Oeltjen et al. 2002). This was however the only usable system available at the time when Dr. Schmidt (University of Frankfurt) designed the transformation experiments. The homologous recombination in *P. tricornutum* has not been reported so far and doubts have been expressed if it exists (Falciatore and Bowler 2002; de Riso et al. 2009). This implies that the targeted knock out of a specific gene is not possible. Therefore in the recombinant strain, FcpA1.2, the

----

His-tagged Fcp was expressed along with a background of all Fcps leading to an effective low expression level of the recombinant protein. Meanwhile targeted knockdown of specific genes has become possible using interference RNA technology (de Riso et al. 2009). This might lead to a higher expression of a recombinant protein and will be the strategy in upcoming projects. Further the usage of a light independent promoter to drive the expression of *fcp* genes would create the possibility of a higher expression rate. Several groups have started the usage of the transformation vector pPhaNR which allows for the usage of a nitrate reductase as a molecular switch to turn on the expression of the gene under control which is expected to deliver better results than a light dependent promoter like pfcpA (Hempel et al. 2010, Miyagawa-Yamaguchi et al. 2011).

5.1.1 Pigment content of $FcpA_{His}$ and WT Fcps.

Western blotting using anti-His antibody and anti-Fcp antibody could prove that the affinity purified product was indeed His-tagged Fcp (figure 27). In spite of loading same concentrations of Chl *a*, signals obtained in case of WT Fcp pool were consistently lesser than that in case of $FcpA_{His}$ (figure 26 and 27). Lavaud and colleagues have reported pigment content of *P. tricornutum* cells where Fx content was 0.68±0.03 per mole of Chl *a* and Chl *c* was 0.15±0.003 per mol of Chl *a*. No xanthophyll cycle pigments were detected in whole cells (Lavaud et al. 2003). The pigment content in this study was significantly higher than the previously reported values (table 32). Fx content lay between 0.78-0.80 mol/mol of Chl *a* and Chl *c* between 0.21-0.23 mol per mol of Chl *a*. The total amount of XC pigments (i.e. Ddx+Dtx) were similar at 0.12 mole per mol of Chl *a* in both cultures. One of the major reasons for the higher pigment values in this study can be attributed to the method and duration of cultivation of the cells. The report of Lavaud was also based on cultures grown using sterile airlifts which bubbled air continuously through the cultures. However the cells were allowed to grow only for 3-4 days after which pigment content was determined.

Unfortunately no mention is made about the cell number or the chlorophyll content at this time point. In this study cells were allowed to grow under continuous gaseous exchange for 10 days before harvesting. At the point where cells were harvested the cultures appeared intense dark brown and the cell number was also extremely high (43-59 million cells/ml culture; table 30). One possibility is that during culturing, when cell number increased exponentially, enough light was not available to all cells. To keep photochemistry at optimum the cross section of absorbance of excitation energy had to be increased which means that the amount of Fcps and therefore of the photosynthetic pigments was upregulated. Interesting differences were observed also when the pigment content of the WT Fcp pool was compared with that of pure $FcpA_{His}$ (table 33). The Fx content associated with the pure WT Fcps (1.710±0.137) was tremendously high as compared to that of $FcpA_{His}$ (1.199±0.090). While the Chl *c* content remained similar in both cases (0.36-0.37 mol per mol Chl *a*) the amount of XC pigments was at least 4 folds higher in case of the WT Fcp pool than $FcpA_{His.}$ The total pool of Fcps named LHCF obtained after sucrose density gradient centrifugation contained 1.1±0.059 mol per mol of Chl *a* in reports by (Lavaud et al. 2003). In another study the Fcp pool, named F, was shown to contain 1.22±0.061 mol Fx/mol Chl *a* and 0.066±0.003 Ddx per mol of Chl *a* (Guglielmi et al. 2005). A fraction enriched in Fx and Ddx named fraction 'D' was localized at a height above the fcp band in SDG. But from spectroscopic investigations and polypeptide analyses it could be seen that this band did not represent an exclusive Fcp population.

Mass spectrometric analyses of the $FcpA_{His}$ purified over affinity chromatography had revealed it to be a complex consisting also of FcpE subunits (table 34). Detailed investigation about subcomplexes within the major pool of the trimeric light harvesting complexes from *P. tricornutum* has been carried out and it has been observed that several other trimeric complexes apart from FcpA-E exist (K.Gundermann, University of Frankfurt, personal

communication). Lepetit analysed the trimeric Fcp pool of *P. tricornutum* for population identity and found that this pool consisted of all the major known Lhcf along with Lhcr proteins and a few Lhcx proteins (Lepetit et al. 2007, Lepetit et al. 2010). The composition of the WT Fcp pool in this study must therefore be comparable to these reports.

Both FcpA and FcpE fall into Lhcf type (group I of Fcps) which are known to be the classical light harvesting proteins. It was therefore unexpected to find lower amounts of Fx in the FcpA$_{His}$ complexes compared with the WT Fcp pool. Lhcx type of proteins are postulated to play a key role in photoprotection by modulating the amount of bound xanthophyll cycle pigments Ddx and Dtx. Additional Ddx is sysnthesised under HL stress and associated with Lhcx like proteins (Beer et al. 2006, Zhu and Green 2010). A correlation in the fluorescence quenching and the amount of Dtx has been shown (Gundermann and Büchel 2008). Thus the amount of at least XC pigments has been shown to vary under different conditions as a response to light acclimation. It is therefore logical to assume that the different Fcps are differently pigmented. The high amount of Fx and XC pigments can be attributed to the different Fcps other than FcpA and FcpE in the WT Fcp pool. The second reason for the high pigment content of the WT Fcp pool can also be attributed to the process of purification. Most of the pigment data reported for Fcps has been generated where the purification process was solely sucrose density gradient centrifugation (Guglielmi et al. 2005, Lepetit et al. 2007). In this study a combined approach was used for the purification of the WT Fcp pool i.e. a second purification step of gel filtration that should reduce contamination due to proteins comigrating on SDG. It is known that the xanthophyll cycle pigments can be lost from the antenna complexes more easily than Fx, Chl *c* and Chl *a* due to their probable peripheral binding site (Beer et al. 2006). It was therefore not surprising that the concentrations of Ddx+Dtx were higher in the WT Fcp fraction than in the FcpA$_{His}$ complex (Table 33), because WT Fcp was not subjected to the slightly harsher condition of IMAC during

----

purification. In the case of the FcpA$_{His}$ complex, the pigment data include only the pool of pigments tightly associated with the polypeptides, which seem to be the 'core' pigments quite similar in all FCP complexes isolated so far. Thus, a characterization of several individual Fcps of the three different classes, Lhcf, r and x, is needed to prove that the different Fcps can bind different pigments in different stoichiometries.

5.1.2   Oligomeric organisation of Fcps

FcpA$_{His}$ as well as the WT Fcp from SDG eluted from the analytical gel filtration column at the same time (figure 30) in one single peak. A small trailing peak was observed in case of WT Fcp which was possibly contamination with free pigment due to imprecise extraction of the Fcp band from SDG. The trimeric FCPa complex from *C. meneghiniana* also eluted from the same column at identical time like that of the WT Fcp and FcpA$_{His}$. Thus both WT Fcp and FcpA$_{His}$ were trimers. Neither monomers nor higher oligomers were obtained. Fcp populations have been isolated from different organisms in different oligomeric states. FCPa; a trimeric complex and FCPb; a higher oligomeric complex (suggested to be hexameric or nonameric) could be isolated in co-existence from *C. meneghiniana*. Trimeric Fcp populations were isolated from *P. tricornutum* when thylakoids were solublilised using α-DDM using Chl to det ratio of 1:15 (Guglielmi et al. 2005). Using very mild solubilisation of thylakoids using β-DDM (chl: det :: 1:5) a higher oligomeric complex FCPo was isolated and using relatively harsher solubilisation (chl:det:: 1:20 or 1:40) trimeric FCP complexes could be isolated (Lepetit et al. 2007). Unfortunately the existence of this higher oligomer in *P. tricornutum* has not been reported or studied further. Thus, trimers and higher oligomers of Fcps seem to co-exist in *C. meneghininina* however not in *P. tricornutum*. In this study the Chl *a*: det ratio was set to 1:30 which explains the observation that the complexes were trimeric. The hypothesis that trimers are the basic stable units of organization of Fcps in *P. tricornutum* can be confidently supported from the results of this study.

5 Discussion

5.1.3 Spectroscopic investigations

The absorption spectra of FcpA$_{His}$ and the WT Fcp pool were similar in spectral shape. The WT Fcp pool showed a very huge shoulder between 450-550 nm which was absent in case of FcpA$_{His}$ (figure 28A). From difference spectrum it was shown that this huge shoulder arose only due to the presence of high amounts of carotenoids (figure 28B). In the previous comments about pigment content it was discussed that different Fcps might be differently pigmented depending upon their function (please refer section 5.1.1).

Excitation spectra and fluorescence emission spectra demonstrated that the transfer of energy from Chl *c* and Fx to Chl *a* was intact in both WT Fcp pool and FcpA$_{His}$. A small shoulder was observed at around 640 nm when Chl *c* in FcpA$_{His}$ was preferentially excited and the fluorescence emission was recorded (figure 31C) which was an indication that some Chl *c* was decoupled from the FcpA$_{His}$ complex during purification. However this shoulder disappeared when an additional gel filtration was performed (figure 31C). It suggests that the Chl *c* emission observed after IMAC was not due to uncoupled Chl *c* but rather due to free Chl *c* independent of the FcpA$_{His}$ complex which could have co-eluted during purification. The additional gel filtration that was performed with FcpA$_{His}$ not only confirmed its oligomeric state but also indicated that the complex was stable and could retain an intact energy transfer capacity after a series of purification processes.

5.1.4 Organisation of pigments on polypeptide backbone of Fcps

In the absorbance spectrum the Qy max of Chl *a* absorption was seen at 672 nm for both FcpA$_{His}$ and WT Fcp pool. In case when a circular dichroism spectra was recorded a 3 nm shift was seen where a prominent (-) 669 nm band was observed in FcpA$_{His}$ (figure 32). This was suggestive of the presence of a heterogeneous pool of Chl *a* (Mimuro et al. 1990). Further in this area of the spectrum no split signal was associated with the (-) 669 nm band. The same was true also for WT Fcp pool (-) 670 nm band. This indicates that Chl *a*-Chl *a*

----

interactions do not exist in case Fcps of *P. tricornutum*. The same finding, i.e. the absence of split signals in the red region, has been reported in case of all oligomeric states of the brown alga *Dictyota dichotoma.* The only report of Chl *a*- Chl *a* interactions in the red region were from the trimeric FCPa and higher oligomeric complex FCPb from the cyclic diatom *C. meneghiniana* (Büchel 2003). In both FCPa and FCPb small signals were observed at (-) 663 and (-) 674 nm separated by more positive (+) 669 nm signal. The (-) 663 nm band was more pronounced in case of higher oligomeric FCPb complex composed of 19 kDa proteins. It was suggested that the binding of Chl *a* to the 19 kDa polypeptides could be different than to the 18kDa polypeptides or Chl *a*- Chl *a* interactions could be present only in higher oligomeric states. The second suggestion for the origin of the split signal in red region does not seem to be correct since no similar signals in red region were observed on case of the higher oligomeric FCPo complex of *P. tricornutum* (Lepetit et al. 2007). Thus the origins of CD signals in the red region need more investigation. The loss of CD signals in FCP complexes in the red region of the spectrum has been investigated by recording CD of whole cells. In the whole cells of *P. tricornutum* and *P. meringensis*, it has been shown that a psi-type CD signal is present between (-) 679 nm and (+) 693 nm which is attributed to chiral macrodomain organizations within the thylakoid membrane which is lost as cells as disrupted during isolation of Fcps (Szabó et al. 2008). In the present study French press disruption of the cells to would have led to the loss of CD signals in the red region.

An excitonic CD signal in the blue region was indicative that the organization of pigments on the isolated proteins was still intact and that the proteins have retained the native state like that seen in the thylakoid membrane. The split signal in Soret region between (-) 467 nm and (+) 470 nm for both WT Fcp pool and FcpA$_{His}$ was a clear indicative of the presence of an excitonic dimer of a Chl *a*-Chl *c* or Chl *a*-carotenoid dimer. Some contribution of carotenoids in this band cannot be ruled out since the (-) 467 band was broad and Fx is known to absorb

----

light in this region of the spectrum. However the contribution of Chl *c* or Fx in this signal is a matter of debate. The circular dichroism shape reported in this study is well comparable to that reported for the trimeric Fcp population as well as the higher oligomeric FCPo complex (Lepetit et al. 2007). The common excitonic split signal in the blue region also reported in case of FCPa and FCPb from *C.meneghiniana* and in the LHC of a xanthophyte alga (Büchel and Garab 1997) is suggestive that the presence of a Chl *a*-carotenoid or Chl *a*-Chl *c* excitonic dimer is a conserved feature in Chl *a /c* containing algae.

5.1.5   Towards 2D crystallization of FcpA_{His} from *P. tricornutum*:

MGDG and PC have been shown to associate with highly pure antenna complexes of both *C.meneghiniana* and *P. tricornutum* both under low light and high light conditions (Goss et al. 2009, Lepetit et al. 2011). MGDG has been proposed to carry out several functions like a reservoir for excess Ddx during HL, solubilisation of Ddx which allows effective action of the enzyme diadinoxanthin deepoxidase. It was therefore not surprising the FcpA_{His} could be reconstituted into vesicles using MGDG. However it is a thumb rule in crystallization that the amount of impurities is responsible for disturbance in the crystal formation, growth and homogeneity (Kühlbrandt 1992). Low yields of purification of FcpA_{His} (refer 4.2.3) could not allow a single purification batch to be utilized for crystallization trials and this necessitated a mixing of different batches of purified protein and thus involved freeze-thawing of proteins to some extent. It has been shown that freeze-thaw cycles lead to the monomerisation of the trimers in *P. tricornutum* (Lepetit et al. 2007). The existence of a heterogeneous pool of Fcps (monomers plus trimers) cannot be ruled out which effectively a step-back in the reconstitution of FcpA_{His}. One strategy that can be applied to overcome this effect can be the resolubilisation of a trimeric FcpA_{His} containing complex and subsequent purification of the His-tagged FcpA monomers and crystallization trials with a homogenous pool of protein. Such a strategy has been successfully used for crystallization of LHCII-His in *N. tabacum*

(Flachmann and Kühlbrandt 1996). The other aspect that can be considered while making fresh crystallization trials, can be the isolation of native lipids from thylakoid membranes of *P. tricornutum* and attempting reconstitution using additional lipids. Use of native lipids has been demonstrated to give better results in some cases for e.g.: in 2D crystallization of PSII cores (Hankamer et al. 2001). The choice of the second detergent used in this study was solely influenced by the available data concerning 2D crystallization of the trimeric FCPa complex from *C. meneghiniana* in which NG was used as the second detergent. A thorough and systematic investigation for the right choice of secondary detergent and additive will create a wider web of potential crystallization conditions and improve the existing reconstitution results.

5.2   Specific interaction of Lhcf type proteins with photosystem I

For the purpose of isolation of PS-Fcp complexes, two different solubilisation conditions were applied to separate pigment protein complexes on a sucrose density gradient centrifugation. When 10 mM β-DDM or 15mM β-DDM was used only 3 distinct coloured bands containing free pigment, free Fcp complexes and photosystems were obtained. Milder solubilisation conditions than those used for the purification of pure Fcps were used in order to keep the functional and structural association between photosystems and Fcps intact (refer table 7). From the several different solubilisation conditions used in this study and the pattern obtained on the SDG (figures 21 and 33) it was clear that only a single green band corresponding to the presence of both photosystems can be obtained in case of *P. tricornutum*. As against this, the separation of PSI and PSII can be easily achieved in the centric diatom *C.meneghiniana* using SDG centrifugation (Veith et al. 2009). The mildest solubilisation (10mM β-DDM) led to a poor separation of complexes on the SDG and the photosystem band appeared much closer to the Fcp band than in the case when 15mM β-DDM solubilisation was used (figure 33). After a further ion exchange purification of the

----

green PSs bands from SDG it could be suspected that only peak 2 might contain a PS-Fcp complex due to its significant absorbance at 530 nm (figure 34). Polypeptide analysis using gel electrophoresis led to a band pattern in peak 2 which was similar to that reported for PSI-Fcp supercomplex (Veith and Büchel 2007). The band pattern resembled more closely to that reported by Berkaloff for a PSI-Fcp complex in *P. tricornutum* where a native complex was isolated on a SDG by solubilising thylakoids using the mild detergent digitonin and subsequent solubilisation of the native PSI-Fcp complex using β-DDM on a second SDG (Berkaloff et al. 1990). The PSI-Fcp complex was shown to retain proteins of 17 kDa and 19 kDa corresponding to the molecular mass of Fcps also after a second solubilisation. In this thesis, three distinct proteins of 19, 18 and 17 kDa were observed to be associated with PSI. In case of PSII containing fraction i.e. Peak 5, two smeared bands were observed around 19 and 20 kDa (figure 36). An antibody against all Fcps from *C. meneghiniana* showed signals only in peak 2 and peak 5. Peak 2 was assigned to PSI after comparison of the band pattern of PSI-Fcp complex and also due to immune reaction with antibody against core proteins PsaA and PsaB (figure 38). Peak 5 was attributed to PSII due to immune reaction with core protein D2 (figure 38). It was also shown to contain some Fcp proteins which were apparently higher in molecular mass than those found in the PSI sample.

No signal could be obtained either in peak 2 or 5 with an antibody against His-tag. One of the main considerations for this result should be the fact that the amount of His tagged FcpA in the total pool of Fcps was only ~ 1.5 % on Chl *a* basis. The concentration of the His-tag and possibly its masking by other WT Fcps seems to have been the problem that the His-tag was not detected by the antibody.

Mass spectrometry remained the only tool available for the identification of the Fcps associated with the two photosystems. The Lhcf group of proteins viz. FcpE , A, C and F were identified to be associated with PSI (table 35). FcpE was the most abundantly found

protein among these. The bands that were identified as Fcps from western blotting (figure 38) in PSII were identified as the intrinsic light harvesting protein CP43 of PSII. It has to be noted that the antibody against all Fcps from *C. meneghinaina* was raised from a Fcp pool which was purified only using sucrose density gradient centrifugation and this could be one of the reasons for cross reactivity against PSII core antenna proteins. From the spectroscopic investigations on PSI-Fcp sample it was observed that the fluorescence emission was quenched to a very high extent (~ 75 %) in the PSI-Fcp containing sample as compared to energetically intact pure Fcps (figure 39). The quantum efficiency of PSI at RT is ~1 meaning every photon that is absorbed by PSI leads to a charge separation at RC and thereby PSI is a fluorescence quencher. Therefore the intensity of quenching was significant in establishing that the Fcps were energetically coupled to the PSI.

In chromophytic algae there has been no evidence for the spatial separation of photosystems in the thylakoid membrane. One study has shown that the outer lamellae of the thylakoid membranes are slightly enriched in PSI compared to the inner stacks of the membrane which contain more PSII (Pyszniak and Gibbs 1992). However a 3D model explaining the thylakoid architecture in diatoms is not present. In higher plants electron tomographic results have been helpful in strengthening the helical model of grana and stroma architecture (Austin and Staehelin 2011). The grana stacks in higher plants lie in one plane while the parallel arranged stromal thylakoids wind helically around the grana. The grana and stroma thylakoids are interconnected by slits in the grana margins and the size of the slits might be controlled by plants to regulate the movement of protons and membrane proteins between the stacked grana and the unstacked stroma. This spatial separation of photosystems by granum formation in higher plants has been seen as an evolutionary response to separate the kinetically slow PSII from the fast trapping PSI and thereby avoiding a spillover from PSII to PSI. LHCI and LHCII constitute the specific light harvesting antenna of PSI and PSII in higher plants. The

Lhcs of rhodophytes and Chl *c* containing algae form a sister clade to most chlorophyte (higher plant) Lhc sequences which suggests that Chl *c* containing Lhcs diverged independently than those in the green lineage (Durnford et al. 1999, de Martino et al. 2000). Proteins homologous to LHCII which associate specifically with PSII in higher plants are thought to have evolved independently in Chl *c* containing algae. Due to the independent evolution of the Fcps in Chl *c* containing algae they are believed to be photosystem unspecific (Green and Parson 2003, Hoffman et al. 2011).

However, Veith and coworkers proved the association of a Lhcr type protein, Fcp4, with PSI in *C. meneghiniana* and extended the proposition of Eppard and Rhiel based on sequence homologies that Lhcr family of proteins might be specifically bound with PSI core (Veith et al. 2009). It was also suggested that Fcp1-3 and 5 represented typical subunits of PSII. However, using immune-blotting experiments it was shown that Fcp2 (Lhcf type) and Fcp4 (Lhcr type) are associated with both photosystems in *C. cryptica*. The presence of Fcp 2 associated with PSI was suggestive that photosystem specific antenna systems do not exist in diatoms (Brakemann et al. 2006) This concept has been proposed before through several studies where only one major Fcp pool could be purified from diatoms and related brown algae (Katoh and Ehara 1990, Berkaloff et al. 1990). Furthermore the antenna proteins copurified with PSI were similar to the main antenna complex (Berkaloff et al. 1990).

From a more intensive study on identification of specific Fcps from free fcp pool or PSI associated compexes, it was shown that 8 out of the 14 Lhcrs whereas only one Lhcf type protein (Lhcf3/4) was associated with PSI-Fcp enriched fractions (Lepetit et al. 2010). In the supplementary material reported for this paper additional 6 Lhcfs are indicated to be associated and identified by tandem mass spectrometry although with low sequence coverage. This paper presents results based on the purification of PSI-Fcp complex by means of only a sucrose density gradient centrifugation. Fcps associated with PSI in *C. meneghiniana* were

----

not reported since complete genomic data are not available for this organism. In the results obtained in this thesis study FcpE was identified as the most abundantly present protein associated with PSI core in addition to 3 other Fcps. Unfortunately no Lhcr type of protein could be identified. Several studies on the purification of pigment protein complexes in *P. triornutum* which use the mild detergent β-DDM have reported the presence of only 1 green band corresponding to the mixture of PSI and PSII (Joshi-Deo et al. 2010, Juhas M 2009). The crude separation of PSI and PSII from *P. tricornutum* on a discontinuous sucrose density gradient using a very mild solubilisation Chl: det:: 1:10 using β-DDM has been shown (Lepetit et al. 2007). However the PSI and PSII bands were not distinctly separated. This unclear separation between PSI and PSII on sucrose density gradient might create a situation where some of the proteins that are identified could represent a co-migrating pool. We used a very stringent purification protocol comprising of a sucrose density gradient centrifugation followed by ion exchange chromatography. The Fcps identified to be associated with PSI must therefore represent a strong attachment with the PSI core. Furthermore the energy transfer from Fcps to PSI was intact which was shown using excitation spectra (figure 39). A mere co-purification of Fcps would have led to a higher fluorescence contribution than observed.

A topology of the diatom thylakoid membrane has been proposed recently (Lepetit et al. 2011). It was suggested previously that PSI and their specific antennae (Lhcrs) exist preferentially in the outer lamellae of the thylakoid stacks. The outer lamellae are not free of PSII and peripheral antennae but contain lower amounts and perhaps in different oligomeric states than in the inner lamellae. This is thought to prevent a strong spillover from PSII to PSI. Under high light conditions it is suggested that Lhcx proteins are synthesized and associate with PSII as its photoprotectants. The possibility that a part of the peripheral Fcp complex dissociates from PSII under high light stress and forms higher order aggregates is

5 Discussion

----

also suggested. This model assumes that the thylakoid membrane of diatoms is divided into structural domains which provide the opportunity for the spatial separation and regulation of the diverse functional tasks associated with the thylakoid membrane.

In summary, the existence of a mixed population of PSII and PSI in the thylakoid membrane due to the lack of differentiation into grana and stroma as in higher plants leads to some degree of spillover from PSII to PSI which effectively reduces the working capacity of PSII. To overcome this energy loss, PSII amounts must be higher than PSI. PSII to PSI ratios varying from 1.3 to 4 has been reported in several diatoms (Trissl and Wilhelm 1993). It seems logical in this case that the distribution of excitation energy between the two photosystems occurs using an alteration of the amounts of PSII and PSI. Two different light harvesting systems operating specifically for photosystems might not be needed in this case. It is fully justifiable that the Lhcf type of proteins were found associated strongly and functionally to PSI core in this study especially when the two photosystems are randomly distributed in the thylakoid membranes of diatoms. The presence of Lhcr as a specific antenna of PSI cannot be doubted at least in the case of the centric diatom *C. meneghiniana*. However it might serve different function other than light harvesting for e.g. photoprotection. However this needs to be investigated in further details in a species independent manner, e.g. centric diatoms vs. pennate diatoms.

5.3 Conclusion

During this work it was possible to isolate for the first time a specific Fcp containing complex, FcpA$_{His}$, from a diatom species viz. *P. tricornutum*. Using gel filtration it was shown that this complex was a stable trimer. Furthermore using mass spectrometric analysis it could be shown that the binding partner of FcpA in the trimer is the FcpE polypeptide. Spectroscopic investigations indicated that the excitation energy transfer from the pigments Chl *c* and fucoxanthin to Chl *a* was intact in the purified complex. Circular dichroism spectra

5 Discussion

----

indicated that at least one Chl *a* molecule and one fucoxanthin molecule bound on the Fcp polypeptide interact excitonically.

A protocol was developed for the reconstitution of FcpA$_{His}$ into 2D crystals which grew mainly in the form of vesicles. This highly pure and stable FcpA$_{His}$ preparation and a protocol to reconstitute it form a solid background for further crystallization attempts.

A PSI-Fcp supercomplex could be isolated from *P. tricornutum* using a very mild solubilisation of thylakoids and subsequent ion exchange chromatography. Using spectroscopic analyses it could be proved that the Fcps were energetically coupled to PSI and mainly FcpE was identified to be associated with PSI after mass spectrometry. From molecular weights of Fcps associated with PSI and PSII after gel electrophoresis, it can be said that the stably bound Fcps seem different. However from this thesis it was evident that Lhcf type proteins are also associated with PSI and act as their light harvesting antenna. Since no Lhcr or Lhcx type of proteins could be identified, their interaction either with PSI or PSII remains unclear. From sequence homologies with LHCII it can be assumed that the Lhcf type of proteins might also act as the light harvesting antenna of PSII. The isolation of PSII-Fcp supercomplex using more refined methods and the subsequent identification of Fcps using sequencing will be the solution to solve this enigma.

A cartoon demonstrating the topology of the diatom thylakoid membrane based on conclusions from this work as well as information from literature is presented. A comparison is also made between the methods used in literature to purify Fcps and photosystem-Fcp complexes.
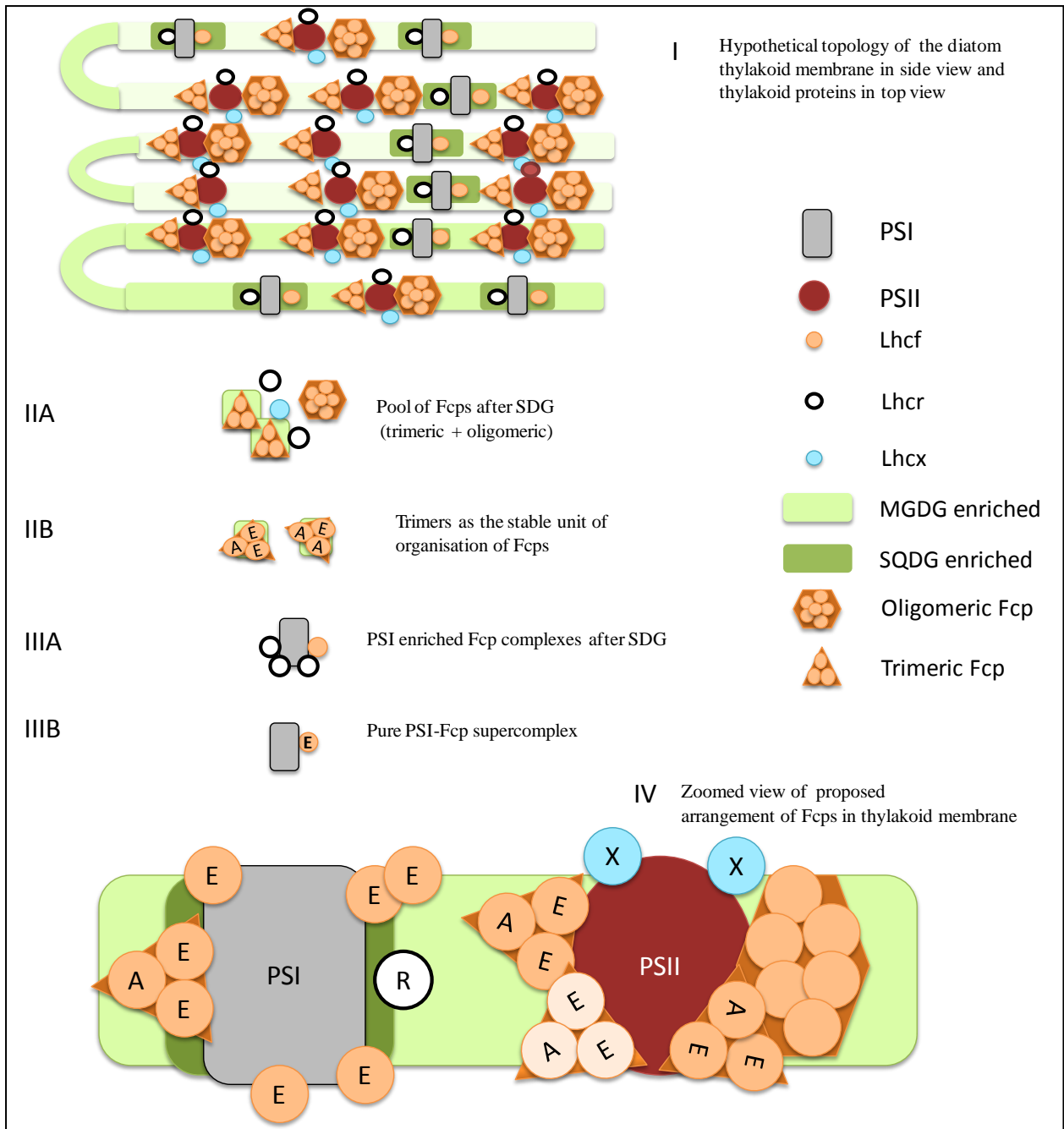
Figure 42: Hypothetical cartoon of the topology of the thylakoid membrane of diatoms in side view of thylakoid structure and top view of proteins. The cartoon considers only photosystems and Fcps for ease of interpretation. Cytb$_6$f complex and ATP synthase are not depicted.

Figure 42 depicts a hypothetical model of the topology of side view of thylakoid structure

and top view of proteins in diatom thylakoids. The model is based on information in literature

and a final interpretation of results combined from this thesis and from literature is also done.

In this figure, roman numbers, for e.g. 'I' refers to the text mentioned below marked with 'I' and so on, respectively.

I	The thylakoid membrane of diatoms consist of three parallel arranged membranes. PSI is more likely present in the outer thylakoid membrane than inner lamellae (Gibbs 1962; Pyszniak and Gibbs 1992). SQDG patches are hypothesized to separate PSI and PSII and reduce spillover of excitation energy (Lepetit et al. 2010, Lepetit et al. 2011). Mild purification methods like sucrose density gradient centrifugation have shown that Fcps are either higher oligomeric or trimeric in state both in *C. meneghiniana and P. tricornutum* (Büchel 2003, Beer et al. 2006, Lepetit et al. 2007, Joshi-Deo et al. 2010). MGDG is shown to be associated peripherally with Fcps as a shield and thought to be anchor the enzyme DDE responsible for conversion of Ddx to Dtx during the XC cycle (Goss et al. 2009, Goss et al. 2007). The exact location of the different types of Fcps and their association with PSs is unclear. For ease of interpretation concerning Fcps, the remaining important constituents of the membrane viz. $cytb_6f$ complex and ATP synthase complex are not shown.

IIA	Separation of protein complexes on sucrose density gradient centrifugation has indicated that

- In *P. tricornutum*, Fcp proteins from all three families (Lhcf, r and x) are found in the common pool of Fcps which are separated very well from photosystems (Lepetit et al. 2007, Lepetit et al. 2010, Joshi-Deo et al. 2010).

- They are shown to be associated with the lipid MGDG (Lepetit et al. 2010, Beer A 2010, Goss and Jakob 2010).

- Fcps can either be higher oligomeric (most probably hexameric) or trimeric (Lepetit et al. 2007, Büchel 2003) both in pennate and centric diatoms.

IIB	In *P. tricornutum*, trimers are the basic stable unit of organization. FcpA and FcpE form specific trimers (Joshi-Deo et al. 2010). There is data available concerning existence of

other specific trimeric complexes apart from FcpA and E complex (unpublished data K. Gundermann).

IIIA   PSI-Fcp complex from *C. meneghiniana* purified using 2 successive SDGs shows the stable association of Fcp4, an Lhcr type protein, with PSI (Veith et al. 2009). PSI-Fcp complex from *P. tricornutum* separated on sucrose density gradient contains largely Lhcr proteins and small amount of Lhcf proteins (Lepetit et al. 2010).

IIIB   A highly pure PSI-Fcp obtained using SDG and subsequent IEX associated only with FcpE (Lhcf type). Lhcr proteins seem to bind more peripherally and are therefore more easily lost than Lhcf5 proteins. The oligomeric organization of the Lhcfs associated with PSI has not been investigated.

IV   In summary, until intact PSII-Fcp complex can be isolated it is hypothesized that most of the Lhcfs and some Lhcx proteins associate with PSII. Lhcf function in light harvesting and Lhcx in photoprotection of PSII. One of the Fcp specific complexes is trimeric FcpA-E. FcpE also associates with PSI and acts as its light harvesting antenna. Lhcr proteins seem to be less tightly bound with PSI than Lhcf and might act as the photoprotection agents of PSI (Lepetit et al. 2010).

----

6   Summary

Diatoms contribute largely to the total primary production of the ecosphere and are key players in global biogeochemical cycles. Their chloroplasts are surrounded by four membranes owing to their secondary endosymbiotic origin. Their thylakoids are arranged into three parallel bands and differentiation of thylakoid membranes into grana or stroma is not observed. The fucoxanthin chlorophyll a/c binding proteins act as the light harvesting proteins and play a role in photoprotection during excess light as well. The diatom genome encodes three different families of antenna proteins. Family I are the classical light harvesting proteins called 'Lhcf'. Family II are the red algae related Lhca-R1/2 proteins called 'Lhcr' and family III are the photoprotective LI818 related proteins called 'Lhcx'.

All known Fcps have a molecular weight in the range of 17-23 kDa. They are membrane proteins and have shorter loops and termini compared to LHCs of higher plants and are therefore extremely hydrophobic. This makes the isolation of single specific Fcps using routine protein purification techniques difficult.

The purification of a specific Fcp containing complex has not been achieved so far and until this is done several questions concerning light harvesting antenna systems of diatoms cannot be answered. For e.g. Which proteins interact specifically? Are various Fcps differently pigmented? Which pigments interact with each other and how? Which proteins contribute to photosystem specific antenna systems? Can pure Fcps be reconstituted into crystals like LHCII proteins? In order to answer these questions specific Fcp containing complexes have to be purified.

The primary aim of this study was isolation of a single specific Fcp, namely the Lhcf protein family representative; FcpA, in its native state and to characterize it spectroscopically and biochemically. From transmission electron microscopy on WT and recombinant whole cells it could be observed that the morphology of whole cells and the organization of thylakoid

----

membranes was unaffected by the addition of six extra histidine residues on the C- terminus of FcpA. Further a protocol was developed to achieve a highly pure preparation of His-tagged FcpA protein of the pennate diatom *P. tricornutum* using sucrose density gradient and affinity chromatography. The complex was found to be a stable trimer. Mass spectrometry indicated that the binding partner of FcpA in the trimer was FcpE which is also a protein that belongs to the Lhcf family of proteins. Spectroscopic investigations indicated that the Fcp complex was absolutely intact in excitation energy transfer from Chl *c* and Fx to Chl *a*. Furthermore spectroscopic recordings upon specific excitation of Chl *c* or Fx and subsequent energy transfer indicated that these pigments were energetically coupled to Chl *a*. Pigment analysis verified that the complex contained 1 Fx molecule per Chl *a* which is was in line with literature values concerning mixed Fcp populations. However pigment analysis on highly pure Fcp preparations using sucrose density gradient ultracentrifugation and gel filtration of wildtype Fcp pool indicated that some Fcps were differentially pigmented and contributed to a higher XC pigment content as well as higher amounts of Fx in comparison to FcpA$_{His}$ and also to literature values.

Circular dichroism spectroscopy indicated that at least one of the Chl *a* molecules in the FcpA$_{His}$ and possibly one Fx molecule interacted excitonically. The characteristic split signal in the blue region of the spectrum observed in the FCP complexes of *C. meneghiniana* and *P. tricornutum* as well as in the xanthophyte alga *P. meringensis* indicate that the Chl *a*-carotenoid excitonic dimer is probably a conserved feature of the Chl a/c containing algae.

Furthermore, the FcpA$_{His}$ complex purified via sucrose density gradient centrifugation and a subsequent IMAC could be used for 2D crystallization experiments and analysed using transmission electron microscopy. 2D crystals in the form of vesicles could be obtained using the lipid MGDG and second detergent NG. However all crystals that were formed showed only a poor diffraction pattern under the TEM after negative staining. Nevertheless, the

----

reconstitution into vesicles was reproducible and this protocol is a sound fundamental point towards more crystallization trials.

To study the specific association either FcpA$_{His}$ or FcpE with photosystems, PSI-Fcp, PSII-Fcp and free Fcps were isolated from *P. tricornutum* using combination of mild solubilisation using β-DDM followed by SDG and ion exchange chromatography. Mass spectrometric analyses verified that the Fcps bound to PSI were mainly FcpE and 3 other Fcps viz. FcpA, C and F, all of which belong to the light harvesting family of proteins. These Fcps were found to be energetically coupled to PSI after spectroscopic investigations. Mass spectrometry could not identify any Fcps associated with PSII. Intact PSII-Fcp complexes need to be purified from this organism to identify PSII specific Fcps. Based on the fact that Lhcf proteins share a high sequence homology with LHCII it is assumed that Lhcf proteins also harvest light for PSII in diatoms. However this study indicates clearly that they also act as the light harvesting antenna also of PSI. Thus, at least certain Fcps are shared as a common light harvesting antenna system in *P. tricornutum*.

7 Zusammenfassung

----

7 Zusammenfassung

Diatomeen tragen maßgeblich zu der Primärproduktion der Ökosphäre bei und sind Hauptakteure in den globalen biogeochemischen Stoffkreisläufen. Ihre Chloroplasten sind aufgrund ihrer Entstehung durch sekundäre Endosymbiose von vier Membranen umgeben. Die Thylakoide sind in drei parallelen Bändern angeordnet und eine Differenzierung der Thylakoidmembranen in Grana- und Stromathylakoide liegt nicht vor. Die Fucoxanthin – Chlorophyll *a/c* – Bindeproteine fungieren hauptsächlich als Lichtsammelproteine und besitzen darüber hinaus auch eine Schutzfunktion bei überschüssiger Lichteinstrahlung.

Die Genomsequenzen von Diatomeen kodieren drei verschiedene Familien von Antennenproteinen: Proteine der Familie I sind die klassischen Lichtsammelproteine und werden als „Lhcf" bezeichnet. Familie II Proteine sind durch ihre strukturelle Ähnlichkeit zu dem einzigen membranintrinsischen Lichtsammelprotein der Rotalgen, *lhca*-R1/2, charakterisiert. Sie werden demnach auch als „Lhcr"-Proteine bezeichnet. Die Proteine der Familie III besitzen Lichtschutzfunktion und werden als „Lhcx" bezeichnet. Sie zeichnen sich durch ihre nahe Verwandtschaft zu den LI818-Proteinen der Grünalgen aus.

Alle bekannten Fcps besitzen eine relative ähnliche molekulare Masse in der Größenordnung von 17 – 21 kDa. Als Membranproteine sind sie zudem stark hydrophob, was eine Trennung spezifischer Fcp-Komplexe voneinander über die üblichen Proteinisolationsmethoden zusätzlich erschwert.

Die Isolation spezifischer Fcp-Komplexe konnte bisher nicht erreicht werden und aus diesem Grund sind bestimmte Fragestellungen betreffend der Lichtsammelproteine der Diatomeen immer noch unbeantwortet. Zum Beispiel, welche Proteine interagieren spezifisch miteinander? Sind die verschiedenen Fcps unterschiedlich pigmentiert? Welche Pigmente interagieren miteinander und auf welche Art und Weise? Welche Proteine sind Bestandteil von photosystem-spezifischen Antennensystemen? Ist es möglich, isolierte Fcp-Komplexe zu

----

kristallisieren, um ihre dreidimensionale Struktur aufzuklären, wie es bereits bei LHCII-Proteinen gelungen ist? Um all diese Fragen beantworten zu können, ist es unabdingbar, Fcp-Komplexe spezifisch zu isolieren.

Das primäre Ziel dieser Arbeit war demnach die spezifische Isolation eines einzigen Fcp in seinem nativen Zustand und zwar ein Vertreter der Lhcf-Familie, FcpA. Der gereinigte FcpA-Komplex sollte im Anschluss biochemisch sowie spektroskopisch weiter charakterisiert werden.

Untersuchungen am Transmissionselektronenmikroskop von ganzen rekombinanten sowie Wildtypzellen von *Phaeodactylum* zeigten, dass weder die Morphologie der Zellen, noch die Organisation der Thylakoidmembranen, durch den Anhang von sechs zusätzlichen Histidinresten an den C-Terminus von FcpA, verändert bzw. beeinflusst wurden.

Des Weiteren wurde in der vorliegenden Arbeit ein Protokoll entwickelt, durch das hoch reine Fcp-Komplexe über ein His_6-markiertes FcpA ($FcpA_{His}$) mittels Saccharosedichtegradientenzentrifugation (SDGZ) und Affintitätschromatographie isoliert werden konnten. Der reine Komplex wurde als stabiles Trimer isoliert und die massenspektrometrische Analyse identifizierte FcpE, ein weiteres Mitglied der Lhcf-Familie, als Bindungspartner von FcpA in den Trimeren. Darüber hinaus war die Weiterleitung der Anregungsenergie innerhalb des Fcp-Komplexes von Chl *c* und Fx zum Chl *a* vollkommen intakt. Die Fluoreszenzspektroskopischen Untersuchungen nach spezifischer Anregung von Chl *c* oder Fx und dem darauf folgenden Energietransfer belegten die energetische Kopplung dieser beiden Pigmente mit Chl *a*. Die Pigmentanalyse der Komplexe bestätigte ein bereits für heterogene Fcp-Komplexe publiziertes Verhältnis von einem Molekül Fx pro Chl *a*. Eine weitere Pigmentanalyse der durch SDGZ und Gelfiltration gereinigten gesamt FCP-Fraktion des *Phaeodactylum* Wildtyps zeigte jedoch im Vergleich zur Literatur höheren Gehalt an Fx und Xanthophyllzykluspigmenten unter den gegebenen Anzuchtsbedingungen. Die Analyse

----

der FcpA$_{His}$-Komplexe durch Circulardichroismus zeigte, dass mindestens eines der Chl *a* Moleküle mit einem oder mehreren Molekülen Fx excitonisch interagiert. Das gemeinsame charakteristische [zweigeteilte] Signal im blauen Spektralbereich der Spektren von FCP-Komplexen aus *C. meneghiniana* und *P. tricornutum*, sowie der Goldalge *P. meringensis* belegen, dass es sich bei diesem [excitonischen Dimer] aus Chl *a* und Fucoxanthin sehr wahrscheinlich um ein konserviertes Charakteristikum von Fcps in Chl *a/c* haltigen Organismen handelt.

Der über SDGZ und anschließender Ni-NTA-Affinitätschromatographie gereinigte FcpA$_{His}$-Komplex konnte darüber hinaus für zweidimensionale Kristallisationsexperimente verwendet werden, die im Anschluss mittels Transmissionselektronenmikroskopie analysiert wurden. Mit Hilfe des Lipids MGDG und einem weiterem Detergenz NG konnten zweidimensionale Kristalle der FcpA$_{His}$-Komplexe in vesikulärer Form rekonstituiert werden. Allerdings zeigten die produzierten Kristalle nach ihrer Anfärbung lediglich schwache Beugungsmuster unter dem Transmissionselektronenmikroskop. Gleichwohl war die Rekonstitution der Komplexe in vesikulärer Form reproduzierbar und das dabei etablierte Protokoll stellt eine wesentliche und wichtige Grundlage für weitere Kristallisationsexperimente dar.

Um die spezifische Assoziation des FcpA$_{His}$ bzw. des FcpE mit den Photosystemen zu untersuchen, wurden Superkomplexe aus PSI-Fcp, PSII-Fcp, sowie Fcp-Komplexe ohne Photosysteme aus *P. tricornutum* über eine Kombination aus milder Solubilisierung mit β-DDM und darauf folgender SDGZ und Ionenenaustauscherchromatographie isoliert. Es konnte gezeigt werden, dass die mit PSI assoziierten Fcps allesamt Vertreter der Lichtsammelprotein-Familie I sind. Dabei konnten hauptsächlich FcpE, A, C und F identifiziert werden. Durch spektroskopische Analysen wurde belegt, dass diese Fcps auch energetisch mit dem PSI gekoppelt sind. PSII spezifisch assoziierte Fcps konnten über massenspektrometrische Analyse nicht identifiziert werden. Um PSII spezifische Fcps in

----

Phaeodactylum identifizieren zu können, müssten intakte PSII-Fcp-Superkomplexe isoliert und weiter charakterisiert werden. Beruhend auf der Tatsache, dass die Lhcf Proteine eine hohe Sequenzhomologie mit LHCII aufweisen, wird allerdings vermutet, dass sie auch in Diatomeen Lichtsammelfunktion für das PSII ausüben müssten. Durch die vorliegende Arbeit konnte jedenfalls deutlich gezeigt werden, dass sie darüber hinaus auch als Lichtsammelantennen des PS I fungieren.

8   References

Amunts, A.; Toporik, H.; Borovikova, A.; Nelson, N. (2010): Structure determination and improved model of plant photosystem I. In: *J. Biol. Chem* 285 (5), 3478–3486.

Amunts, A.; Nelson, N. (2008): Functional organization of a plant Photosystem I: Evolution of a highly efficient photochemical machine. In: *Plant Physiology and Biochemistry* 46 (3), 228–237.

Anderson, J. M.; Chow, W. S.; de Las Rivas, J. (2008): Dynamic flexibility in the structure and function of photosystem II in higher plant thylakoid membranes: the grana enigma. In: *Photosyn. Res* 98 (1-3), 575–587.

Apt, K. E.; Kroth-Pancic, P. G.; Grossman, A. R. (1996): Stable nuclear transformation of the diatom *Phaeodactylum tricornutum*. In: *Mol. Gen. Genet* 252 (5), 572–579.

Apt, K. E.; Zaslavkaia, L.; Lippmeier, J. C.; Lang, M.; Kilian, O.; Wetherbee, R. et al. (2002): In vivo characterization of diatom multipartite plastid targeting signals. In: *J. Cell. Sci* 115, 4061–4069.

Armbrust, E. V. (2004): The Genome of the Diatom *Thalassiosira Pseudonana*: Ecology, Evolution, and Metabolism. In: *Science* 306 (5693), 79–86.

Austin, J. R.; Staehelin, L. A. (2011): Three-dimensional architecture of grana and stroma thylakoids of higher plants as determined by electron tomography. In: *Plant Physiol* 155 (4), 1601–1611.

Barclay, W.; Meager, K.; Abril, J. (1994): Heterotrophic production of long chain omega-3 fatty acids utilizing algae and algae-like microorganisms. In: *Journal of Applied Phycology* 6 (2), 123–129.

Barka Frederik (2008): Charakterisierung von Fucoxanthin-Chlrophyll-Protein-Mutanten der Diatomee *Phaeodactylum tricornutum*. Diplomarbeit. University of Frankfurt.

Bathke, L.; Rhiel, E.; Krumbein, W. E.; Marquardt, J. (1999): Biochemical and Immunochemical Investigations on the Light-Harvesting System of the Cryptophyte Rhodomonas sp.: Evidence for a Photosystem I Specific Antenna. In: *Plant Biology* 1 (5), 516-523.

Beer Anja (2010): Auswirkungen von Licht - and Eisenstress auf Morphologie und Photosynthese von *Cyclotella meneghiniana* (Bacillariophyceae) unter besonderer Berücksichtigung der Lichtantennenproteine (FCPs). PhD thesis. University of Frankfurt.

Beer, A.; Gundermann, K.; Beckmann, J.; Büchel, C. (2006): Subunit Composition and Pigmentation of Fucoxanthin−Chlorophyll Proteins in Diatoms: Evidence for a Subunit Involved in Diadinoxanthin and Diatoxanthin Binding. In: *Biochemistry* 45 (43), 13046–13053.

Berkaloff, C.; Caron, L.; Rousseau, B. (1990): Subunit organization of PSI particles from brown algae and diatoms: polypeptide and pigment analysis. In: *Photosynthesis Research* 23, 181–193.

Bhattacharya, D.; Medlin, L. (1998): Algal Phylogeny and the Origin of Land Plants. In: *Plant Physiology* 116 (1), 9–15.

Bhaya, D.; Grossman, A. R. (1993): Characterization of gene clusters encoding the fucoxanthin chlorophyll proteins of the diatom *Phaeodactylum tricornutum*. In: *Nucl Acids Res* 21 (19), 4458–4466.

Borowitzka, M.A.; Volcani, B. E. (1978): The Plymorphic diatom *Phaeodactylum tricornutum*: Ultrastructure of its morphotypes. In: *Journal of Phycology* 14 (1), 10-21.

Bouck, G. B. (1965): Fine structure and organelle association in brown algae. In: *J. Cell Biol* 26 (2), 523–537.

Bowler, C.; Allen, A. E.; Badger, J. H.; Grimwood, J.; Jabbari, K.; Kuo, A. et al. (2008): The *Phaeodactylum* genome reveals the evolutionary history of diatom genomes. In: *Nature* 456 (7219), 239–244.

Brakemann, T.; Schlörmann, W.; Marquardt, J.; Nolte, M.; Rhiel, E. (2006): Association of fucoxanthin chlorophyll a/c-binding polypeptides with photosystems and phosphorylation in the centric diatom *Cyclotella cryptica*. In: *Protist* 157 (4), 463–475.

Bricker, T.M.; Frankel, L. K. (2002): The structure and function of CP47 and CP43 in Photosystem II. In: *Photosyn. Res* 72 (2), 131–146.

Büchel, C. (2003): Fucoxanthin-Chlorophyll Proteins in Diatoms: 18 and 19 kDa Subunits Assemble into Different Oligomeric States. In: *Biochemistry* 42 (44), 13027–13034.

Caron, L.; Brown, J. (1987): Chlorophyll-Carotenoid Protein Complexes from the Diatom, *Phaeodactylum tricornutum*: Spectrophotometric, Pigment and Polypeptide Analyses. In: *Plant and Cell Physiology* 28 (5), 775–785.

Dekker, J. P.; Boekema, E. J. (2005): Supramolecular organization of thylakoid membrane proteins in green plants. In: *Biochim. Biophys. Acta* 1706 (1-2), 12–39.

Dunahay, T.; Jarvis, E.; Dais, S.; Roessler, P. (1996): Manipulation of microalgal lipid production using genetic engineering. In: *Applied Biochemistry and Biotechnology* 57-58 (1), 223–231.

Durnford, D. G.; Aebersold, R.; Green, B. R. (1996): The fucoxanthin-chlorophyll proteins from a chromophyte alga are part of a large multigene family: structural and evolutionary relationships to other light harvesting antennae. In: *Molecular and General Genetics* 253 (3), 377–386.

Durnford, D. G.; Deane, J. A.; Tan, S.; McFadden, G. I.; Gantt, E.; Green, B. R. (1999): A phylogenetic assessment of the eukaryotic light-harvesting antenna proteins, with implications for plastid evolution. In: *J. Mol. Evol* 48 (1), 59–68.

Enami, I.; Okumura, A.; Nagao, R.; Suzuki, T.; Iwai, M.; Shen, J.R. (2008): Structures and functions of the extrinsic proteins of photosystem II from different species. In: *Photosyn. Res* 98 (1-3), 349–363.

Eppard, M.; Rhiel, E. (1998): The genes encoding light-harvesting subunits of *Cyclotella cryptica* (Bacillariophyceae) constitute a complex and heterogeneous family. In: *Mol. Gen. Genet* 260 (4), 335–345.

Eppard, M.; Krumbein, W. E.; Haeseler, A. von; Rhiel, E. (2000): Characterization of *fcp4* and *fcp12*, Two Additional Genes Encoding Light Harvesting Proteins of *Cyclotella cryptica* (Bacillariophyceae) and Phylogenetic Analysis of this Complex Gene Family. In: *Plant Biology* 2 (3), 283-289.

Falciatore, A.; Bowler, C. (2002): Revealing the molecular secrets of marine diatoms. In: *Annu Rev Plant Biol* 53, 109–130.

Falciatore; C.; Leblanc; A.; Bowler C. (1999): Transformation of Nonselectable Reporter Genes in Marine Diatoms. In: *Mar. Biotechnol* 1 (3), 239–251.

Falkowski, P. G.; LaRoche, J. (1991): Acclimation to spectral irradiance in algae. In: *Journal of Phycology* 27 (1), 8-14.

Fawley, M. W.; Grossman, A. R. (1986): Polypeptides of a Light-Harvesting Complex of the Diatom *Phaeodactylum tricornutum* are Synthesized in the Cytoplasm of the Cell as Precursors. In: *Plant Physiology* 81 (1), 149–155.

Ferreira, K. N.; Iverson, T. M.; Maghlaoui, K.; Barber, J.; Iwata, S. (2004): Architecture of the photosynthetic oxygen-evolving center. In: *Science* 303 (5665), 1831–1838.

Fey, H.; Piano, D.; Horn, R.; Fischer, D.; Schmidt, M.; Ruf, S. et al. (2008): Isolation of highly active photosystem II core complexes with a His-tagged Cyt b_{559} subunit from transplastomic tobacco plants. In: *Biochim. Biophys. Acta* 1777 (12), 1501–1509.

Fischer, H.; Robl, I.; Sumper, M.; Kröger, N. (1999): Targeting and covalent modification of cell wall and membrane proteins heterologously expressed in the diatom *Cylindrotheca fusiformis* (Bacillariophyceae). In: *Journal of Phycology* 35 (1), 113-120.

Flachmann, R.; Kühlbrandt, W. (1996): Crystallization and identification of an assembly defect of recombinant antenna complexes produced in transgenic tobacco plants. In: *Proc. Natl. Acad. Sci. U.S.A* 93 (25), 14966–14971.

Gibbs, S. (1962): The ultrastructure of the chloroplasts of algae. In: *Journal of Ultrastructure Research* 7 (5-6), 418–435.

Goss, R.; Nerlich, J.; Lepetit, B.; Schaller, S.; Vieler, A.; Wilhelm, C. (2009): The lipid dependence of diadinoxanthin de-epoxidation presents new evidence for a macrodomain organization of the diatom thylakoid membrane. In: *J. Plant Physiol* 166 (17), 1839–1854.

Goss, R.; Latowski, D.; Grzyb, J.; Vieler, A.; Lohr, M.; Wilhelm, C.; Strzalka, K. (2007): Lipid dependence of diadinoxanthin solubilization and de-epoxidation in artificial membrane systems resembling the lipid composition of the natural thylakoid membrane. In: *Biochim. Biophys. Acta* 1768 (1), 67–75.

Goss, R.; Jakob, T. (2010): Regulation and function of xanthophyll cycle-dependent photoprotection in algae. In: *Photosyn. Res* 106 (1-2), 103–122.

Green, B. R.; Durnford, D. G. (1996): The chlorophyll-carotenoid proteins of oxygenic photosynthesis. In: *Annu. Rev. Plant. Physiol. Plant. Mol. Biol* 47 (1), 685–714.

Green, B. R.; Parson, W. W. (2003): Light-harvesting antennas in photosynthesis. Dordrecht: Kluwer.

Green, B. R.; Pichersky, E. (1994): Hypothesis for the evolution of three-helix Chl a/b and Chl a/c light-harvesting antenna proteins from two-helix and four-helix ancestors. In: *Photosynthesis Research* 39 (2), 149–162.

Gruber, A.; Vugrinec, S.; Hempel, F.; Gould, S.; Maier, U.G.; Kroth, P. (2007): Protein targeting into complex diatom plastids: functional characterisation of a specific targeting motif. In: *Plant Molecular Biology* 64 (5), 519–530.

Guglielmi, G.; Lavaud, J.; Rousseau, B.; Etienne, A. L.; Houmard, J.; Ruban, A. V. (2005): The light-harvesting antenna of the diatom Phaeodactylum tricornutum. In: *FEBS Journal* 272 (17), 4339-4348.

Gundermann, K.; Büchel, C. (2008): The fluorescence yield of the trimeric fucoxanthin–chlorophyll–protein FCPa in the diatom *Cyclotella meneghiniana*; is dependent on the amount of bound diatoxanthin. In: *Photosynthesis Research* 95 (2), 229–235.

Hankamer, B.; Barber, J.; Boekema, E. J. (1997): Structure and membrane organization of photosystem II in green plants. In: *Annu. Rev. Plant Physiol. Plant Mol. Biol* 48, 641–671.

Hankamer, B.; Morris, E.; Nield, J.; Gerle, C.; Barber, J. (2001): Three-Dimensional Structure of the Photosystem II Core Dimer of Higher Plants Determined by Electron Microscopy. In: *Journal of Structural Biology* 135 (3), 262–269.

Hempel, F.; Felsner, G.; Maier, U. G. (2010): New mechanistic insights into pre-protein transport across the second outermost plastid membrane of diatoms. In: *Molecular Microbiology* 76 (3), 793–801.

Heukeshoven, J.; Dernick, R. (1988): Increased sensitivity for Coomassie staining of sodium dodecyl sulfate-polyacrylamide gels using PhastSystem Development Unit. In: *Electrophoresis* 9 (1), 60–61.

Hobe, S.; Prytulla, S.; Kühlbrandt, W.; Paulsen, H. (1994): Trimerization and crystallization of reconstituted light-harvesting chlorophyll a/b complex. In: *EMBO J* 13 (15), 3423–3429.

Hoffman, G. E.; Puerta, M. V.; Delwiche, C. F. (2011): Evolution of light-harvesting complex proteins from Chl c-containing algae. In: *BMC Evol Biol* 11 (1), 101.

Ikeda, Y.; Komura, M.; Watanabe, M.; Minami, C.; Koike, H.; Itoh, S. et al. (2008): Photosystem I complexes associated with fucoxanthin-chlorophyll-binding proteins from a marine centric diatom, *Chaetoceros gracilis*. In: *Biochim. Biophys. Acta* 1777 (4), 351–361.

Ishikita, H.; Loll, B.; Biesiadka, J.; Kern, J.; Irrgang, K. D.; Zouni, A. et al. (2007): Function of two beta-carotenes near the D1 and D2 proteins in photosystem II dimers. In: *Biochim. Biophys. Acta* 1767 (1), 79–87.

Jeffrey, S. W.; Humphrey, G. F. (1975): New Spectrophotomteric equations for determining chlorophylls *a, b, c1* and *c2* in higher plants, algae and natural phytoplankton. In Biochemie und Physiologie der Pflanzen. 167 (2), 191–194.

Joshi-Deo, J.; Schmidt, M.; Gruber, A.; Weisheit, W.; Mittag, M.; Kroth, P. G.; Büchel, C. (2010): Characterization of a trimeric light-harvesting complex in the diatom *Phaeodactylum tricornutum* built of FcpA and FcpE proteins. In: *Journal of Experimental Botany* 61 (11), 3079–3087.

Juhas Matthias (2009): Veränderungen des molekularen Aufbaus im Photosystem I bei Diatomeen. Diplomarbeit. University of Frankfurt.

Katoh, T.; Ehara, T. (1990): Supramolecular Assembly of Fucoxanthin-Chlorophyll-Protein Complexes Isolated from a Brown Alga, *Petalonia fascia*. Electron Microscopic Studies. In: *Plant and Cell Physiology* 31 (4), 439–447.

Kaufmann Thomas (2006): Detergent-Protein and Detergent-Lipid Interactions: Implications for Two-dimensional Crystallization of Membrane Proteins and Development of Tools for High Throughput Crystallography. PhD thesis. University of Basel.

Kereïche, S.; Kiss, A. Z.; Kouril, R.; Boekema, E. J.; Horton, P. (2010): The PsbS protein controls the macro-organisation of photosystem II complexes in the grana membranes of higher plant chloroplasts. In: *FEBS Lett* 584 (4), 759–764.

Kilian, O.; Kroth, P.G. (2005): Identification and characterization of a new conserved motif within the presequence of proteins targeted into complex diatom plastids. In: *The Plant Journal* 41 (2), 175-183.

Kröger, N.; Poulsen, N. (2008): Diatoms-from cell wall biogenesis to nanotechnology. In: *Annu. Rev. Genet* 42, 83–107.

Kudo, I.; Miyamoto, M.; Noiri, Y.; Maita, Y. (2000): Combined effects of temperature and iron on the growth and physiology of the marine diatom *Phaeodactylum tricornutum* (Bacillariophyceae). In: *Journal of Phycology* 36 (6), 1096-1102.

Kühlbrandt, W. (1992): Two-dimensional crystallization of membrane proteins. In: *Q. Rev. Biophys* 25 (1), 1–49.

Lacapère, Jean-Jacques (Hg.) (2010): Methods in Molecular Biology. Totowa, NJ: Humana Press.

Larkum, A. W. D. (2004): Light-Harvesting Systems in Algae. In: Govindjee, Anthony W. D. Larkum, Susan E. Douglas and John A. Raven (Hg.): Photosynthesis in Algae, Springer Netherlands (Advances in Photosynthesis and Respiration), 277–304.

Lavaud J (2007): Fast Regulation of Photosynthesis in Diatoms: Mechanisms, Evolution and Ecophysiology. In: *Functional Plant Science and Biotechnology* 1, 267–287.

Lavaud, J.; Rousseau, B.; Etienne, A. L. (2003): Enrichment of the Light-Harvesting Complex in Diadinoxanthin and Implications for the Nonphotochemical Fluorescence Quenching in Diatoms. In: *Biochemistry* 42 (19), 5802–5808.

Lepetit, B.; Volke, D.; Gilbert, M.; Wilhelm, C.; Goss, R. (2010): Evidence for the Existence of One Antenna-Associated, Lipid-Dissolved and Two Protein-Bound Pools of Diadinoxanthin Cycle Pigments in Diatoms. In: *Plant Physiology* 154 (4), 1905–1920.

Lepetit, B.; Volke, D.; Szabó, M.; Hoffmann, R.; Garab, G.; Wilhelm, C.; Goss, R. (2007): Spectroscopic and Molecular Characterization of the Oligomeric Antenna of the Diatom *Phaeodactylum tricornutum*. In: *Biochemistry* 46 (34), 9813–9822.

Lepetit, B.; Goss, R.; Jakob, T.; Wilhelm, C. (2011): Molecular dynamics of the diatom thylakoid membrane under different light conditions. In: *Photosynthesis Research*.

Lewin, J. C.; Lewin, R. A.; Philpott, D. E. (1958): Observations on *Phaeodactylum tricornutum*. In: *Microbiology* 18 (2), 418–426.

Liu, Z.; Yan, H.; Wang, K.; Kuang, T.; Zhang, J.; Gui, L. et al. (2004): Crystal structure of spinach major light-harvesting complex at 2.72A° resolution. In: *Nature* 428 (6980), 287–292.

Lohr, M.; Wilhelm, C. (1999): Algae displaying the diadinoxanthin cycle also possess the violaxanthin cycle. In: *Proc. Natl. Acad. Sci. U.S.A* 96 (15), 8784–8789.

Lohr, M.; Wilhelm, C. (2001): Xanthophyll synthesis in diatoms: quantification of putative intermediates and comparison of pigment conversion kinetics with rate constants derived from a model. In: *Planta* 212 (3), 382–391.

Loll, B.; Kern, J.; Saenger, W.; Zouni, A.; Biesiadka, J. (2005): Towards complete cofactor arrangement in the 3.0A° resolution structure of photosystem II. In: *Nature* 438 (7070), 1040–1044.

Lopez, P.J.; Descles, J.; Allen, A. E.; Bowler, C. (2005): Prospects in diatom research. Plant biotechnology/ Food biotechnology. In: *Current Opinion in Biotechnology* 16 (2), 180–186.

Maheswari, U. (2004): The Diatom EST Database. In: *Nucleic Acids Research* 33 (Database issue), D344.

Maheswari, U.; Mock, T.; Armbrust, E. V.; Bowler, C. (2009): Update of the Diatom EST Database: a new tool for digital transcriptomics. In: *Nucleic Acids Research* 37, D1001.

----

de Martino, A.; Douady, D.; Quinet-Szely, M.; Rousseau, B.; Crépineau, F.; Apt, K.; Caron, L. (2000): The light-harvesting antenna of brown algae. In: *European Journal of Biochemistry* 267 (17), 5540-5549.

McKay, R. M. L.; Geider, R. J.; LaRoche, J. (1997): Physiological and Biochemical Response of the Photosynthetic Apparatus of Two Marine Diatoms to Fe Stress. In: *Plant Physiol* 114 (2), 615–622.

Mimuro, M.; Katoh, T.; Kawai, H. (1990): Spatial arrangement of pigments and their interaction in the fucoxanthin-chlorophyll ac protein assembly (FCPA) isolated from the brown alga Dictyota dichotoma. Analysis by means of polarized spectroscopy. In: *Biochimica et Biophysica Acta (BBA) - Bioenergetics* 1015 (3), 450–456.

Miyagawa-Yamaguchi, A.; Okami, T.; Kira, N.; Yamaguchi, H.; Ohnishi, K.; Adachi, M. (2011): Stable nuclear transformation of the diatom *Chaetoceros sp.* In: *Phycological Research* 59 (2), 113-119.

Murata, N.; Kume, N.; Okada, Y.; Hori, T. (1979): Preparation of girdle lamella-containing chloroplasts from the diatom *Phaeodactylum tricornutum*. In: *Plant and Cell Physiology* 20 (6), 1047–1053.

Nagao, R.; Ishii, A.; Tada, O.; Suzuki, T.; Dohmae, N.; Okumura, A. et al. (2007): Isolation and characterization of oxygen-evolving thylakoid membranes and photosystem II particles from a marine diatom *Chaetoceros gracilis*. In: *Biochim. Biophys. Acta* 1767 (12), 1353–1362.

Nelson, N.; Ben-Shem, A. (2004): The complex architecture of oxygenic photosynthesis. In: *Nat Rev Mol Cell Biol* 5 (12), 971–982.

Niyogi, K. K.; Li, X. P.; Rosenberg, V.; Jung, H. (2005): Is PsbS the site of non-photochemical quenching in photosynthesis? In: *Journal of Experimental Botany* 56 (411), 375–382.

Oeltjen, A.; Krumbein, W. E.; Rhiel, E. (2002): Investigations on Transcript Sizes, Steady State mRNA Concentrations and Diurnal Expression of Genes Encoding Fucoxanthin Chlorophyll a/c Light Harvesting Polypeptides in the Centric Diatom *Cyclotella cryptica*. In: *Plant Biology* 4 (2), 250-257.

Papagiannakis, E.; van H. M. Stokkum, I.; Fey, H.; Büchel, C.; van Grondelle, R. (2005): Spectroscopic Characterization of the Excitation Energy Transfer in the Fucoxanthin–Chlorophyll Protein of Diatoms. In: *Photosynthesis Research* 86 (1), 241–250.

Peers, G.; Truong, T. B.; Ostendorf, E.; Busch, A.; Elrad, D.; Grossman, A. R. et al. (2009): An ancient light-harvesting protein is critical for the regulation of algal photosynthesis. In: *Nature* 462 (7272), 518–521.

Pickett-Heaps, J. D.; Tippit, D. H.; Leslie, R. (1980): Light and electron microscopic observations on cell division in two large pennate diatoms. Hantzschia and Nitzschia. II. Ultrastructure. In: *Eur. J. Cell Biol* 21 (1), 12–27.

Premvardhan, L.; Bordes, L.; Beer, A.; Büchel, C.; Robert, B. (2009): Carotenoid structures and environments in trimeric and oligomeric fucoxanthin chlorophyll a/c2 proteins from resonance Raman spectroscopy. In: *J Phys Chem B* 113 (37), 12565–12574.

Premvardhan, L.; Robert, B.; Beer, A.; Büchel, C. (2010): Pigment organization in fucoxanthin chlorophyll a/c$_2$ proteins (FCP) based on resonance Raman spectroscopy and sequence analysis. In: *Biochim. Biophys. Acta* 1797 (9), 1647–1656.

Provasoli, L.; Mclaughlin, J. J.; Droop, M. R. (1957): The development of artificial media for marine algae. In: *Arch Mikrobiol* 25 (4), 392–428.

Pyszniak, A. M.; Gibbs, S. P. (1992): Immunocytochemical localization of photosystem I and the fucoxanthin-chlorophyll a/c light-harvesting complex in the diatom *Phaeodactylum tricornutum*. In: *Protoplasma* 166 (3), 208–217.

Reynolds, E. S. (1963): The use of lead citrate at high pH as an electron-opaque stain in electron microscopy. In: *J. Cell Biol* 17, 208–212.

Richard, C.; Ouellet, H.; Guertin, M. (2000): Characterization of the LI818 polypeptide from the green unicellular alga *Chlamydomonas reinhardtii*. In: *Plant Molecular Biology* 42 (2), 303–316.

Rigaud, J. L.; Chami, M.; Lambert, O.; Levy, D.; Ranck, J. L. (2000): Use of detergents in two-dimensional crystallization of membrane proteins. In: *Biochimica et Biophysica Acta (BBA) - Biomembranes* 1508 (1-2), 112–128.

de Riso, V.; Raniello, R.; Maumus, F.; Rogato, A.; Bowler, C.; Falciatore, A. (2009): Gene silencing in the marine diatom *Phaeodactylum tricornutum*. In: *Nucleic Acids Res* 37 (14), e96.

Ruban, A. V.; Wentworth, M.; Yakushevska, A. E.; Andersson, J.; Lee, P. J.; Keegstra, W. et al. (2003): Plants lacking the main light-harvesting complex retain photosystem II macro-organization. In: *Nature* 421 (6923), 648–652.

Schaegger, H.; von Jagow, G. (1987): Tricine-sodium dodecyl sulfate-polyacrylamide gel electrophoresis for the separation of proteins in the range from 1 to 100 kDa. In: *Analytical Biochemistry* 166 (2), 368–379.

Shi, L. X.; Lorković, Z. J.; Oelmuller, R.; Schroder, W. P. (2000): The low molecular mass PsbW protein is involved in the stabilization of the dimeric photosystem II complex in *Arabidopsis thaliana*. In: *J. Biol. Chem* 275 (48), 37945–37950.

Standfuss, J.; Kühlbrandt, W. (2004): The Three Isoforms of the Light-harvesting Complex II. In: *Journal of Biological Chemistry* 279 (35), 36884–36891.

Suorsa, M.; Regel, R. E.; Paakkarinen, V.; Battchikova, N.; Herrmann, R. G.; Aro, E. M. (2004): Protein assembly of photosystem II and accumulation of subcomplexes in the absence of low molecular mass subunits PsbL and PsbJ. In: *Eur. J. Biochem* 271 (1), 96–107.

Szabó, M.; Lepetit, B.; Goss, R.; Wilhelm, C.; Mustárdy, L.; Garab, G.(2008): Structurally flexible macro-organization of the pigment–protein complexes of the diatom *Phaeodactylum tricornutum*. In: *Photosynthesis Research* 95, 237–245.

Thornber, J. P. (1975): Chlorophyll-Proteins: Light-Harvesting and Reaction Center Components of Plants. Annual Review of Plant Physiology. In: *Annu. Rev. Plant. Physiol* 26 (1), S. 127–158.

Trissl, H. W.; Wilhelm, C. (1993): Why do thylakoid membranes from higher plants form grana stacks? In: *Trends Biochem. Sci* 18 (11), 415–419.

Veith Thomas (2009): Biochemical Characterisation of Photosystem I Complexes in Diatoms. PhD thesis. University of Frankfurt.

Veith, T.; Büchel, C. (2007): The monomeric photosystem I-complex of the diatom *Phaeodactylum tricornutum* binds specific fucoxanthin chlorophyll proteins (FCPs) as light-harvesting complexes. In: *Biochimica et Biophysica Acta (BBA) - Bioenergetics* 1767 (12), 1428–1435.

8 References

Veith, T.; Brauns, J.; Weisheit, W.; Mittag, M.; Büchel, C. (2009): Identification of a specific fucoxanthin-chlorophyll protein in the light harvesting complex of photosystem I in the diatom *Cyclotella meneghiniana*. Radical species, mitochondria and cardiac function. In: *Biochimica et Biophysica Acta (BBA) - Bioenergetics* 1787 (7), 905–912.

Wilhelm, C.; Büchel, C.; Fisahn, J.; Goss, R.; Jakob, T.; LaRoche, J. et al. (2006): The Regulation of Carbon and Nutrient Assimilation in Diatoms is Significantly Different from Green Algae. In: *Protist* 157 (2), 91–124.

Zaslavskaia, L. A.; Lippmeier, J. C.; Kroth, P. G.; Grossman, A. R.; Apt, K. E. (2000): Transformation of the diatom *Phaeodactylum tricornutum* (Bacillariophyceae) with a variety of selectable marker and reporter genes. In: *Journal of Phycology* 36 (2), 379-386.

Zhu, S. H.; Green, B. R. (2008): Light-Harvesting and Photoprotection in Diatoms: Identification and Expression of LI818-Like Proteins. In: John F. Allen, Elisabeth Gantt, John H. Golbeck and Barry Osmond (Hg.): Photosynthesis. Energy from the Sun: Springer Netherlands, 261–264.

Zhu, S. H.; Green, B. R. (2010): Photoprotection in the diatom *Thalassiosira pseudonana*: Role of LI818-like proteins in response to high light stress. In: *Biochimica et Biophysica Acta (BBA) - Bioenergetics* 1797 (8), 1449–1457.

Zigmantas, D.; Hiller, R. G.; Sharples, F. P.; Frank, H. A.; Sundström, V.; Polívka, Tomáš (2004): Effect of a conjugated carbonyl group on the photophysical properties of carotenoids. In: *Phys. Chem. Chem. Phys* 6 (11), 3009.

Appendix I

Appendix I – Nomenclature of Fcps identified in *P. tricornutum* genome

Protein	Alternative name	Phatr2 proteinID

Lhcf type- GroupI Fcps- function in light harvesting

Protein	Alternative name	Phatr2 proteinID
FcpA	Lhcf1	18049
	Lhcf2	25172
FcpC	Lhcf3	50705
FcpD	Lhcf4	25168
FcpE	Lhcf5	30648
FcpB	Lhcf6	30643
	Lhcf7	29266
	Lhcf8	22395
	Lhcf9	30031
	Lhcf10	22006
FcpF	Lhcf11	51230
	Lhcf12	16302
	Lhcf13	22680
	Lhcf14	25893
	Lhcf15	48882
	Lhcf16	34536
	Lhcf17	56310

Lhcr type- Group II Fcps- supposed to be PSI specific antenna

Alternative name	Phatr2 proteinID
Lhcr1	44601
Lhcr2	22956
Lhcr3	50725
Lhcr4	17766
Lhcr5	29472
Lhcr6	56319
Lhcr7	43522
Lhcr8	32294
Lhcr9	43860
Lhcr10	50086
Lhcr11	23257
Lhcr12	54027
Lhcr13	38121
Lhcr14	47813

Lhcx type-GroupIII Fcps- function in photoprotection

Alternative name	Phatr2 proteinID
Lhcx1	27278
Lhcx2	54065

Lhcx3   44733
Lhcx4   38720

Appendix II- Pigment analysis of PI-Fcp complex.

Pigment analysis of the PSI-Fcp sample (please refer section 4.3.4). Values reported here are an average of 2 measurements on 2 different samples of the same preparation.

Mol/mol Chl *a*	Fx	Chl *c*	Ddx+Dtx	β-carotene
PSI-Fcp sample	0.138	0.05	0.014	0.127

E R K L Ä R U N G

Ich erkläre hiermit, dass ich mich bisher keiner Doktorprüfung unterzogen habe.

Frankfurt am Main, den.................................. ....

……………………………………...
(Unterschrift)

Eidesstattliche Versicherung

Ich erkläre hiermit an Eides Statt, dass ich die vorgelegte Dissertation über

....

....

....

selbständig angefertigt und mich anderer Hilfsmittel als der in ihr angegebenen nicht bedient habe, insbesondere, dass alle Entlehnungen aus anderen Schriften mit Angabe der betreffenden Schrift gekennzeichnet sind.

Ich versichere, nicht die Hilfe einer kommerziellen Promotionsvermittlung in Anspruch genommen zu haben.

Frankfurt am Main, den................................. ....
(Unterschrift)

Curriculum vitae

Jidnyasa Joshi

Contact:
joshi@bio.uni-frankfurt.de
joshi3010@gmail.com
Rotdornweg 6
36037, Fulda, Germany.

Nationality: **Indian**
Date of Birth: **30th October 1984**
Place of Birth: **Goregaon (India)**
Marital status: **Married**

Education

06/2008 to date	**Johann Wolfgang GoetheUniversity, Frankfurt am Main, Germany** **Doctoral student in Biological Sciences, Plant Cell Physiology group under supervision of Prof. Dr. C. Büchel.**
Project	Biochemical characterization of Fucoxanthin Chlorophyll proteins and their interaction with photosystems in the diatom *Phaeodactylum tricornutum*.

08/2007 to 05/2008 Jacobs University Bremen, Germany, Graduate studies in Molecular life sciences
Biopysics laboratory supervision of Prof. Dr. M. Winterhalter
Project Electrophysiological investigation of antibiotic translocation through OmpF and OmpC in black lipid membranes**.**

08/2005-08/2007 **University of Pune, India, Master of Science in Biochemistry, Grade 'Outstanding'**
Project Molecular characterization of urinary isolates of *Acinetobacter* species.

08/2002-06/2005 **Fergusson College,Pune,India, Bachelor of Science in Chemistry and Biotechnology**
Grade 'First class with Distinction'

Research Experience

08/2008 to date **Scientific research associate, Plant Cell Physiology Laboratory, Johann Wolfgang GoetheUniversity, Frankfurt am Main, Germany.**
-Algae culture, Membrane protein purification –Affinity chromatography, Gel filtration, Ion exchange, HPLC.
-Spectroscopy-UV/Vis, Fluorescence, Circular Dichroism
-Transmission electron microscopy CM12 Philips- 2D crystal handling, ultrathin sections for structural investigations.

Scientific Communication

Publications: **Jidnyasa Joshi-Deo, Matthias Schmidt, Ansgar Gruber, Wolfram Weisheit, Maria Mittag, Peter G. Kroth and Claudia Büchel. Characterization of a trimeric light-harvesting complex in the diatom *Phaeodactylum tricornutum* built of FcpA and FcpE proteins. J. Exp. Botany, June 2010. Vol. 61, No. 11, pp. 3079–3087.**

Oral Presentations:	8th European Biophysics Congress, 23rd -27th August 2011, Budapest, Hungary. *Characterization of the light harvesting antenna system in the diatom Phaeodactylum tricornutum.*

Oral Presentations: 8th European Biophysics Congress, 23rd -27th August 2011, Budapest, Hungary. *Characterization of the light harvesting antenna system in the diatom Phaeodactylum tricornutum.*

International Summer School, August 2011, 'Current techniques in Membrane Proteomics' at the Center for Membrane Proteomics, University of Frankfurt (M), Germany. *The light harvesting antenna system in the diatom Phaeodactylum tricornutum.*

Photosynthesis Workshop, August 2010, at the University of Frankfurt (M). *Function of light harvesting protein FcpA in the diatom Phaeodactylum tricornutum.*

Symposium Botanik, January 2010, University of Frankfurt (M). *Purification and Characterization of light harvesting protein FcpA from Phaeodactylum tricornutum.*

Posters: VAAM 2008, Frankfurt am Main,Germany. Srivastava A., Joshi J., Ullrich M. Mapping the transcriptional start site of levansucrase genes in *Pseudomonas syringae.*

Botanikertagung der Deutsche Botanische Gesselschaft, 2009, Leipzig,Germany. Jidnyasa Joshi-Deo and Frederik Barka, Matthias Schmidt, Claudia Büchel. Towards the characterization of single light harvesting-proteins from the diatom *Phaeodactylum tricornutum.*

Botanikertagung der Deutsche Botanische Gesselschaft, 2009, Leipzig, Germany. Gundermann Kathi, Barka Frederik, Joshi-Deo Jidnyasa and Büchel Claudia. Genetically modified *Phaeodactylum tricornutum* cells expressing additional polypeptides analogue to Ll818 in the light harvesting complexes (FCP).

8th European Biophysics Congress, 2011, Budapest, Hungary. *Characterization of the light harvesting antenna system in the diatom Phaeodactylum tricornutum.*

Practical Experience

09/2007-05/2008 **Jacobs University Bremen, Germany**
Investigation of antibiotic efflux through ion channels using black lipid bilayer and patch clamp technique.

05/ 2006-07/2006 **National Institute of Immunology, New Delhi, India**
Identification of potential allergens from *Coffea arabica.* (Purification and characterization of potential allergenic proteins).

05/ 2004-06/2004 **Summer job at Vaccine trial division, Venkateshwara Hatcheries, Pune, India**

05/2003-06/2003 **Summer job at Serum Institute of India, Quality Control Department, Pune, India**

Skills and Achievements

Languages:	Marathi: mother tongue	Hindi: fluent
	English: fluent	German: thorough working knowledge

Awards:

05/2005 3rd rank, Advanced Diploma in German Language, University of Pune, India.

05/2006-07/2006 Indian Academy of Sciences Fellowship for development of Excellence in Research in young scientists (www.ias.ac.in)

09/2007-05/2008 Jacobs University Bremen Scholarship for graduate studies.